Investigating extracellular vesicle-mediated interactions between *Enterococcus faecalis*, monocyte-derived macrophages, and endothelial cells

Dissertation

zur Erlangung des Grades

des Doktors der Naturwissenschaften

der Naturwissenschaftlich-Technischen Fakultät

der Universität des Saarlandes

von

Arefeh Kardani

Saarbrücken

2024

Tag des Kolloquiums:	10.07.2025
Dekan:	Prof. Dr.-Ing. Dirk Bähre
Berichterstatter:	Prof. Dr. Alexandra K. Kiemer Prof. Dr. Gregor Fuhrmann
Akad. Mitglied:	Dr. Oskar Staufer
Vorsitz:	Prof. Dr. Uli Müller

To my mom.

Contents

Abstract

The bidirectional exchange of EVs between the host and its microbiome or pathogenic bacteria serves as a fundamental mechanism for communication and regulation of various physiological processes and immune responses, especially in microbiome-related disorders. Enterococci bloodstream infections are a prevalent cause of healthcare-associated infections. This study investigated the interactions of *Enterococcus faecalis* and host cells through EVs.

Chapter I contributed to a more comprehensive understanding of EVs secreted by Gram-positive *Enterococcus faecalis* and their role in activating host immune cells. Bacterial EVs were isolated, characterized, and assessed for their cytotoxic effect in host cells. Furthermore, their internalization and potential to affect the inflammatory gene expression were studied.

In chapter II, an *in vitro* flow culture model was utilized to culture endothelial cells under laminar flow conditions that allowed the isolation of endothelial EVs. EVs from static and flow cultures were isolated and examined for their characteristics and cargo content. Furthermore, the expression of bacterial genes involved in virulence was studied after exposure to endothelial EVs.

Zusamenfassung

Der bidirektionale Austausch von EVs zwischen dem Wirt und seinem Mikrobiom bzw. pathogenen Bakterien stellt einen grundlegenden Mechanismus für die Kommunikation und Regulierung verschiedener physiologischer Prozesse und Immunreaktionen, insbesondere bei mikrobiombedingten Erkrankungen. *Enterokokken*-Infektionen der Blutbahn sind eine häufige Ursache für Infektionen im Zusammenhang mit dem Gesundheitswesen. In dieser Studie wurden die Wechselwirkungen zwischen *Enterococcus faecalis* und Wirtszellen durch EVs untersucht.

Kapitel I trug zu einem umfassenderen Verständnis der von Gram-positiven *Enterokokken* abgesonderten EVs und ihrer Rolle bei der Virulenz bei. Die bakteriellen EVs wurden isoliert, charakterisiert und auf ihre zytotoxische Wirkung in den Wirtszellen untersucht. Darüber hinaus wurden ihre Internalisierung und ihr Potenzial zur Beeinflussung des entzündlichen Genexpressionsprofils untersucht.

In Kapitel II wurde ein *in vitro* Strömungskulturmodell verwendet, um Endothelzellen unter laminarer Strömung zu kultivieren, was die Isolierung von endothelialen EVs ermöglichte. EVs aus statischen und Fließkulturen wurden isoliert und auf ihre physiologischen Eigenschaften und den Gehalt an Fracht untersucht. Darüber hinaus wurde die Expression von Bakteriengenen, die an der Virulenz beteiligt sind, nach der Exposition gegenüber endothelialen EVs untersucht.

1 Introduction

1.1 Enterococcus faecalis

Enterococcus faecalis, a Gram-positive bacterium, typically resides as a natural component of the gut microbiota. However, it is also recognized as an opportunistic pathogen capable of causing a range of infections including urinary tract infections (Abat et al. 2016), endocarditis (Barnes, Frank, and Dunny 2021) and sepsis (Linden 2003). Its pathogenicity is notably elevated in individuals with compromised immune systems or other underlying health conditions. Hence, *E. faecalis* is frequent in clinical settings, especially during hospitalization and in cases of surgical wounds, making it one of the most commonly encountered species in clinical isolates (Beganovic et al. 2018).

The primary component of the cell wall in Enterococci is peptidoglycan (PG). Alongside the polymerization of glycan strands, Enterococci decorate their peptidoglycan layer and cell membrane with diverse proteins. These proteins are either covalently linked to the peptidoglycan layer, including polysaccharides, teichoic acids, and surface-anchored proteins, or covalently attached to the plasma membrane, such as lipoteichoic acids (LTA) and lipoproteins (Hancock, Murray, and Sillanpää 2014).

1.1.1 Virulence-related factors

The progression of bacterial infections involves a series of stages: colonization, adherence to host tissues, tissue invasion, and resistance to host defence mechanisms. The exploration of the mechanisms in enterococci that facilitate these stages has identified a set of genes potentially associated with enterococcal virulence.

Extracellular matrix (ECM) binding: The primary step crucial to *E. faecalis* pathogenesis involves adherence to host tissues, particularly in urinary tract infections (UTIs) (Flores-Mireles et al. 2015). Virulence factors associated with this adherence include an aggregation substance (Agg), and the adhesin to collagen (Ace), which facilitate adhering to and colonizing in the host tissues (Șchiopu et al. 2023). Furthermore, *E. faecalis* has the capability to form biofilms (Oli et al. 2022), which have been shown to impart antibiotic resistance (Khalil et al. 2023), making them more vulnerable to antibiotic therapy.

Pili: The endocarditis and biofilm-associated pili (Ebp) play a significant role in the pathogenicity of *E. faecalis*, as highlighted by various studies (Nielsen et al. 2012; Sillanpää et al. 2013; Kavindra V. Singh, Nallapareddy, and Murray 2007; Nallapareddy et al. 2006)**.** The ebp locus comprises three genes, ebpA, ebpB, and ebpC, forming an operon responsible for encoding the pilus subunits (Sillanpää et al. 2013; Nallapareddy et al. 2006)**.** Ebp are important for biofilm formation and adherence of bacteria to host ECM proteins, including fibrinogen and collagen, a process that is considered crucial in the initial steps of infection (Nallapareddy and Murray 2008; Nallapareddy et al. 2011)**.**

ECM digestion: Gelatinase is a zinc-containing metalloproteinase produced by *E. faecalis* that is capable of hydrolyzing gelatin, collagen, casein, hemoglobin, and other peptides (Mäkinen et al. 1989), contributing to the development of chronic intestinal inflammation by impairing epithelial barrier integrity (Steck et al. 2011). Certain peptides, generated as a consequence of collagen fragmentation attract monocytes (Postlethwaite and Kang 1976), macrophages (Laskin et al. 1994), and neutrophils (Riley et al. 1988) to the site of breakdown.

Pore formation: Enterococcal cytolysin is a pore-forming exotoxin that affects a broad range of eukaryotic and prokaryotic cell types (Coburn and Gilmore 2003). Contribution of cytolysin in virulence has been studied in various infection models (Ike, Hashimoto, and Clewell 1984; K. V. Singh et al. 1998; Chow et al. 1993; Jett et al. 1992; Stevens et al. 1992). Cytolysin is associated with acute mortality in humans (Huycke, Spiegel, and Gilmore 1991) and evading host defense by inhibiting macrophage activation (Bebien et al. 2012).

1.1.2 Enterococcal infection and immunity

The initial line of defense in the innate immune system against pathogen invasion relies on recognition of pathogen-associated molecular patterns (PAMPs) present in pathogens. Cells within the innate immune system, such as macrophages, serve as primary defenses against invaders. These cells possess robust phagocytic properties and are equipped with pattern recognition receptors (PRRs), which enable them to identify and eliminate microorganisms by recognizing common patterns expressed by various pathogens, referred to as pathogen-associated molecular patterns or damage-associated molecular patterns (DAMPs) (D. Li and Wu 2021).

Toll-like receptors (TLRs), which comprise a significant subgroup of PRRs, play pivotal roles in recognizing both commensal and pathogenic bacteria. When specific compounds are recognized, TLRs initiate signal transduction pathways, such as the NF-κB pathway or MAP kinase pathways. In turn, these pathways result in the recruitment of transcription factors, leading to the activation of inflammatory gene expression and protein secretion (Fitzgerald and Kagan 2020). For instance, bacterial surface patterns such as lipopolysaccharides (LPS) from Gram-negative bacteria or LTA from Gram-positive bacteria can induce the secretion of inflammatory mediators through TLR4 and TLR2, respectively (Kawasaki and Kawai 2014).

Using a mouse model, Leendertse et al. showed that enterococcal bacteria are recognized by peritoneal macrophages through TLR2, mediating neutrophil influx to the site of infection and bacterial clearance (Leendertse, Willems, Giebelen, Roelofs, Bonten, et al. 2009). It was also found that peritoneal macrophages (Leendertse, Willems, Giebelen, Roelofs, van Rooijen, et al. 2009), neutrophils (Leendertse, Willems, Giebelen, Roelofs, Bonten, et al. 2009) and the complement system (Leendertse et al. 2010) are essential for the rapid eradication of this bacterium in the early stages of the infection.

1.1.3 Clinical manifestations

Enterococci are among the most common sources of infections acquired in hospitals, with *E. faecalis* accounting for 80–90% of infection cases (Weiner et al. 2016; Suetens et al. 2018; Orsi and Ciorba 2013). Enterococci typically affect older individuals, those with compromised immune systems, those with significant underlying illnesses, individuals undergoing broad-spectrum antibiotic treatment, and those with concurrent bacterial infections. Enterococci are responsible for a range of infections, including urinary tract infections (UTIs), endocarditis, meningitis, wound infections, and intra-abdominal and pelvic infections. (Moellering 1992).

Normally, enterococcal infections follow specific routes: (1) spread of the patient's regular microbial flora to different body sites, frequently triggered by extensive antibiotic usage or improper antibiotic application (referred to as opportunistic infections); (2) spread of antibiotic-resistant bacterial strains within a hospital setting; and (3) wound infections (largely attributed to surgery, decubitus ulcers, and burn wounds).

According to the International Society for Infectious Diseases and the Center for Disease Control, UTIs are among the most common infections in hospitalized patients (Öztürk and Murt 2020). Enterococci contribute to over 30% of UTIs in patients using urinary catheters and have been identified as the leading pathogen in catheter–associated UTI (Kline and Lewis 2016). The host immune response proved inadequate in eliminating infection, indicating an increased risk of colonization and infection in individuals undergoing immunosuppressive therapies (Guiton et al. 2013).

Bacteremia occurs when the organism enters the bloodstream. Individuals experiencing enterococcal bacteremia face an elevated risk of developing endocarditis, which is characterized by bacterial damage to the cardiac valves and a decline in cardiac function (Dahl et al. 2019; Escolà-Vergé et al. 2021). The formation and progression of bacterial biofilms have been observed during *E. faecalis* colonization of

the murine gastrointestinal tract (Barnes et al. 2016). Biofilm formation also represents a significant pathogenic factor in animal models of enterococcal catheter-associated urinary tract infections and endocarditis (Barnes, Frank, and Dunny 2021).

1.2 Host microbiome interaction

The term "microbiota" refers to a community of microorganisms that encompasses commensal, symbiotic, and pathogenic microorganisms, that literally share our body spaces (Hou et al. 2022). As we are abruptly and continuously exposed to the environment after birth, trillions of normally non-pathogenic bacteria rapidly colonize the gut. While the composition and metabolic functions of the gut microbiota show greater similarities in early life, the microbiota diversity becomes more pronounced over time. In healthy individuals, the composition of the gut microbiota remains relatively stable, dominated mainly by a few phyla that form complex biochemical interaction networks between themselves and their hosts (Hui Xu et al. 2020; Shkoporov and Hill 2019; Sender, Fuchs, and Milo 2016; Huttenhower et al. 2012). Nevertheless, there is notable diversity in bacterial populations among individuals, attributed to variances in the host genome and influenced by lifestyle factors such as diet, drug usage, and environmental exposure (Thriene and Michels 2023; Tamburini et al. 2016).

The gut microbiota maintains a symbiotic relationship within the human host, which plays a pivotal role in shaping overall health. Interactions between the gut microbiota and intestinal cells actively regulate barrier functions and consistently prompt the immune system to mount defenses against potential pathogens (Cao et al. 2022; Yoo et al. 2020; De Santis et al. 2015).

The balance between the ratios of epithelial barrier-protective, pro-inflammatory, and anti-inflammatory cytokines determines the inflammatory or homeostatic state of the gut (Fakharian et al. 2023; Cicchese et al. 2018; Rescigno 2011). The detection of pathogen-associated molecular patterns by antigen-presenting cells (APCs) through pattern recognition receptors is integral to the innate immune response. PRRs enable APCs to identify PAMPs, which, in turn, initiate a cascade of inflammatory responses. For example structural components of the microbiota, such as LPS and peptidoglycan, directly engage with host intestinal cells through Toll-like receptors (Zheng, Liwinski, and Elinav 2020; Larsson et al. 2012).

The gut epithelium and vascular barrier regulate the entry of the host tissue beyond the intestinal epithelial barrier and into circulation. Functionally, the intestinal epithelial barrier separates the luminal contents from the immune cells found in the gut and prevents systemic dissemination of pathogens to other organs (Di Vincenzo et al. 2024; Scalise et al. 2021) (Figure 1-1).

Impaired intestinal integrity can lead to bacterial translocation, defined as the movement of gut bacteria into sterile tissue. Contrary to the belief that live bacteria must breach the gut epithelial barrier for sepsis, the term includes the movement of intact bacteria, toxins, and microbial products from the gut into circulation, resulting in systemic inflammation and diverse diseases (Wheeler et al. 2023; Twardowska et al. 2022; Nagpal and Yadav 2017).

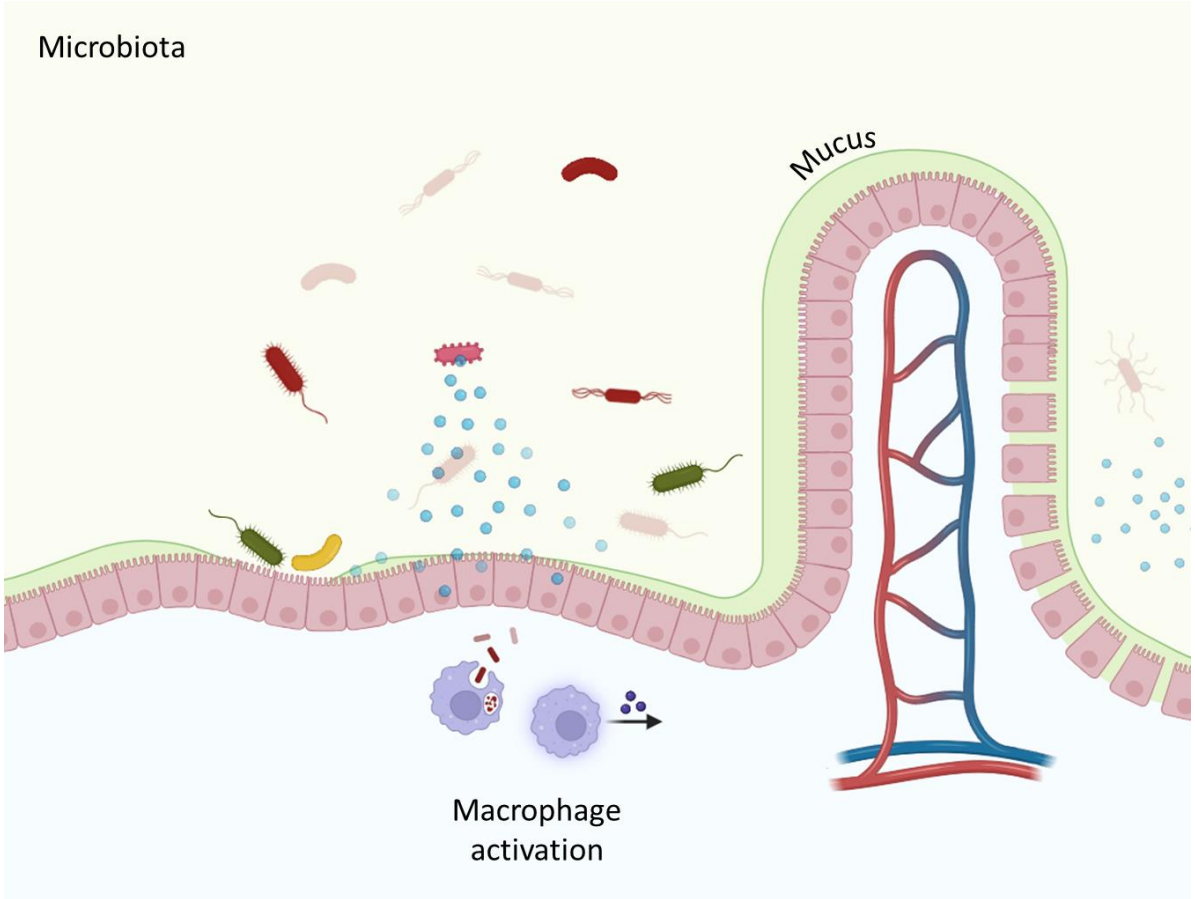

FIGURE 1-1. Interaction between gut microbiota and the host: Impaired intestinal barrier function results in bacterial and microbiome-derived metabolites permeating the underlying tissue, leading to inflammation. Created with BioRender.com.

1.3 Extracellular vesicles

The interaction between bacteria and host cells extends beyond direct cell contact, with the release of bacterial extracellular vesicles (EVs) emerging as a significant mechanism (Yang et al. 2022; Rodrigues et al. 2018). EVs are nano-sized membrane-bound structures released by almost all cell types in their external environment. The significance of EVs has been underestimated for a long time, with EVs being initially referred to as cellular 'dust' (Cocucci, Racchetti, and Meldolesi 2009; Wolf 1967). It is now well recognized that EVs carry bioactive molecules, such as proteins, nucleic acids, and lipids. These vesicles play a crucial role in intercellular communication and influence various physiological and pathological processes in the recipient cells (van Niel et al. 2022; Berumen Sánchez et al. 2021).

The impact of EV production on pathogenesis has become an increasingly active research field (EL Andaloussi et al. 2013). It is now well established that many pathogenic bacteria use their EVs to deliver toxic compounds to infected cells (Bitto et al. 2017), whereas eukaryotic EVs are involved in many important human pathologies, including cancer, cardiovascular, and neurodegenerative diseases, and have the potential to be used as biomarkers or delivery vehicles for therapeutic action (Yáñez-Mó et al. 2015; Robbins, Dorronsoro, and Booker 2016; Thompson et al. 2016; Shu Liu et al. 2017; Mateescu et al. 2017).

1.3.1 Bacterial EVs

Bacterial EVs are heterogeneous populations of EVs with various size, density, and cargo content, whose production and relative distribution change with the physiological state. Bacteria exhibit various types of cell envelope that affect the nature of their EVs. Gram-negative bacteria have an outer membrane (OM) containing LPS and a thin layer of peptidoglycan located in the periplasmic space that is between the outer and inner membranes. In contrast, gram positive bacteria have a single membrane covered with a thick layer of peptidoglycan (Effah et al. 2024; Dauros Singorenko et al. 2017; Kim et al. 2015).

EVs produced by Gram-negative bacteria are mostly derived from the OM and are referred to as outer membrane vesicles (OMVs). The OM 'blebs' outwards and pinches off, forming spherical vesicles containing periplasmic components (Furuyama and Sircili 2021; Schwechheimer and Kuehn 2015) (Figure 1-2).

The limited attention paid to EVs in Gram-positive bacteria was attributed to the assumption that the thick cell wall acts as a physical barrier, hindering the release of EVs into the extracellular space. The release of EVs through the cell wall may be facilitated by the application of post-release pressure from the plasma membrane (Figure 1-2), the presence of cell wall-modifying enzymes released alongside EVs, and the potential transit through channels (Jeong et al. 2022; Brown et al. 2015).

Bacterial EVs play a role in delivering their contents to the recipient bacteria, contributing to cellular communication, biofilm formation (Turnbull et al. 2016; Liao et al. 2014), antibiotic resistance (Rumbo et al. 2011), stress response (Maredia et al. 2012), toxin delivery (Rompikuntal et al. 2012), and nucleic acid transfer (Sjöström et al. 2015).

In addition, bacterial EVs are known to transport their contents to eukaryotic cells and have been associated with pathogenic processes and immune system homeostasis (Muraca et al. 2015; Rakoff-Nahoum, Coyne, and Comstock 2014). Bacterial EVs can cross the mucosal barrier, reach gut mucosal macrophages and initiate intestinal inflammation (Christovich and Luo 2022; Pathirana and Kaparakis-Liaskos 2016; Hickey et al. 2015).

1.3.2 Eukaryotic EVs

EVs produced by human cells are present in various biological fluids, facilitating the delivery of their cargo not only to neighboring cells within the tissue microenvironment and over long distances throughout the bodies of multicellular organisms (Kalra, Drummen, and Mathivanan 2016).

Eukaryotic EVs are usually classified into three main categories, based on their size and mode of production (van Niel, D'Angelo, and Raposo 2018). Microvesicles are formed by outward budding of membrane vesicles from the cell surface (Muralidharan-Chari et al. 2009). Exosomes originate from the endocytic pathway through the 'outward' budding of the late endosomal membrane. Initially, they accumulate in structures known as multivesicular bodies (MVBs), which later fuse with the plasma membrane and release their contents as exosomes into the extracellular space (M. Xu et al. 2023). The third major type of eukaryotic EVs, called apoptotic bodies, is produced by cells undergoing programmed cell death by outward budding from the surface of apoptotic cells (Kakarla et al. 2020) (Figure 1-2).

For cargo transfer, EVs undergo fusion with the membranes of target cells, either directly integrating with the plasma membrane or merging with the endosomal membrane following endocytic uptake. Cells exhibit the ability to internalize EVs through direct fusion and diverse endocytic pathways, including clathrin-dependent endocytosis and clathrin-independent routes such as caveolin-mediated uptake, macropinocytosis, phagocytosis, and lipid raft–mediated internalization (Y.-J. Liu and Wang 2023; Mulcahy, Pink, and Carter 2014).

Owing to variations in their biogenesis processes, subtypes of EVs exhibit changes in composition even when they originate from the same cell (Vagner et al. 2019). Under specific circumstances, specific cell types produce several types of EVs. For example, large oncosomes are produced by cells from advanced cancers (Minciacchi, Freeman, and Di Vizio 2015), and migrasomes are produced during cell migration (Jiang et al. 2023; Ma et al. 2015).

EVs carry a diverse range of cellular components and originate from the packaging of cytoplasmic contents within the membrane-bound vesicles. For instance, EVs harbor numerous proteins, and the presence of these proteins can provide valuable insights into the biogenesis and physiological functions of EVs (Greening et al. 2017). Moreover, encapsulated RNAs within vesicles can significantly influence recipient cells by transferring between different cell types. This transformation may manifest as the production of novel proteins in the case of mRNA transfer or regulation of gene expression by miRNAs (Valadi et al. 2007).

The composition of EVs is not only influenced by the source but also by the methods used for initial isolation or enrichment. Therefore, caution is necessary before attributing specific functions to one type of EV because these functions could potentially arise from other EVs present in the preparation (Sharma et al. 2020; Tkach and Théry 2016; Théry et al. 2006a).

Cell culture supernatants are the most used source of EV isolation (Stam et al. 2021). Fetal calf serum (FCS) is a commonly used supplement in cell culture media because it provides a rich source of nutrients, growth factors, and hormones necessary for cell growth and proliferation. However, its use in EV isolation has been a subject of controversy due to the potential for FCS-derived components to co-isolate with EVs and interfere with downstream applications (Wei et al. 2016; Lehrich, Liang, and Fiandaca 2021). To avoid these concerns, several alternatives to FCS-containing medium have been proposed for EV isolation purposes, including serum-free and EV-depleted FCS medium (Théry et al. 2006b), or using supplements like insulin-transferrin-selenium (ITS) solution (Baxter et al. 2019; Schulz et al. 2020). However, it is recommended to monitor the changes in cell's behaviour and evaluate the

background of the analytes of interest to ensure that the chosen method does not affect EV characteristics (Urzì, Bagge, and Crescitelli 2022).

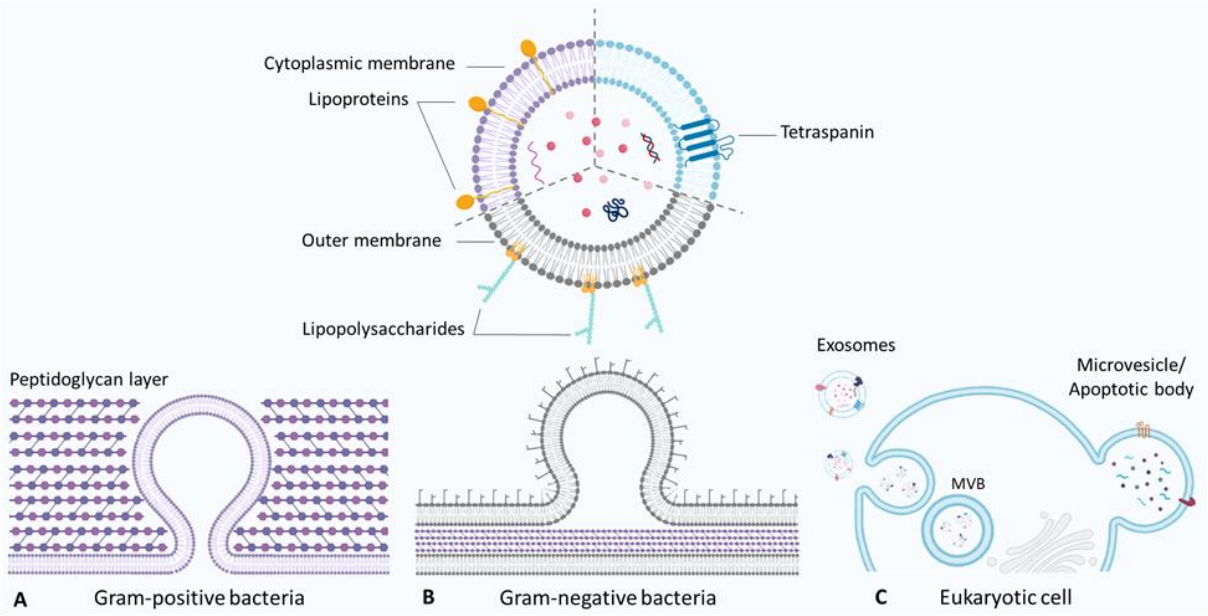

FIGURE 1-2**.** EV secretion from bacteria and eukaryotic cells. Gram-positive bacterial EVs originate from cytoplasmic membrane **A)**, while EVs produced by Gram-negative bacteria derive from the outer membrane **B)**. The process of releasing eukaryotic exosomes contains intracellular trafficking of MVBs, and fusion of MVBs with the plasma membrane. Microvesicles and apoptotic bodies arise from the direct outward budding of the plasma membrane **C)**. Created with BioRender.com.

1.4 Shear stress

Endothelial cells, which line the interior surface of blood vessels, are constantly exposed to the mechanical force exerted by flowing blood. This force, known as shear stress, plays a crucial role in maintaining endothelial cell function and vascular homeostasis (Tun et al. 2019), and modulating host defense (Bastounis et al. 2022). Since most cell culture protocols are designed for static cultures, and experiments with ECs are predominantly conducted under these non-physiological conditions, it is important to develop a model for culturing ECs under flow conditions that more closely mimics their physiological environment.

It is widely recognized that atheroprotective wall shear stress in arteries generally ranges from 10 to 40 dyn cm^{-2} (Ortega Quesada et al. 2024; Tanaka et al. 2021; Roux et al. 2020; Davies 1995). However, shear stress varies across the vasculature in different patterns and influences various cellular processes, including signaling (McQueen and Warboys 2023), gene expression (Rojas-González et al. 2023), and cell morphology (Sun, Zhang, and Xia 2021). Therefore, understanding the effects of shear stress on endothelial cells using experimental models is essential to elucidate the mechanisms underlying vascular health and disease.

2 Aim of thesis

2.1 Aim of chapter one

Bacterial EV-mediated interactions between the microbiome and the host, and their role in the onset of various pathophysiological processes including inflammation and infection have been widely investigated (Luo et al. 2023). While a direct interaction between *E. faecalis* and host cells has been documented, we hypothesized that an interaction between *E. faecalis*-derived EVs and host cells may also contribute to the virulence. Therefore, in the chapter one of this work we aimed to study the interaction of *E. faecalis*-derived EVs with primary human monocyte-derived macrophages (HMDMs) and human umbilical vein endothelial cells (HUVECs) *in vitro*.

2.2 Aim of chapter two

Endothelial cells experience shear stress associated with blood flow. Such shear stress regulates endothelial function by altering cell physiology. EVs produced by endothelial cells contribute to the physiological functions of endothelium. In the second chapter of this thesis, we aim to:

- Apply different media for culturing HUVECs under static and laminar flow to obtain the optimal condition for EV isolation.
- Isolate extracellular vesicles from HUVECs cultured in static and under laminar flow conditions and examine their characteristics.
- Investigate the cargo content of HUVEC-derived EVs to test the hypothesis that endothelial EVs from cells cultured under static versus shear flow conditions differ due to the simulation of physiological conditions, thereby impacting EV-mediated communication.

In addition, since Enterococci are a clinically significant cause of bloodstream infections (Billington et al. 2014; Ubeda et al. 2010; Freedberg et al. 2018), and previous reports suggested bacterial gene expression is affected by mammalian cargo (Shirong Liu et al. 2016; 2019; Santos et al. 2020), we aim to:

- Investigate the effect of endothelial cell-derived EVs on *E. faecalis*.

3 Chapter I

3.1 Materials and Methods

3.1.1 Cell culture

Human umbilical vein endothelial cells (HUVEC) were isolated from fresh umbilical cords from female individuals (Klinikum Saarbrücken, Germany, consent of the Local Ethics Committee, permission no. 131/08) under sterile condition using 0.1 g/l collagenase for digestion (Roche) at 37 °C. To stop the digestion, veins were rinsed with Earle`s medium 199 (PAA, # P04-07500) containing 10% fetal calf serum (FCS) (#F7524, PAA), 100 U/ml penicillin G, and 100 µg/ml streptomycin (#P4333). After centrifugation (10 min, 200 *g*) cells were resuspended in 5 ml endothelial cell growth medium with supplement mix (# C-22010, Promocell) containing 10% FCS, 100 U/ml penicillin G, 100 µg/ml streptomycin, and 0.1% Kanamycin (#K0254, Sigma), and cultivated at 37 °C and 5% CO_2 in a 25 cm^2 cell culture flask. After one day, cells were washed three times with PBS (phosphate buffered saline, 7.20 g/l NaCl, 0.43 g/l KH_2PO_4, 1.48 g/l Na_2HPO_4) and cultivated until confluence. Cells were cryopreserved in passage #1 and used for further experiments.

Monocytes were isolated from buffy coats of healthy blood donors (Blood Donation Center, Klinikum Saarbrücken, Germany) with the consent of the local ethics committee (permission no. 173/18). Peripheral blood mononuclear cells (PBMCs) were isolated by density gradient centrifugation using lymphocyte separation medium 1077 (#C-44010, PromoCell) and LeucoSep tubes (#227290, Greiner). Monocytes were obtained by magnetic cell sorting using anti-CD14 microbeads (#130-050-201, Miltenyi), seeded, and differentiated to human monocyte-derived macrophages (HMDMs) in complete RPMI medium supplemented with 20 ng/ml human recombinant colony-stimulating factor (M-CSF, #130-096-492, Miltenyi) for a duration of 6 days prior to their use in various treatments (Dahlem et al. 2020).

3.1.2 Bacterial culture, extracellular vesicle (EV) isolation and purification

Enterococcus faecalis (DSM 20478, German Collection of Microorganisms and Cell Cultures (DSMZ)) was grown in BHI medium (#53286, Merck) under static condition at 37 °C (Afonina et al. 2021). When reaching confluency (Optical density = 1, at the end of exponential stage), the bacterial culture was centrifuged at 5000 *g* for 15 min at 4 °C to pellet the bacterial cells, then the supernatant was pushed through 0.45 µm bottle top PVDF filters (#6-0039, Neolab) to remove any remaining cell. The sterility of the filtrate was checked *via* overnight incubation of the filtered supernatant on agar plates.

The supernatants were then loaded in 70 ml ultracentrifuge tubes (#355655, Beckman Coulter, Germany) and ultracentrifuged (UC) at 160,000 *g* for 3 hours at 4 °C (rotor SW 45Ti, Optima L-90k, Beckman Coulter, Germany) to obtain the EVs. The supernatants were removed and EV pellets were re-suspended in 100 µl of 0.2 µm filtered (#99255, TPP, Switzerland) phosphate buffered saline (PBS tablets, #D2049.2100, Genaxxon).

Size exclusion chromatography (SEC) was performed to separate the EVs from other proteins and diluents. 5oo µl of EV pellet was loaded on top of a 40 ml column containing Sepharose CL-2B) #17-0140-01, GE Life Science, UK). 45 fractions were collected in 1.7 ml tubes (#MCT-175-A, Axygen, Corning Incorporated, Mexico) by passing the 0.2 µm filtered PBS through the column. Fractions were stored at -80 °C for further use.

3.1.3 EV characterization

3.1.3.1 Bicinchoninic acid (BCA) assay

The protein concentration of the fractions was determined using the bicinchoninic assay kit (BCA) (#QPBCA, QuantiPro™ BCA Kit, Sigma Aldrich) according to the manufacturer's instructions. The samples were analyzed in triplicate using a standard calibration curve generated from bovine serum albumin (BSA).

3.1.3.2 Nanoparticle Tracking Analysis (NTA)

Particle size distribution and yield of EV preparations were analyzed by nanoparticle tracking analyzer (NTA, LM-10, Malvern, UK). 150 µl of diluted sample in 0.2 µm filtered PBS was introduced into a green laser-illuminated chamber to maintain vesicle concentration within the range of 20 –120 particles/frame, and a high-sensitivity video with camera level 13–15 was captured; three videos of 30 s length were recorded and processed by the NanoSight 3.4 software.

3.1.3.3 Cryo-TEM imaging

Purified EVs were subjected to cryogenic transmission electron microscopy (cryo-TEM). In this process, a 5 µl sample was placed onto a holey carbon grid (type S147-4, Plano, Wetzlar, Germany) and allowed to settle for 2 s before being rapidly submerged into liquid ethane at a temperature of -165 °C using a Gatan (Pleasanton, CA, USA) CP3 cryo plunger. The sample was then transferred under liquid nitrogen to a Gatan model 914 cryo-TEM sample holder. Low-dose TEM bright-field imaging was conducted at a temperature of -173 °C using a JEOL (Tokyo, Japan) JEM-2100 LaB6 microscope operating at an accelerating voltage of 200 kV. Images were acquired at a resolution of 1024×1024 pixels using a Gatan Orius SC1000 CCD camera with an imaging time of 4 s and a binning factor of 2.

3.1.4 Cytotoxicity assay

HUVECs and HMDMs were seeded in a 96-well plate at a density of 10,000 and 40,000 cells per well respectively. Both cell types were exposed to varying concentrations of bacterial extracellular vesicles: 1000, 5000, and 10,000 EVs per cell, in 200 µl fresh medium. After 24 hours of incubation, the supernatants were aspirated, and cells were treated with 100 µl 3-(4,5-dimethylthiazol-2-yl)-2,5-diphenyltetrazolium bromide containing medium (0.5 mg/ml in medium) (#M5655, Sigma Aldrich, USA) for 2 hours. Subsequently, the medium was removed, and cells were lysed using 100 µl of DMSO. The absorbance at a wavelength of 560 nm was measured using a microplate reader (GloMax® Discover Multimode Microplate Reader, Promega).

3.1.5 Macrophage morphology analysis

HMDMs were cultured and treated with bacterial EVs as described above. Cells were analyzed for their morphology using the IncuCyte® S3 system cell-by-cell analysis software and grouped based on their eccentricity into either round or elongated shapes (Dahlem et al. 2020).

3.1.6 Bacterial EV labeling

Fluorescent labeling of pelleted EVs obtained through UC was carried out using 2 µl of DiI (#V22885, Vybrant DiI Cell Labeling Solution, Thermo Fisher, Germany) incubated for 30 min at 37 °C. To remove any unincorporated dye, SEC was employed, and the fractions exhibiting the highest fluorescence intensity / protein content were selected for subsequent analysis (Mehanny et al. 2020).

3.1.7 EV uptake study

Primary monocytes were freshly isolated and seeded at a density of 250,000 cells per well in a 24-well plate containing 500 µl fresh medium in each well. HEK-Dual hTLR2 and HEK-Blue hTLR4 cells were both seeded 50,000 and 100,000 cells/well in a 24 well plate with 500 µl medium per well, and HUVECs were seeded at the same density in a 12 well plate with 1 ml medium per well and incubated overnight. After the incubation period, cells were treated with DiI-labeled bacterial EVs (30,000 EV/cell). For measuring EV uptake in TNF-treated HUVECs, cells were seeded 25,000 and 50,000 cells/well in a 12-well plate. The next day, cells were treated with 100 ng/ml TNF for 24 h. DiI-labeled bacterial EVs were added to the pre-stimulated cells (30,000 EVs/cell), either after TNF removal or in the presence of refreshed TNF. To measure the percentage of EV uptake after 24 h and 48 h incubation at 37 °C, cells were washed with PBS and detached using Accutase (#A6964, Sigma Aldrich, Germany). Cells were

centrifuged at 500 *g* for 4 min, and pellets were then re-suspended in PBS containing 2% FCS and used for flow cytometry analysis (LSRFortessa, BD Bioscience, USA).

3.1.8 Gene expression study

HMDMs (250,000 cell/ well in a 24 well plate) and HUVECs (100,000 cell/well in a 24 well plate) were treated with bacterial EVs for 24 h or 48 h (1000, 5000, and 10,000 EVs/cell in 500 µl medium). Three individual donors were used for each cell type. Total RNA was isolated using the Direct-zol™ RNA MiniPrep Kit (#R2052, Zymo Research). Concentration of isolated RNA was quantified by NanoDrop™ (Thermo Fisher Scientific). Equal amounts of RNA were reverse transcribed using the High Capacity cDNA Reverse Transcription Kit (#4368813, Thermo Fisher Scientific) in the presence of RNase inhibitor (#10777-019, Invitrogen) according to the manufacturer's instructions. Amplifications were carried out in 10 µl reaction solutions containing 0.25 µl of each primer, and 2 µl of 5x Hot FIREPol EvaGreen qPCR Mix (#08-24-00020, Solis BioDyne). The primer sequences for each transcript are detailed in supplementary table 1. The PCR was performed in a CFX96 touch™Real-Time PCR detection system (BioRad). Data were normalized to the beta-actin housekeeping gene (*ACTB*).

TABLE 3-1. Primer sequences used for qPCR (10 µM stock)

Gene	Accession number	Primer forward sequence	Primer reverse sequence
ACTB	NM_001101.3	TGCGTGACATTAAGGAGAAG	GTCAGGCAGCTCGTAGCTCT
CCL2	NM_002982.4	TTGATGTTTTAAGTTTATCTTTCATGG	CAGGGGTAGAACTGTGGTTCA
CXCL8	NM_000584.4	GAGAAGTTTTTGAAGAGGGCTGA	GCTTGAAGTTTCACTGGCATCT
ICAM	NM_000201.3	TGACCGTGAATGTGCTCTCC	TCCCTTTTTGGGCCTGTTGT
IL10	NM_000572	CAACAGAAGCTTCCATTCCA	AGCAGTTAGGAAGCCCCAAG
IL1A	NM_000575.5	GCGTTTGAGTCAGCAAAGAAGT	CATGGAGTGGGCCATAGCTT
IL1B	NM_000576.3	GGCTGCTCTGGGATTCTCTT	AGTCATCCTCATTGCCACTGTAA
IL6	NM_000600.5	ACATCCTCGACGGCATCTCA	TCACCAGGCAAGTCTCCTCATT
NOS3	NM_001160109.1	AACCCCAAGACCTACGTGC	CATGGTAACATCGCCGCAGA
TLR2	NM_003264.3	GGAGTTCTCCCAGTGTTTGGT	GCAGTGAAAGAGCAATGGGC
TNF	NM_000594.4	CTCCACCCATGTGCTCCTCA	CTCTGGCAGGGGCTCTTGAT
TSC22D3	NM_004089.3	CATGTGGTTTCCGTTAAGCTGG	AGGATCTCCACCTCCTCTCTC
VCAM	NM_001078.4	TTTGGATAATGTTTGCAGCTTCTCA	CACCTTCCCATTCAGTGGACTA
VEGFA	NM_001171623.1	CGCTTACTCTCACCTGCTTCTG	GGTCAACCACTCACACACACAC

3.1.9 Reporter cells

To determine NF-κB/AP-1 activity and the involved receptor, HEK-Dual hTLR2 cells (#hkd-htlr2ni, Invivogen) and HEK-Blue hTLR4 cells (#hkb-htlr4, Invivogen) expressing secreted embryonic alkaline phosphatase (SEAP) were used. Cells were seeded in 96-well plates at a density of 50,000 cells in 200 µl medium per well, and simultaneously treated with 2000, 1000, or 200 EVs per cell. Ultrapure LPS from *E. coli* K12 (#tlrl-peklps, Invivogen) and Pam_3CSK_4 (#tlrl-pms, Invivogen) were used at a concentration of 10 ng/ml as positive controls for HEK-TLR4 and HEK-TLR2 ells, respectively. After overnight incubation, 20 µl of cell culture supernatant from each well was mixed with 180 µl of QUANTI-Blue Solution (#REP-QB2, Invivogen) and incubated at 37 °C for 30 min. Secreted embryonic alkaline phosphatase (SEAP) activity was measured with a microplate reader (PromegaTM GloMax Plate Reader Madison, WI, USA) at 600 nm (Heinrich et al. 2023).

3.1.10 Flow cytometry

The levels of TLR2 were measured in resting and TNF-treated HUVEC in the same donors that were used for the gene expression study. Cells were seeded at a density of 50,000 and 100,000 cells in 1 ml medium per well in a 12-well plate and incubated overnight. After the incubation period, new media was added to the cells with or without 100 ng/ml TNF (#300-01A, PeproTech). TLR2 was assessed 24 h and 48 h after the media change. Subsequently, cells were washed with PBS and detached with

Accutase. The resulting cellular suspensions were centrifuged at 500 *g* for 4 min and cell pellets were resuspended in 100 µl FACSwash (PBS containing 2% FCS). Each sample was stained with 5 µl of fluorescently labeled antibodies directed against TLR2 (Anti-Hu/Mo CD282 PE, clone T2.5, #12-9024-89, eBioscience) or the respective isotype control (#12-4714-82, eBioscience) on ice in the dark. After 20 min, samples were washed twice with FACSwash buffer and prepared for analysis using flow cytometry (LSRFortessa, BD Bioscience, USA).

3.1.11 Statistics

For HMDMs and HUVECs three individual donors were used. Shapiro-Wilk test was performed to analyze the data distribution. For normally distributed data, means of two groups were compared with Student's t-test. For group analysis, one-way analysis of variance (ANOVA) followed by Dunnett's *post hoc* test was applied to compare every mean with the mean of control group. For data that were not normally distributed, means of two groups were compared by Mann-Whitney test. Means of more than two groups were compared to the control group by Kruskal-Wallis ANOVA followed by Dunn's test. All data are presented as mean ± SD, and $p<0.05$ was considered significant. Data analysis was performed using GraphPad Prism 9 software (GraphPad, USA). $^{*}p<0.05$, $^{**}p<0.01$, $^{***}p<0.001$, $^{****}p<0.0001$.

3.2 Results

3.2.1 EV characterization

EVs were isolated from bacterial cultures at the end of the exponential stage (Figure S1). To purify bacterial EVs and remove impurities, SEC was employed. Among the collected fractions, an EV-rich fraction (number 13, Figure S2) was chosen for further analysis.

NTA revealed an average mean size of 167.7 ± 13.6 nm, mode size of 134.6 ± 6.6 nm, and concentration of $1.067 \times 10^{11} \pm 0.28 \times 10^{11}$ particles per milliliter (Figures 3-1A). The morphology of the EVs was then verified through cryo-TEM, which confirmed their spherical structure (Figure 3-1B).

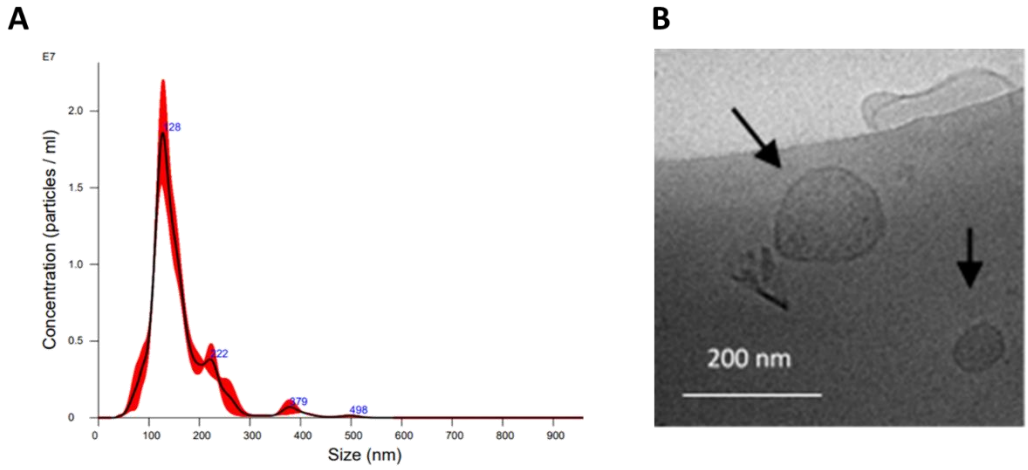

FIGURE 3-1. *E. faecalis* EV characterization. **A)** Representative size distribution of particles in the most concentrated fraction by NanoSight particle tracking analysis. **B)** Representative cryo-TEM image of EVs, scale bar=200 nm.

3.2.2 EVs are not cytotoxic for HMDMs and HUVECs

To investigate the effects of EVs on cell toxicity, MTT assays were performed. For the tested conditions, there was no significant cytotoxicity observed in HMDMs and HUVECs compared to the control (Figure 3-2); therefore, these conditions were used for further investigation.

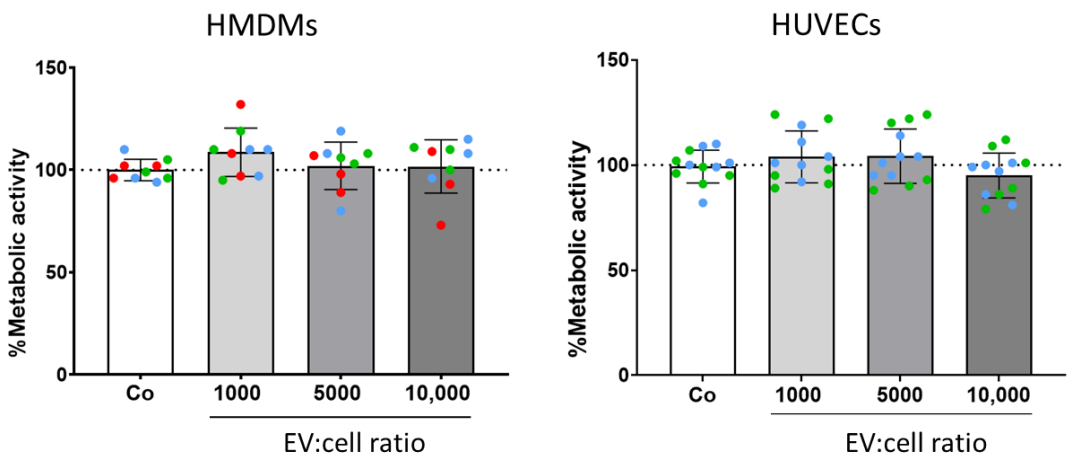

FIGURE 3-2. Metabolic activity of HMDMs and HUVEC cells after 24 h of incubation with EVs remains unchanged. Cells were incubated with EVs (1000, 5000, and 10,000 EVs/cell). Values for

medium-treated cells were used as control (Co). After 24 h of incubation, cell viability was measured by MTT assay. Results are shown as means ± SD of individual donors (indicated with colors) for HMDMs (n=3, triplicates) and two individual donors for HUVECs (n=2, sextuplicates).

3.2.3 HMDMs show inflammatory phenotype after incubation with EVs

Macrophages show different morphology associated with their polarization status with round cells representing an inflammatory phenotype (Rey-Giraud, Hafner, and Ries 2012). Changes in the morphology of HMDMs after EV treatment were analyzed using the Incucyte® system. Our data show that EVs could promote a round shape phenotype after 24 h of incubation in a dose-dependent manner (Figure 3-3).

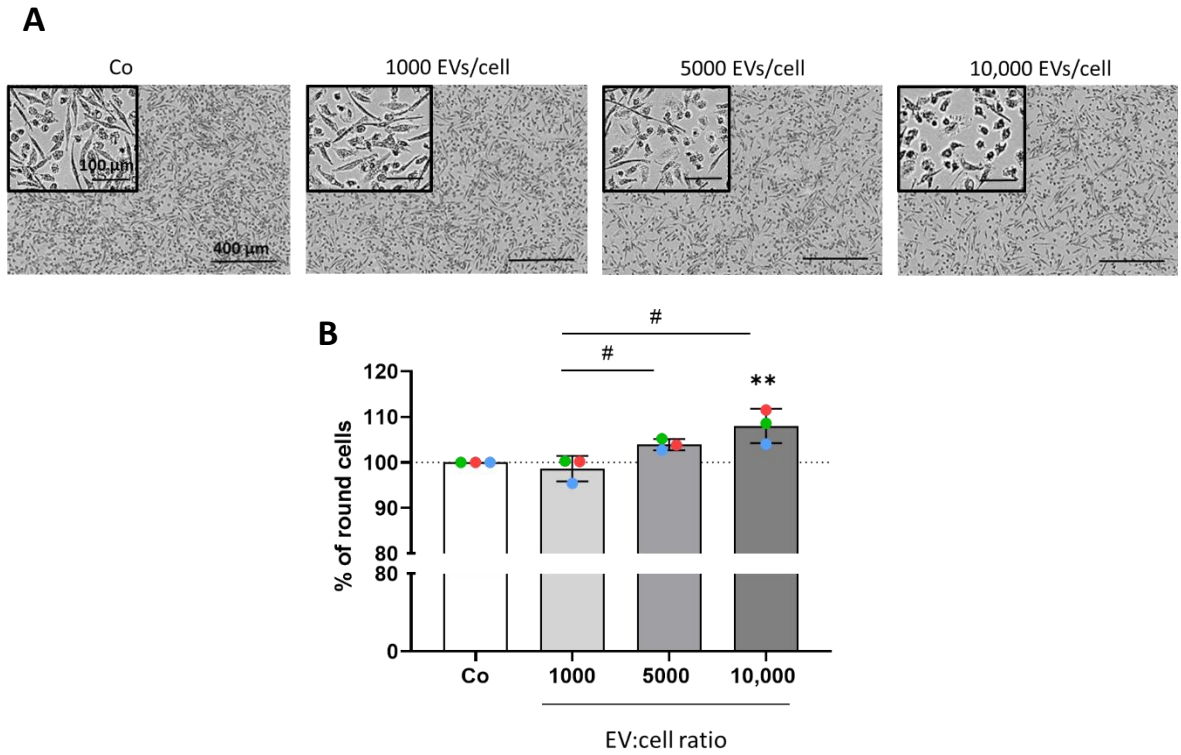

FIGURE 3-3. HMDMs show an inflammatory phenotype after incubation with EVs. **A)** Representative images of macrophages treated with EVs for 24 h. **B)** Percentage of round cells. Data are presented as mean ± SD of three individual donors shown in dots and normalized to medium-treated cells as control (Co). Means of two groups were compared with Student's t-test. For group analysis, one-way analysis of variance (ANOVA) followed by Dunnett's post hoc test was applied to compare every mean with the mean of control group. # shows significant differences between groups. * indicates significant differences compared to the control. $p<0.05$ is considered significant. $^{\#}p<0.05$, $^{**}p<0.01$.

3.2.4 EVs are internalized by HMDMs and HUVECs

To assess whether EVs are taken up by HMDMs and HUVECs, fluorescently labelled EVs were added to the cells. After 24 h, about 90% of primary macrophages had taken up fluorescent EVs (Figure 3-4A), whereas HUVECs demonstrated a less efficient initial uptake. However, this efficiency increased within 48 h, suggesting a gradual enhancement in EV uptake over time (Figure 3-4B).

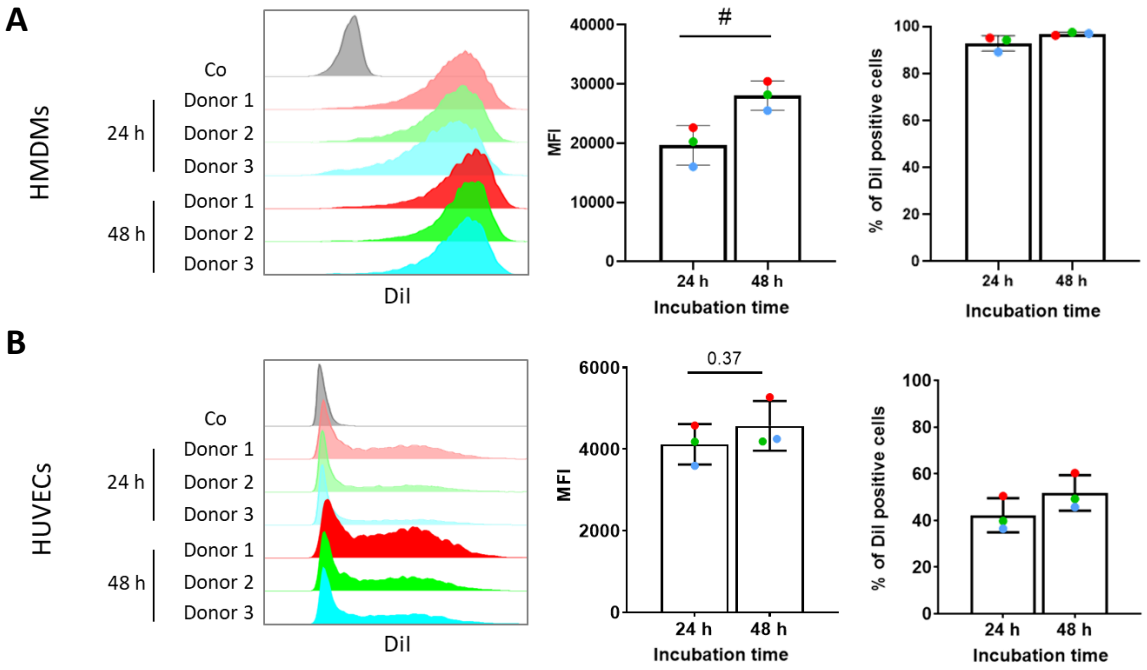

FIGURE 3-4. EVs are internalized into mammalian cells. HMDMs (A) and HUVECs (B) were incubated with DiI-labeled EVs (30,000 EVs/cell) for 24 h and 48 h. Internalization was quantified by measuring phycoerythrin (PE-A) channel fluorescence intensity of three individual donors for each cell type (n=3 individual donors, each). Means of two groups were compared with Student's t-test. # shows significant differences between groups and $p<0.05$ is considered significant. $^{\#}p<0.05$.

3.2.5 EVs modulate HMDM and HUVEC gene expression

The expression of pro- and anti-inflammatory genes was investigated in HMDMs and HUVECs in response to bacterial EVs. The results demonstrated that the gene expression of inflammatory cytokines, such as interleukin (IL)-1α, IL-1β, IL-6, and IL-8 (gene name *CXCL8*) was significantly upregulated in the first 24 h in EV-treated HMDMs in a dose-dependent manner; whereas gene expression of anti-inflammatory IL-10 and glucocorticoid-induced leucine zipper (GILZ, gene name *TSC22D3* (Hahn et al. 2014)) was significantly downregulated compared to the control. The same pattern was observed after 48 h of EV treatment, but to a lower extent (Figure 3-5A, S3). Expression of toll-like receptor 2 (TLR2) mRNA showed a significant increase after 24 h in the group with the highest number of EVs, and this effect persisted even after 48 hours. The expression of tumor necrosis factor (TNF) remained relatively stable, showing a slight increase in the least concentrated group after 24 hours and in the most concentrated group after 48 hours.

In HUVECs we also observed an elevated expression of inflammatory genes and a lower abundance of mRNAs encoding for anti-inflammatory proteins. However, the extent of expression was lower and exhibited variations among individuals (figure 3-5B, S4). Within 24 h, the levels of *TNF*, *IL6*, and *IL1A* mRNA experienced a significant increase in the groups subjected to the highest number of EVs, but these elevations were reduced at later time point. Expression of anti-inflammatory endothelial nitric oxide synthase (eNOS, gene name *NOS3*) and GILZ (*TSC22D3*) was reduced after 24 h, with the effects not lasting for 48 h. Gene expression of monocyte chemoattractant protein-1 (MCP-1, gene name *CCL2*), intercellular adhesion molecule-1 (*ICAM1*) and vascular cell adhesion molecule-1 (*VCAM1*) increased after 48 h, although clear variations were observed in the response of individuals.

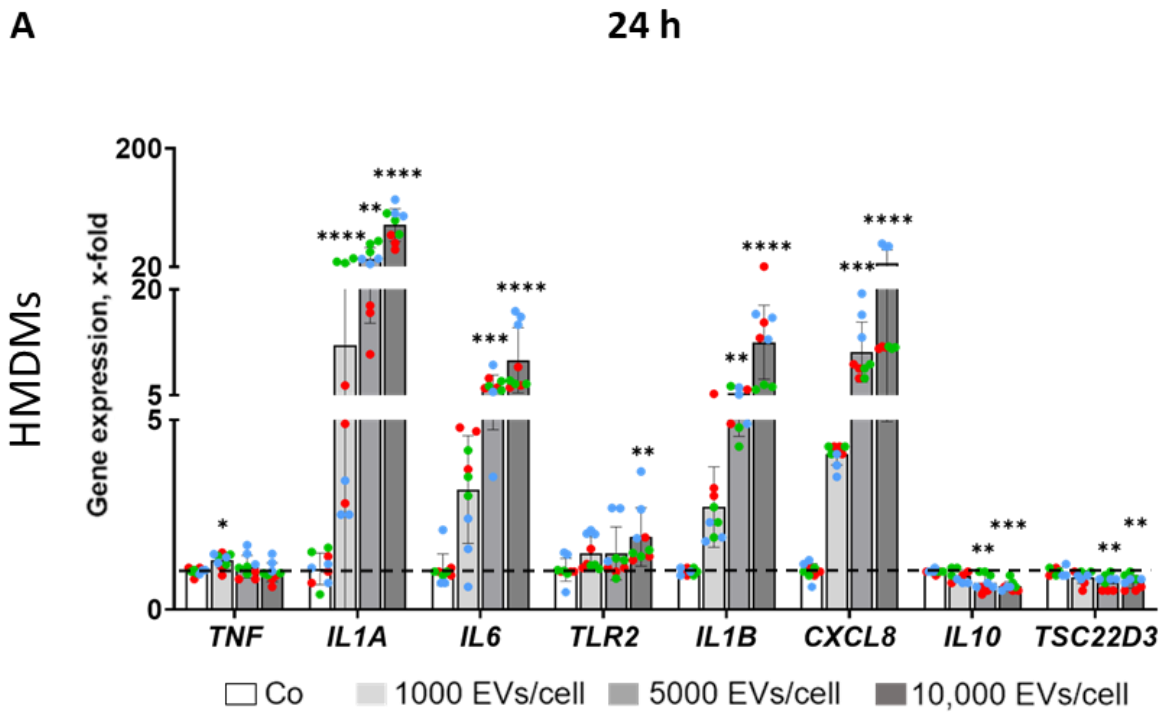
A
24 h
HMDMs
Gene expression, x-fold
200
20
20
5
5
0
TNF
IL1A
IL6
TLR2
IL1B
CXCL8
IL10
TSC22D3
Co
1000 EVs/cell
5000 EVs/cell
10,000 EVs/cell

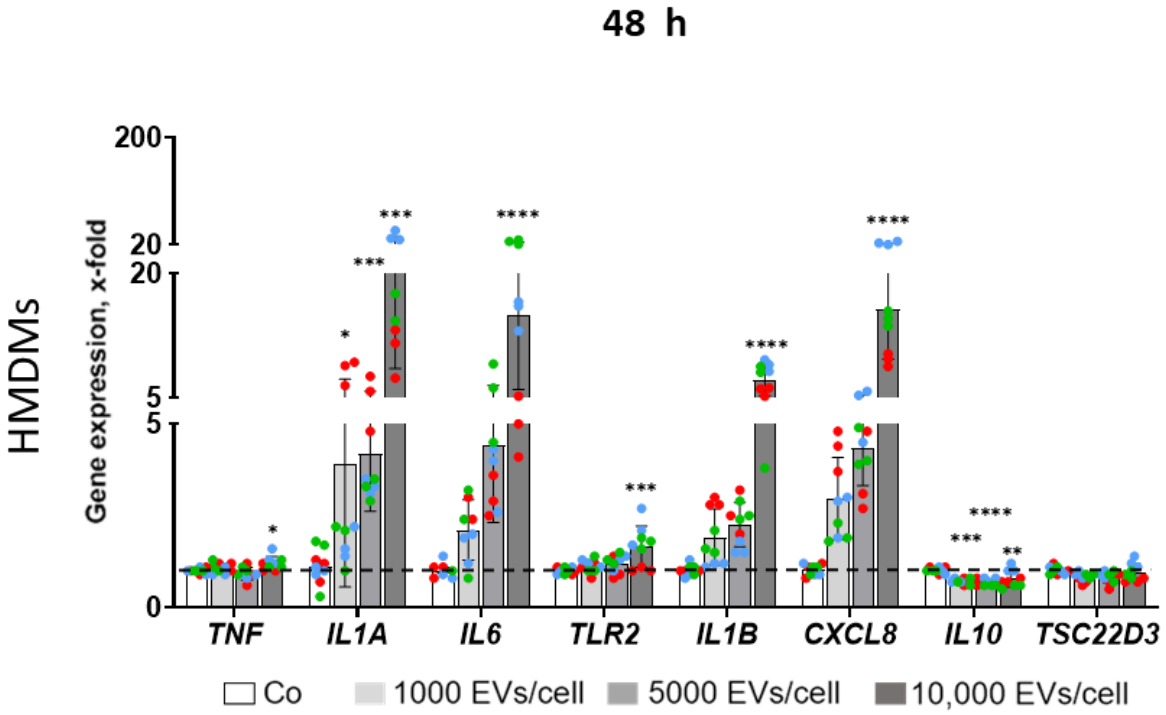
48 h
HMDMs
Gene expression, x-fold
200
20
20
5
5
0
TNF
IL1A
IL6
TLR2
IL1B
CXCL8
IL10
TSC22D3
Co
1000 EVs/cell
5000 EVs/cell
10,000 EVs/cell

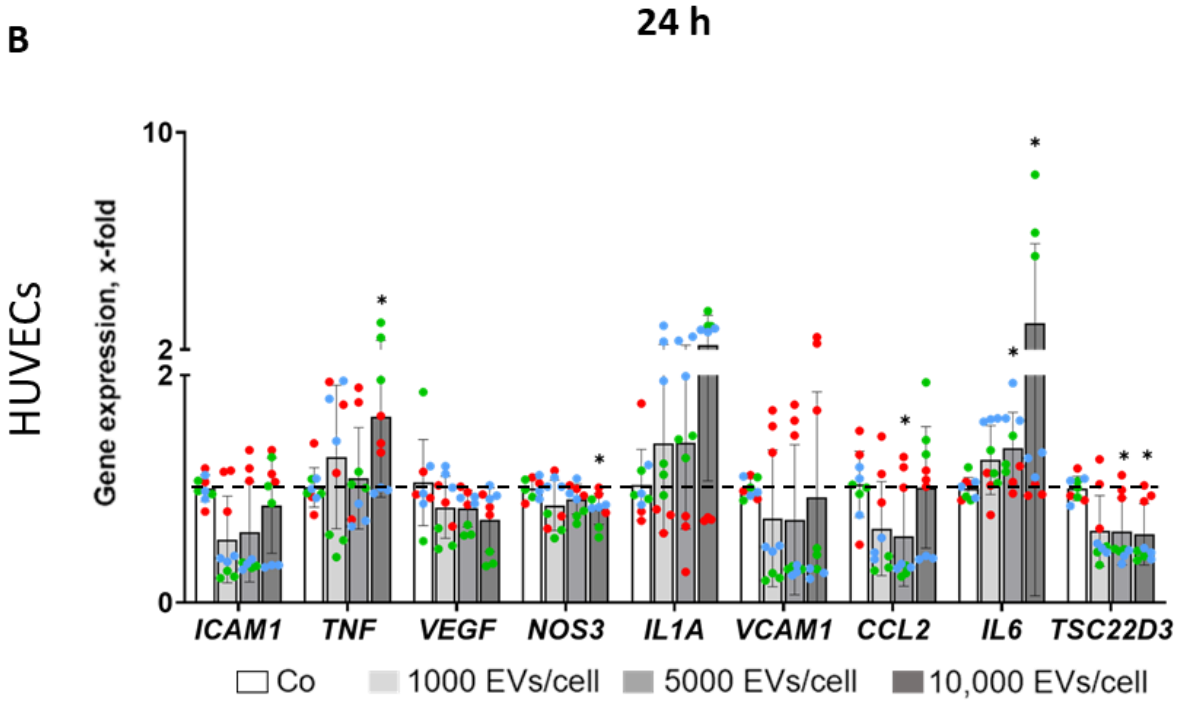
B
24 h
HUVECs
Gene expression, x-fold
10
2
2
0
ICAM1
TNF
VEGF
NOS3
IL1A
VCAM1
CCL2
IL6
TSC22D3
Co
1000 EVs/cell
5000 EVs/cell
10,000 EVs/cell

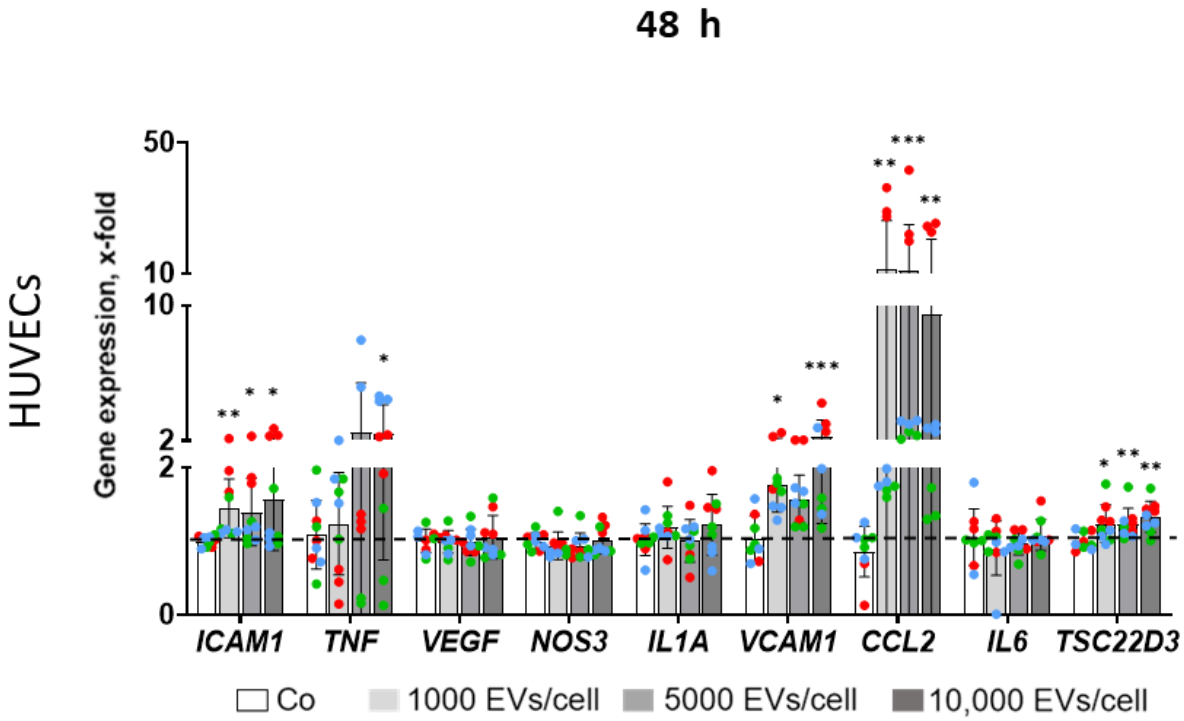
48 h
HUVECs
Gene expression, x-fold
50
10
10
2
2
0
ICAM1
TNF
VEGF
NOS3
IL1A
VCAM1
CCL2
IL6
TSC22D3
Co
1000 EVs/cell
5000 EVs/cell
10,000 EVs/cell

FIGURE 3-5**.** EVs promote pro-inflammatory gene expression in HMDMs and HUVECs. For both cell types three individual donors (n=3, triplicate) were incubated with bacterial EVs at different EV per cell ratios (1000, 5000, and 10,000 EVs/cell) for 24 h and 48 h. Expression levels were analyzed by qPCR using *ACTB* for normalization. Data are shown as the mean ± SD of three individual donors performed in triplicates and normalized to medium-treated cells as control (indicated with a dashed line). Colors belong to each individual donor and dots represent technical replicates. * indicates significant differences compared to the control. p<0.05 is considered significant. *p<0.05, **p<0.01, ***p<0.001, ****p<0.0001.

3.2.6 EVs activate the NF-κB /AP1 pathway through TLR2 signaling

Given the pro-inflammatory activation observed in the gene expression of macrophages upon EV treatment, and considering the involvement of Gram-positive bacterial cell wall components as TLR2 ligands in immune system activation (de Oliviera Nascimento, Massari, and Wetzler 2012; Nguyen et al. 2017), we explored the activation pathway by assessing the NF-κB/AP-1 response in reporter cells exposed to EVs. Our findings indicated a specific dose-dependent activation of HEK-Dual hTLR2 cells (Figure 3-6A), while no response was observed in HEK-hTLR4 cells (Figure 3-6B). Although significantly reduced, the internalization of TLR2 ligand was still recorded in TLR2KO bone marrow–derived DCs (Shen et al. 2014). Therefore, we measured EV uptake in the reporter cells to investigate whether TLR2 affect EV uptake (Figure 3-7). We found that EVs are significantly internalized into HEK-hTLR2 cells after 24 h, while HEK-hTLR4 cells also exhibited EV uptake comparable to their control, the HEK-Blue null cells.

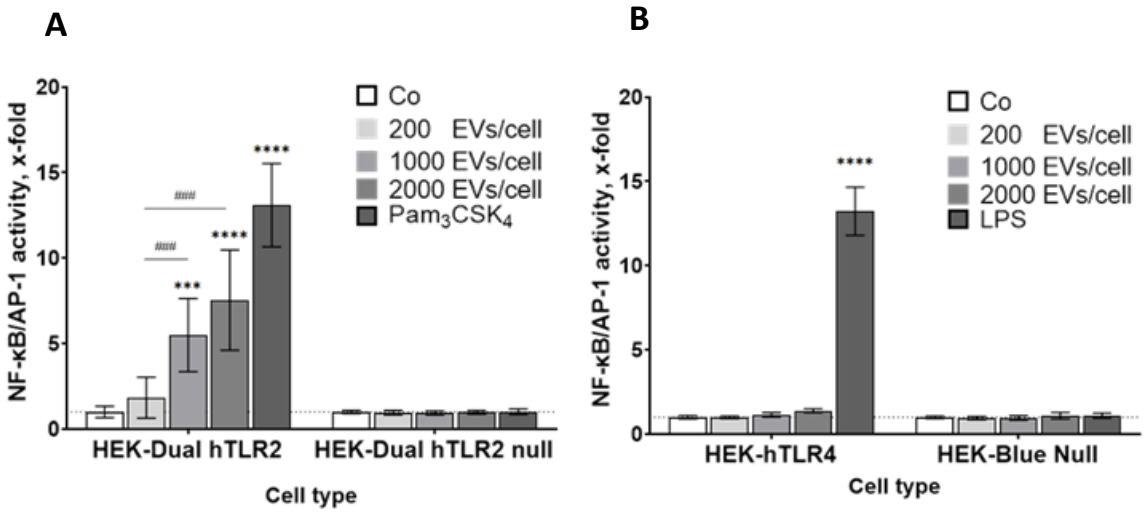

FIGURE 3-6**.** EVs activate the TLR2 pathway. Reporter cells were treated with EVs at concentrations of 200, 1000, and 2000 EVs/cell. Pam_3CSK_4 (TLR2 ligand) and LPS (TLR4 ligand) were used at a concentration of 10 ng/ml as a positive control in **A)** HEK-Dual hTLR2 and **B)** HEK-hTLR4 cells, respectively. The activation of NF-κB/AP-1 was measured as the activity of SEAP and expressed as a fold change of medium-treated cells (indicated by the dashed line). Data are shown as means ± SD of three individual experiments (n=3, triplicate). Means of two groups were compared with Student's t-test. For group analysis, one-way analysis of variance (ANOVA) followed by Dunnett's post hoc test was applied to compare every mean with the mean of control group. # shows significant differences between groups. * indicates significant differences compared to the control. p<0.05 is considered significant. *p<0.05, **p<0.01, ***p<0.001, ****p<0.0001.

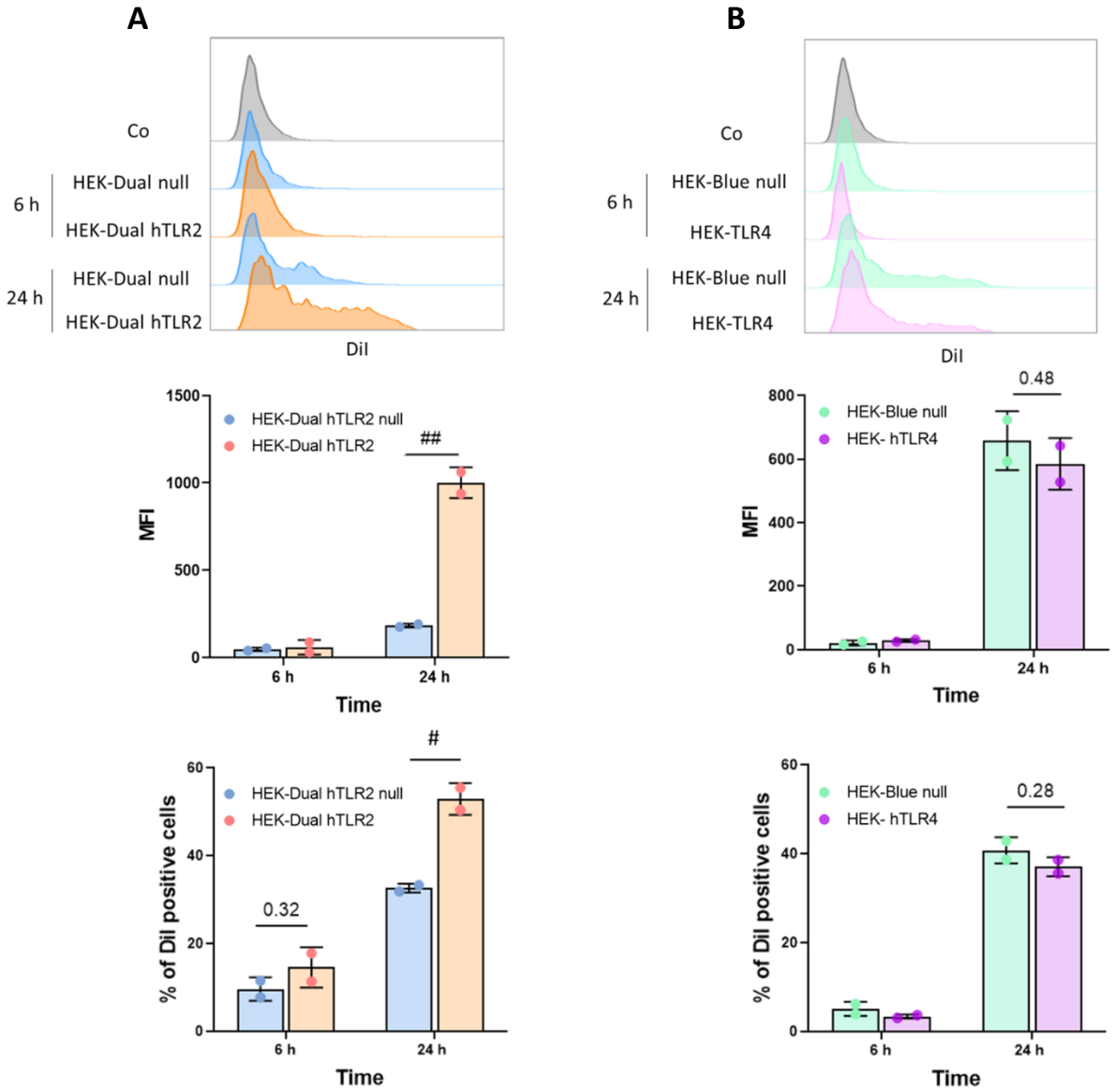

FIGURE 3-7**.** EVs are internalized into reporter cells. Histograms, mean fluorescence intensities (MFIs), and percentage of DiI positive cells of **A)** HEK- hTLR2 and **B)** HEK- hTLR4 cells incubated with DiI-labeled EVs (30,000 EVs/cell) for 6 h and 24 h. Internalization was quantified by measuring phycoerythrin (PE-A) channel fluorescence intensity. Data are represented as mean ± SD (n=2). Means of two groups were compared with Student's t-test. # shows significant differences between groups and $p<0.05$ is considered significant. $^{\#}p<0.05$, $^{\#\#}p<0.01$.

3.2.7 TLR2 expression and EV internalization are elevated in HUVECs upon inflammatory activation

Since we saw a TLR2-dependent uptake and activation for bacterial EVs, we hypothesized that the low responsiveness of HUVECs to EVs is related to their low surface TLR2 content. Furthermore, it has been reported that TLR2 mRNA expression is increased in inflammatory-stimulated HUVECs (Diesel et al. 2012). First, to test this, we measured the levels of *TLR2* mRNA and its protein expression in HUVEC individuals in resting conditions and upon TNF treatment. Our data indicated minimal mRNA and surface protein levels of TLR2 in all HUVEC individuals under baseline conditions (Figure 3-8, S5), which increased following TNF treatment for 24 h. The amounts of surface TLR2 showed a tendency to revert to the baseline level after 48 h when no fresh TNF was added after the first 24 h

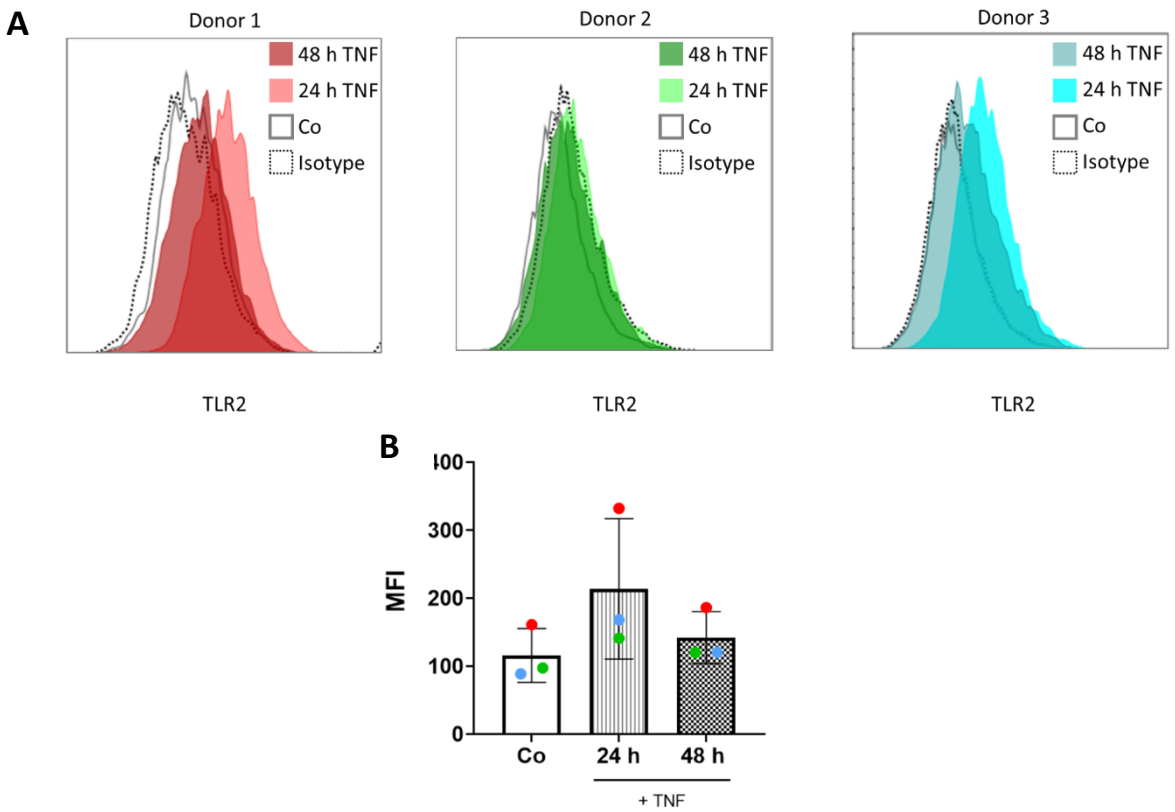

FIGURE 3-8**.** Surface TLR2 is increased in HUVECs after TNF treatment. HUVECs from three individual donors were treated with TNF (100 ng/ml) for 24 and 48 h. Levels of surface TLR2 were quantified by measuring phycoerythrin (PE-A) channel fluorescence intensity. **A)** Histograms. **B)** Mean fluorescence intensities (MFIs). Medium-treated cells were used as control (Co).

Next, we measured EV internalization in stimulated HUVECs upon inflammatory activation by TNF treatment. Our findings indicated that, while there is a donor-dependency in EV uptake, HUVECs consistently exhibited less efficient internalization compared to HMDMs. Inflammatory pre-activation with TNF for 24 h resulted in increased EV uptake at both 24 h and 48 h. The highest uptake was observed in the continuous presence of TNF following the initial 24-hour pre-treatment, i.e., TNF was refreshed daily at the same concentration for an additional 48 h. This uptake pattern correlated with the duration of exposure, as illustrated in Figure 3-9.

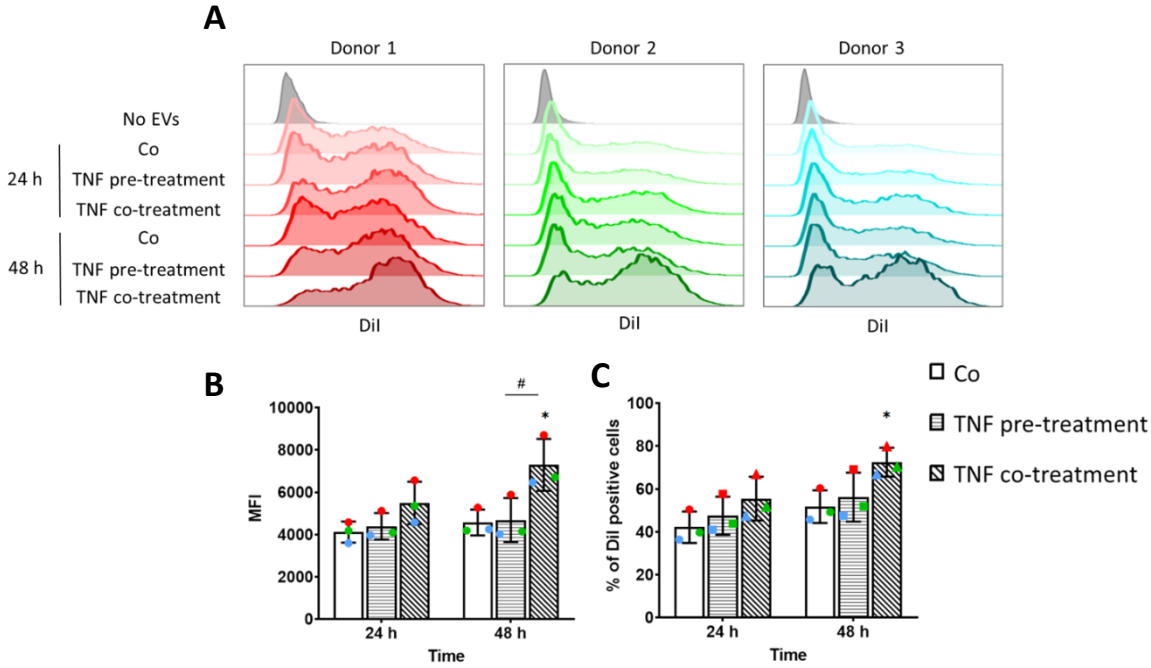

FIGURE 3-9**.** TNF treatment increases EV uptake in HUVECs. HUVECs from three individual donors were pre-treated with TNF (100 ng/ml) for 24 h. Cells were treated with 30,000 EVs/cell in the presence or absence of TNF for 24 and 48 h. Medium-treated cells were used as control (Co). EV uptake was quantified by measuring PE-A channel fluorescence intensity. **A)** Histograms. **B)** Mean fluorescence intensities (MFIs). **C)** Percentage of DiI positive cells. Data are represented as mean ± SD (n=3). Means of two groups were compared with Student's t-test. For group analysis, one-way analysis of variance (ANOVA) followed by Dunnett's post hoc test was applied to compare every mean with the mean of control group. # shows significant differences between groups. * indicates significant differences compared to the control. $p<0.05$ is considered significant. $^{*}p<0.05$.

3.3 Discussion

The interaction between host and microbiome *via* EVs is a widely observed phenomenon. However, Gram-positive bacterial EVs have been less explored in this context, primarily due to the differences posed by their cell wall structure compared to Gram-negative bacteria which argued the existence of EVs from Gram-positive bacteria (Toyofuku, Nomura, and Eberl 2019; Brown et al. 2015). In this study, we have investigated the effect of EVs derived from the opportunistic pathogen *Enterococcus faecalis in vitro* on primary human monocyte-derived macrophages and human umbilical vein endothelial cells isolated from individual donors.

While the number of reports investigating *Enterococcus faecalis*-derived EVs remains limited, similar sizes have been reported for this type of bacterial EVs. In the measurements reported by Costantini et al., non-purified EVs were found to have a mean size ranging from 180 to 210 nm (Costantini et al. 2022). Similar to our data, enterococcal vesicles were described with a particle size range of 50 to 400 nm where Optiprep density gradient fractionation was utilized for purification (Afonina et al. 2021), while our approach involved SEC, which offers a milder process, without compromising EVs' biological activity and integrity (Clos-Sansalvador et al. 2022).

Macrophages constitute a heterogeneous population of host innate immune cells crucial to both health and disease, representing one of the most functionally diverse cells within the hematopoietic system (Shanze Chen et al. 2023). This diversity is underscored by the remarkable plasticity inherent to macrophages, allowing for the development of distinct populations with varying physiological and pathological roles in the face of diverse environmental cues, resulting in mixed population with two contrasting functional extremes: the pro-inflammatory M1 phenotype and the anti-inflammatory M2 phenotype (Shanze Chen et al. 2023; Guilliams and Svedberg 2021). This polarization is reflected in the changes observed in cell shape, with M2 macrophages adopting an elongated form compared to their M1 counterparts (McWhorter et al. 2013). Bacterial EVs affect the inflammatory process by regulating the proportion of M1/M2 macrophages, and the extent of this polarization depends on the bioactive molecules originating from the parental cell and encapsulated within these particles (Dong et al. 2021; Qu, Zhu, and Zhang 2022). While *E. faecalis*-infected murine bone marrow-derived macrophages showed M1-like phenotype (Mohamed Elashiry et al. 2021), our investigation revealed a shift in the polarization of human primary macrophages *in vitro* towards a pro-inflammatory phenotype after incubation with *E. faecalis* EVs. Contradictory to our results, previous findings indicated that EVs from Gram-positive bacteria promote the differentiation of human monocytic THP-1 cells towards anti-inflammatory M2 macrophages. It should be noted that although the utilization of the THP-1 cell line as a human macrophage source is widespread due to its ease of *in vitro* expansion and storage in an undifferentiated state, it might not entirely serve as an ideal model for human primary macrophages (Tedesco et al. 2018; Al-Fityan et al. 2023).

EVs derived from Gram-positive bacteria contain many pathogen-associated molecular patterns (PAMPs) (Bitto et al. 2021). These bacterial ligands in the EVs may interact with specific receptors on host cells and thereby induce inflammatory responses and affect the gene expression profile of the host (Brown et al. 2015). The immunomodulatory effect of *E. faecalis* has been suggested to be due to the activation of NF-kB signaling through lipoprotein-rich EVs in murine macrophages expressing multiple TLRs (Afonina et al. 2021). Since Gram-positive bacterial lipoproteins are recognized by TLR2 (Schenk, Belisle, and Modlin 2009; Drage et al. 2009; Mohammad et al. 2022), we used specific reporter cells to investigate this activation. In agreement with our results, lipoproteins from Gram-positive bacterial EVs were shown to be integral to activate host innate immunity through TLR2 (Bitto et al. 2021; Prados-Rosales et al. 2011), while EVs from mutant bacteria lacking lipoprotein lipidation exhibited deficiencies in TLR2 signaling (Machata et al. 2008). Unlike Gram-negative bacteria, the

pathogenesis of *E. faecalis* is predominantly linked to lipoteichoic acid, a characteristic component in the cell wall structure of Gram-positive bacteria (Park et al. 2013; Ramos, Sansone, and Morales 2021; Guerardel et al. 2020; Hancock, Murray, and Sillanpää 2014). This could explain the lack of activation observed in HEK-hTLR4 cells when exposed to EVs.

We verified the uptake of EVs by HEK-hTLR2 cells, and we observed a clear activation of the NF-κB pathway in a TLR2-dependent manner. Furthermore, we observed internalization of EVs in the absence of TLR2, although no activation of NF-kB pathway was detected. The initiation of the TLR2 pathway activation involves formation of dimers with other co-receptors after ligand recognition (van Bergenhenegouwen et al. 2013). Although signaling requires the presence of the TLR2 receptor, the internalization of the ligand complex still occurred in the absence of TLR2. This was evident when LTA was observed to bind and internalize in HEK/CD14 cells without TLR2 (Triantafilou et al. 2004). CD14-mediated uptake of the ligands was observed when $TLR2^{+}/CD14^{-}$ cells showed less ligand internalization and NF-κB activation (Brandt et al. 2013).

It is worth noting that, in addition to the presence of CD14 in HEK-hTLR4 cells that could potentially contribute to the internalization of EVs, incubation time might also influence the non-specific localization. Shamsul et al. studied the involvement of other receptors in the internalization of TLR2 ligands, where FSL-1 was internalized into peritoneal macrophages from TLR2-deficient mice. It was further shown that CD36 is also responsible for the internalization of TLR2 ligand into HEK293/CD36 transfected cells (Shamsul et al. 2010).

Based on our reporter cell results and given that the interaction between receptors and ligands plays a pivotal role in EV uptake by host cells (Zhou et al. 2020; Torre-Escudero et al. 2019; Rai and Johnson 2019), our attention was directed toward discerning the distinctions in surface molecules between HMDMs and HUVECs to understand the variations in EV internalization and activation of these cells. Since our data suggested a TLR2-dependant response following EV treatment, we aimed to understand whether TLR2 plays a role in ligand internalization and consequently influences activation. Bacterial TLR2 ligands trigger NF-κB-dependent signaling within endosomal compartments in an NF-κB sensitive reporter cell line, even though TLR2 is expressed on the cell surface. The diminished NF-κB activation observed in reporter cells responding to TLR2 ligands, when employing endocytosis inhibitors or immobilizing the ligand implies that the internalization of TLR2 is necessary for NF-κB activation (Brandt et al. 2013).

Surface TLR2 levels vary among different cells (Flo et al. 2001), possibly influencing the extent of receptor interaction with pathogenic molecules, such as EVs. This variability may determine the degree of host activation following exposure to these stimuli. As demonstrated, the observed low levels of surface TLR2 in HUVECs (Shuang Chen et al. 2007), coupled with donor heterogeneity, may underlie the comparatively low EV internalization and activation of these cells in contrast to HMDMs. In addition, the phagocytic nature of the HMDMs might play a role in the rapid EV uptake (Feng et al. 2010).

It is known that septic shock caused by Gram-positive bacteria including *E. faecalis* results in the production and release of pro-inflammatory cytokines (Surbatovic et al. 2015; Zou and Shankar 2016). Earlier research demonstrated that human endothelial cells express higher levels of TLR2 when exposed to inflammatory stimuli (Shuang Chen et al. 2007; Satta et al. 2008). Therefore, we investigated whether this would enhance internalization of Gram-positive bacterial EVs in endothelial cells. Our findings reveal that TNF-stimulated HUVECs exhibited an upregulation of TLR2, and maintaining the cells in a stimulated state while introducing EVs, led to an improvement in EV uptake.

Our study contributed to a deeper understanding of EVs secreted by Gram-positive enterococci and their role in the virulence. We isolated and purified EVs from *E. faecalis*, characterizing them based on morphology, particle size, and concentration. Our results confirmed the internalization of EVs within primary HMDMs, primary HUVECs, and reporter cells *in vitro*. Furthermore, EVs were found to modulate the gene expression of HMDMs and HUVECs towards a pro-inflammatory profile. We observed a TLR2-dependent activation mechanism for EVs. Additionally, our study demonstrated that TLR2 expression and EV internalization are elevated in HUVECs upon inflammatory activation. Future investigations should aim to provide further evidence to validate our *in vitro* findings.

4 Chapter II

4.1 Materials and Methods

4.1.1 Cell culture

Human umbilical vein endothelial cells (HUVECs) were isolated from fresh umbilical cords from female individuals (Klinikum Saarbrücken, Germany, consent of the Local Ethics Committee, permission no. 131/08) under sterile condition using 0.1 g L^{-1} collagenase for digestion (Roche) at 37 °C. To stop the digestion, veins were rinsed with Earle`s medium 199 (PAA, # P04-07500) containing 10% FCS (#F7524, PAA), 100 U ml^{-1} penicillin G, and 100 µg ml^{-1} streptomycin (#P4333). After centrifugation (10 min, 200 g) cells were resuspended in 5 ml endothelial cell growth medium with supplement mix (# C-22010, Promocell) containing 10% FCS, 100 U ml^{-1} penicillin G, 100 µg ml^{-1} streptomycin, and 0.1% kanamycin (#K0254, Sigma), and cultivated at 37 °C and 5% CO_2 in a 25 cm^2 cell culture flask. After one day, cells were washed three times with PBS (phosphate buffered saline, 7.20 g L^{-1} NaCl, 0.43 g L^{-1} KH_2PO_4, 1.48 g L^{-1} Na_2HPO_4) and cultivated until confluence. Cells were cryopreserved in passage #1 and used for further experiments.

4.1.2 Laminar flow

In this work, two different systems were used to generate laminar flow. A parallel plate flow chamber, which not only provided morphological monitoring of the cells, also was suitable for preliminary experiments in a small scale; and a hollow fiber cartridge for cell culture in a larger scale for EV isolation. Details are mentioned bellow:

To assess morphology, viability, immunofluorescence, and gene expression analysis of flow cultures, the following system was utilized as described previously (Hahn et al. 2014) with minor modifications:

Sterilized glass slides (76 x 26 x 1 mm, Roth) were incubated for 30 min in 3 ml collagen (#11179179001, Roche) (50 µg ml^{-1} in 0.2% acetic acid) in 4-well plates. Then, slides were washed with PBS and after drying for 30 min, cells were seeded onto the glass slides. HUVEC-seeded slides were incorporated into the parallel plate flow chambers **(**Figure 4-1A**)**. The chambers were then linked to a peristaltic pump (403U/VM purple/white, Watson Marlow), and filled with different media (Figure 4-1B). Laminar flow rates were regulated to fit a shear stress of 20 dynes cm^{-2} and the flow was unidirectional.

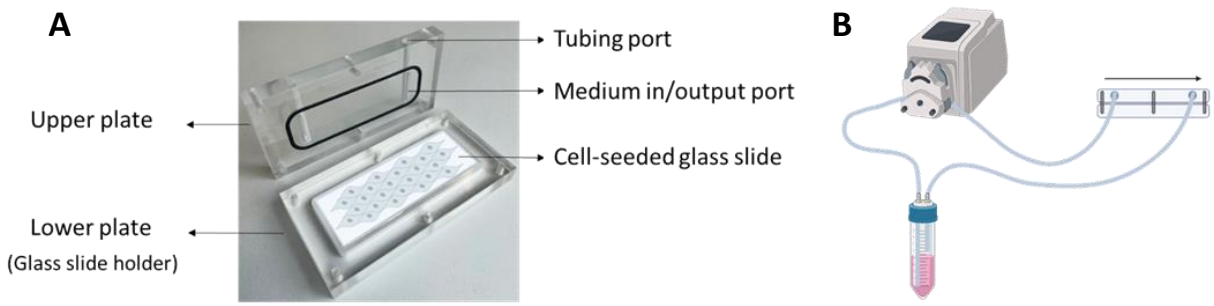

FIGURE 4-1. **A)** One parallel plate flow chamber with cell-seeded glass slide. **B)** Schematic illustration of seeded glass slide connected to the peristaltic pump.

The medium flow rate determines the degree of laminar shear stress. To calculate the flow rate (Q) for reaching the shear stress (τ) of 20 dynes cm^{-2}, the following formula was used:

$$\tau = \frac{6Q\mu}{bh^2}$$

τ = shear stress (dynes cm^{-2})

Q = flow rate (cm^3 s^{-1})

μ = viscosity (0.01 dynes s cm^{-2}) (Frangos, McIntire, and Eskin 1988)

b = channel width (1.9 cm)

h = channel height (= thickness of the middle part of the chamber (1.15 mm) – thickness of the glass slide).

A hollow fiber cartridge (#C2025, FiberCell system) with the FiberCell Systems Duet Pump(Walsby et al. 2014) was used to culture HUVECs for EV isolation experiments **(**Figure 4-2**)** (Ebrahim et al. 2019). Prior to loading the HUVECs into the cartridge, the following preparations were performed according to the manufacturer's instructions.

1. Activation: fibers were activated by injecting 70% absolute ethanol using a luer-lock syringe (#EP97.1, B. Braun, Germany). After ethanol being in contact with the fibers for at least 1 min, excess ethanol was drained, and fibers were rinsed with sterile water.

2. Coating: 1 mg ml^{-1} collagen was injected into the fibers (5-10 ml) and incubated for 30 min. Then the fibers were washed by injecting PBS.

3. Calibration: complete medium was circulated through the fibers for 1 h at 37 °C with degree 10 on the pump, while the extra capillary space was filled with complete medium as well.

4. Seeding was performed according to manufacturer’s instructions.

Laminar flow rates were set to achieve a shear stress of 20 dynes cm^{-2} according to the following formula provided by the manufacturer:

$$\tau = \frac{4Q\eta}{\pi R^3}$$

τ = shear stress (dynes cm^{-2})

Q = fluid flow rate (ml s^{-1}) (per fiber)

η = viscosity (dyne s cm^{-2})

R= internal radius (0.07 cm)

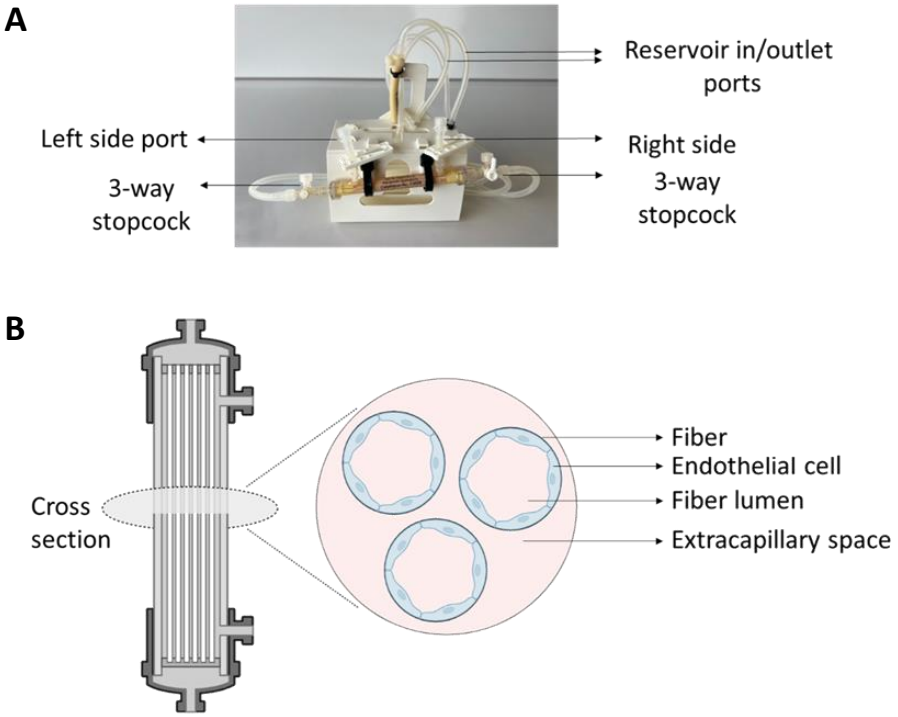

FIGURE 4-2. **A)** One individual cartridge and tubing. **B)** Schematic illustration of the cartridge and its cross section.

4.1.3 Morphological assessment

HUVECs were seeded at 200,000 cells per well in a 6 well plate (2 ml medium per well), and 500,000 cells per sterilized glass slide (76 x 26 x 1 mm, Roth) in a 4 well plate (4 ml medium per well). Cells were incubated overnight to attach. The next day, old medium was removed and replaced with the test medium **(**Table 4-1**)** after PBS wash. Cells were incubated for 72 h under static conditions or under 20 dynes cm^{-2} shear flow. Cells under static culture were imaged with an Incucyte® S3 system every 24 h to monitor morphological changes. Cells under flow condition were imaged with a digital camera (Cannon EODS 400D) attached to a Zeiss AXIOVERT 40 CFL inverted microscope before and after starting the flow.

TABLE 4-1**.** Media options.

10% FCS medium (Co)	# C-22010, Promocell containing 10% FCS (#F7524, PAA)
Endopan medium	# P04-0065K, PAN-Biotech
EGM™ BulletKit™ (Lonza)	# CC-3162, Lonza
ITS solution	# 41400045, Gibco™

4.1.4 Immunofluorescence staining

HUVEC-seeded slides were cut with a glass cutter after the incubation time with different media under laminar flow and used for staining. For static culture, 50,000 HUVECs were placed in each well of an 8 well ibidi slide that was coated with 300 µl of 50 µg ml^{-1} collagen. The cells were then incubated overnight before being washed with PBS and exposed to different media for 72 hours. Following this, the cells were washed with 300 µl PBS and fixed with 300 µl of 1% warm paraformaldehyde (PFA) for 15 min at room temperature. The cells were then washed again with PBS and permeabilized by incubating for 10 min in 300 µl of 0.1% Triton X-100. The cells were subsequently washed with PBS

and blocked with blocking buffer (#MB-070, Rockland) for 30 min. 300 µl medium containing antibodies against actin (#P1951, Sigma) and von Willebrand Factor (vWF) (2 µl per well) (#AHP062F, AbD Serotec) was used to stain the cells for 40 min. Excess antibodies were removed by washing the cells with the same blocking buffer; after which the cells were incubated for 10 min with 300 µl of 1µg ml^{-1} Hoechst 33342 (#62249, Thermo Fisher) to stain the nucleus. HCT116 cells were used as negative control. Finally, the cells were observed under a fluorescence microscope (Leica SP8 Inverted Scanning Confocal Microscope).

4.1.5 Gene expression

Total RNA was isolated using the Direct-zol™ RNA MiniPrep Kit (#R2052, Zymo Research). The concentration of isolated RNA was quantified by NanoDrop™ (Thermo Fisher Scientific). Equal amounts of RNA were transcribed using the High Capacity cDNA Reverse Transcription Kit (#4368813, Thermo Fisher Scientific) in the presence of an RNase inhibitor (#10777-019, Invitrogen) according to the manufacturer's instructions. qPCR was performed using a 5xHotFirePol EvaGreen qPCR Mix (#08-24-00020, Solis BioDyne) and a total volume of 20 µL. The primer sequences for each transcript are detailed in Table 4-2. For each primer pair, an annealing temperature of 60 °C was used (except NOS3 with 62 °C annealing temperature). The PCR was performed in a CFX96 touch™Real-Time PCR detection system (BioRad). Data were normalized to the beta-actin housekeeping gene (*ACTB*).

TABLE 4-2. Primer sequences used for qPCR (10 µM stock).

Gene	Accession number	Primer forward sequence	Primer reverse sequence
ACTB	NM_001101.5	TGCGTGACATTAAGGAGAAG	GTCAGGCAGCTCGTAGCTCT
ICAM	NM_000201.3	TGACCGTGAATGTGCTCTCC	TCCCTTTTTGGGCCTGTTGT
KLF2	NM_016270.2	AGACCACGATCCTCCTTGAC	AAGGCATCACAAGCCTCGAT
NOS3	NM_001160109.1	AACCCCAAGACCTACGTGC	CATGGTAACATCGCCGCAGA
TSC22D3	NM_004089.3	CATGTGGTTTCCGTTAAGCTGG	AGGATCTCCACCTCCTCTCTC

4.1.6 Sex determination of HUVECs

HUVECs were lysed after mixing with 1 µl of Proteinase K (#03115836001, Roche), 5 µl of 10x Taq Buffer (#E00007, Genscript), and 44 µl of water (#A7398, AppliChem) to a total volume of 50 µl. The mixture was then incubated in a heating block set to 55 °C for 60 min at 1500 rpm, followed by 95 °C for 15 min. qPCR was performed as previously described. The primer sequences are detailed in Table 4-3.

TABLE 4-3. Primer sequences used for HUVEC sex determination (10 µM stock).

Gene	Accession number	Primer forward sequence	Primer reverse sequence
RPS4Y1	NM_001008.4	TTTGCTCATGATTTTGGCACTGT	TCCACAAAAGAATGCCGTCCT
RPS4X	NM_001007.5	CAGTGATTAAGTTCTCAGGCAGG	CTTAACAGGGCAGAGGGGTC

4.1.7 EV isolation

To prepare EV-depleted FCS, 30% FCS-containing medium was ultracentrifuged at 100,000 *g* for 18 h at 4 °C, followed by collecting half of the supernatant and filtering through a 0.2 µm stericup filter (Merck Millipore, Germany). The flow-through was used to prepare 2% EV-depleted medium. For each biological replicate, 3 individual female HUVECs were mixed when thawing the cryo tube from -80 °C and let grow until confluency. For static culture, cells were seeded into three T75 flasks with 10^6 cells per flask. The next day, old medium was removed and cells were incubated in 25 ml 2% EV-depleted FCS medium (Promocell) for 48 hours. For flow condition, HUVECs in three T75 flasks were

trypsinised and injected (using a luer-lock syringe) into a collagen-coated hollow fiber cartridge according to the protocol. Cells were let to attach overnight with the 100 ml complete medium flowing through ECS with degree 5 on the duet pump. The next day, medium in the reservoir bottle was refreshed with complete medium and the direction of flow was connected through the fibers on the cells. The flow was set to 5 overnight. The next day medium was replaced with fresh medium, and the flow was increased from 5 to 25 degree gradually from morning to afternoon. The cells were incubated for 48 h under laminar flow (20 dynes cm^{-2}). After the incubation time, conditioned media were collected and centrifuged for 10 min at 300 *g* at 4 °C to remove remaining cells and debris. The supernatant was subjected for 30 min to 10,000 *g* at 4 °C to remove larger particles. EVs were isolated by ultracentrifuging for 4 h at 100,000 *g* at 4 °C using a 45Ti rotor (Beckman). Due to limitations in EV purification methods, such as sample loss, sample dilution and re-concentration, the EV pellets were not further purified in this work.

4.1.8 Nanoparticle Tracking Analysis

Particle size distribution and yield of EV preparations were analyzed by nanoparticle tracking analyzer (NTA, LM-10, Malvern, UK). Preparations of EVs were diluted in 0.22 µm filtered PBS before the analysis. A 500 µl diluted EV sample was introduced into a green laser-illuminated chamber to maintain vesicle concentration within the range of 20 –120 particles/frame, and a high-sensitivity video with camera level 13–15 was captured; three videos of 30 s length were recorded and processed by the NanoSight 3.1 software.

4.1.9 Cryo-TEM imaging

Cryogenic transmission electron microscopy (cryo-TEM) was performed on EV pellets after ultracentrifugation. Three to four microliters of the sample were dropped onto a holey carbon grid (type S147-4, Plano, Wetzlar, Germany) and plotted for 2 s before plunging into liquid ethane at T= −165 °C using a Gatan (Pleasanton, CA, USA) CP3 cryo plunger. The sample was transferred under liquid nitrogen to a Gatan model 914 cryo-TEM sample holder and analyzed at −173 °C by low-dose TEM bright-field imaging using a JEOL (Tokyo, Japan) JEM-2100 LaB6 at 200 kV accelerating voltage. Images with 1024 × 1024 pixels were acquired using a Gatan Orius SC1000 CCD camera at 2 s binning and 4 s imaging time.

4.1.10 Western blot

The EV pellets were lysed with Laemmli lysis buffer (50 mM Tris-HCl, 1% SDS, 10% glycerol, and 0.004% bromophenol blue). HUVECs were also harvested in the same lysis buffer containing 1% protease inhibitors. Samples were boiled for 9 min in 95 °C before loading to the gel. The presence of EV markers was studied by loading equal volumes of samples subjected to 10% sodium dodecyl sulfate-polyacrylamide gel electrophoresis (SDS-PAGE) for 20 min at 90 V. Then the voltage was increased to 110 V for another 45 min. Proteins were transferred to polyvinylidene difluoride (PVDF) membrane (#88518, ThermoFisher), under 250 mA for 75 min in 4 °C. Following 1 h incubation in blocking buffer (#MB144 070, Rockland) membranes were probed with primary antibodies for CD9 (1:1000, #MA1-80307, Thermofischer) and CD63 (1:1000, #sc-5275, Santa Cruz) overnight at 4 °C. Membranes were washed three times with PBS-0.05% Tween 20 and incubated in the dark with IRDye 800 CW goat anti-mouse (1:10,000, Li-COR Biosciences) for 1 h. The blots were then washed three times for 5 min. Bound antibody was visualised by scanning the membrane with an Odyssey Infrared Imaging System (Li-COR Biosciences) in 800 nm channel. All blots were cut in order to detect several proteins on the same blot.

4.1.11 Zeta potential

The surface charge of isolated EVs was measured in triplicates for each batch by DLS using the Zetasizer nano-ZS (Malvern instruments, Malvern). All samples were diluted 1:500 in 0.22 µm filtered PBS before measurements.

4.1.12 Small RNA library preparation

The library was prepared from static and flow EVs and their parental HUVECs, each in three biological replicates, while each biological replicate was a mix of three individual female donors (EVs from this preparation were used for proteomics and bacterial gene expression studies as well). RNAs from EVs and cells were isolated using the miRNeasy Serum/Plasma kit (#217184, Qiagen) and Direct-zol™ RNA MiniPrep Kit (#R2052, Zymo Research) respectively, according to the manufacturer's protocols. RNA concentration was quantified by Nanodrop spectrometer (ThermoFisher Scientific, USA) at 260 nm. Small RNA libraries were prepared according to the MGIEasy small RNA library preparation kit (#1000005269, China). The final small RNA libraries were sequenced by MGI Tech (China).

Fastq sequencing files were analyzed using miRMaster's pipeline with default parameters as previously described (Fehlmann et al. 2021) and using miRbase as reference (release 22.1). As an output, miRMaster generated a list with the expression of all mapped miRNAs. Using the integrated Differential Expression and Pathway Analysis (iDEP) web platform (Ge, Son, and Yao 2018), raw reads were normalized to transcripts per million (TPM) of miRNA mapped reads, and differentially expressed miRNAs were calculated based on TPM values with a threshold of false discovery rate (FDR) < 0.05 and fold-change ≥ 1.5.

4.1.13 Proteomics

EVs from three independent preparations were analyzed. Eighty-eight micrograms of EV protein were precipitated by trichloroacetic acid (TCA) precipitation with an end concentration of 20% TCA. Samples were washed thrice with acetone. After a final centrifugation of 15 min in a SeedVac Plus concentrator (Savant, Thermo Fisher, Waltham, USA), samples were resuspended in 2x Laemmli buffer (4% SDS, 20% glycerol, 120 mM Tris-HCl (pH 6.8), 0.02% bromophenol blue in Millipore water) and denatured at 95 °C for 5 min. Proteins were separated on NuPAGE® 4-12% gradient gels (ThermoFisher Scientific, Karlsruhe, Germany) until the bromophenol dye front reached the center of the gel. Proteins were fixed in the presence of 10% acetic acid /40% ethanol and visualized with colloidal Coomassie stain (10% (v/v) phosphoric acid, 10% (w/v) ammonium sulfate, 20% (v/v) methanol, and 0.12% (w/v) Coomassie G-250). Six gel pieces were cut/ cell lysate, washed, reduced, carbamidomethylated, and trypsin digested as described before (Fecher-Trost et al. 2013). After extraction, 6 µl of tryptic peptides were analyzed by data-dependent nano-LC-ESI-HR-MS/MS analysis using the instrument setup: Ultimate 3000 RSLC nano system equipped with an Ultimate3000 RS autosampler and Nanospray Flex NG ion source coupled to an Orbitrap Eclipse Tribrid mass spectrometer (Thermo Scientific, Germany). Peptides were separated with a gradient generated with buffer A (water and 0.1% formic acid) and buffer B (90% acetonitrile and 0.1% formic acid) at a flow rate of 300 nl/min: 0-5 min 4% B, 5-80 min to 31% B, 80-95 min to 50 % B, 95-100 min to 90% B, 100-105 min hold 90% B, 105-106 min to 4% B and 106-120 min to 4 % B. Peptides were trapped on a C18 trap column (75 µm × 2 cm, Acclaim PepMap100C18, 3 µm,) and separated on a reverse phase column (nano viper Acclaim PepMap capillary column, C18; 2 µm; 75 µm × 50 cm,). The effluent was sprayed into the mass spectrometer using a coated emitter (PicoTipEmitter, 30 µm, New Objective, Woburn, MA, USA, ionization energy: 2.4 keV). MS1 peptide spectra were acquired using the Orbitrap analyzer (R= 120k, RF lens=30% m/z=375-1500, MaxIT: auto, profile data, intensity threshold of 104). Dynamic exclusion of the 10 most abundant peptides was performed for 60 seconds. MS2 spectra were collected in the linear ion trap (isolation mode: quadrupole, isolation window: 1.2, activation: HCD, HCD collision energy: 30%, scan rate: fast, data type: centroid).

Peptides and fragments were analyzed using the MASCOT algorithm and TF Proteome Discoverer (PD) 1.4 software (ThermoFisher, Waltham, USA). Therefore, peptides were matched to tandem mass spectra by Mascot version 2.4.0 by searching of a SwissProt database (2021_05, number of protein sequences

for all taxonomies: 564.638, for taxonomy human: 20.397). Peptides were analysed with the following mass tolerances: peptide tolerance: 10 ppm, fragment tolerance: 0.7 D. The workflow included tryptic digest and up to two missed cleavage sites. Cysteine carbamidomethylation was set as a fixed modification and deamidation of asparagine and glutamine, acetylation of lysine and N-term and oxidation of methionine were set as variable modifications. The PD output files were loaded in the software Scaffold (5, Proteome SoftwareInc., Portland, OR, USA). The identification of two unique peptides per protein was set as the minimum for protein identification.

4.1.14 Bacterial culture

Enterococcus faecalis cryo stock was provided from german collection of microorganisms and cell cultures (DSMZ) (#20478). For long term storage the bacterial stock was stored at -80 °C. As a standard growth medium for *E. faecalis*, BHI (#53286, Sigma) was used. Thirty-seven g of the powder was dissolved in 1 L of distilled water. Another batch was also prepared with the addition of 1.5% Agar and autoclaved before use. The BHI Agar plates were poured into petri dishes and stored at 4 °C.

The bacteria from freezing stock was streaked on the agar plates with a sterile inoculation loop and incubated overnight. One colony from the agar plate was put into 10 ml liquid BHI in a 15 ml falcon and incubated overnight at 37 °C. Then, a new 10 ml bacterial culture was initiated with OD=0.1 and incubated to reach OD=1.

4.1.15 Calculating CFU/ml of bacteria

To obtain the number of bacterial cells when the culture is confluent (optical density (OD) at 600 nm= 1), the colony forming unit (CFU) per one ml of culture was calculated. To do so, 1:10 dilutions were prepared from the confluent culture and 100 µl of each dilution was placed on a BHI Agar plate and incubated overnight. The one plate with 30-300 colonies was choose to calculate the initial culture concentration using the following formula:

$$\mathrm{CFU/ml} = \frac{\text{number of colonies} \times \text{dilution factor}}{\text{volume put on Agar plate}}$$

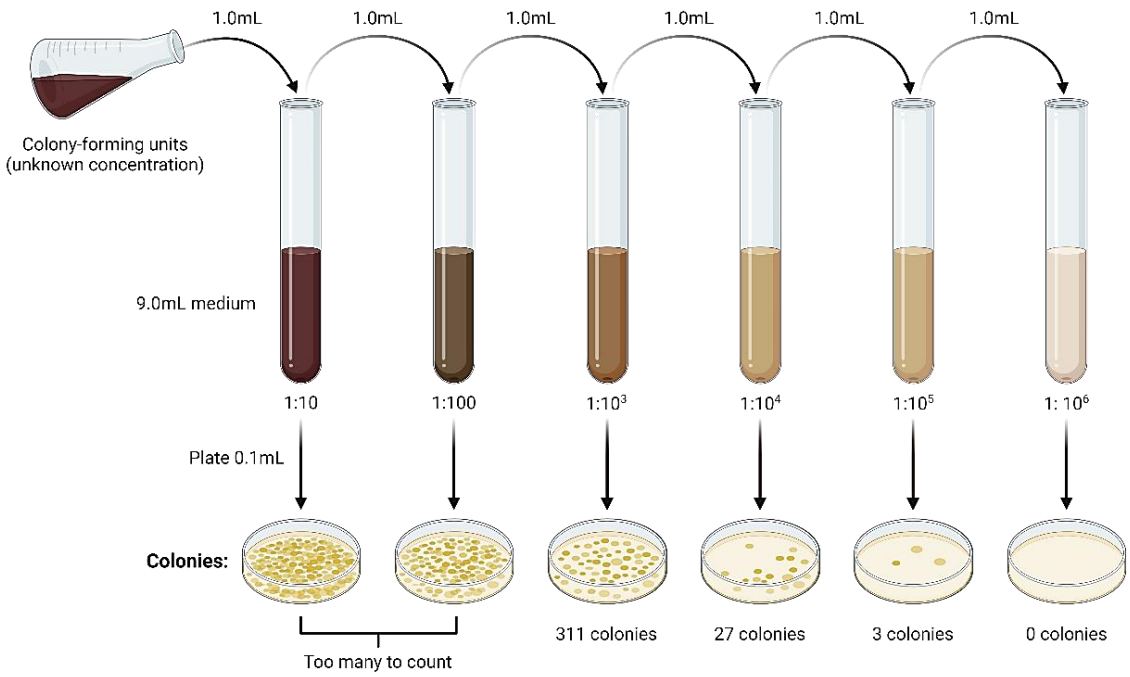

FIGURE 4-3. Schematic illustration of CFU/ml calcuation from BioRender.com

4.1.16 Treatment of bacteria with EVs

HUVEC-derived EVs from static and flow cultures (the EV stock used for RNAseq and proteomics studies) were thawed overnight on ice at 4 °C (in cold room). From confluent bacterial culture, 0.5 µl and 1 µl were incubated with 10 µl of the EV types separately to have 10,000 and 20,000 EVs/CFU. Treatments were incubated in 1.5 ml tubes overnight prior to RNA extraction.

4.1.17 Bacterial gene expression

Bacterial cells were lysed with 3 mg/ml lysosyme (#90082, Thermo Fisher Scientific) prior to isolation of total RNA using the Monarch Total RNA Miniprep Kit (#T2010S, NEB). The concentration of isolated RNA was quantified by NanoDrop™ (Thermo Fisher Scientific). qPCR was performed as described before. Primer sequences for each transcript are detailed in Table 4-4. Data were normalized to the *16s* rRNA housekeeping gene.

TABLE 4-4. Primer sequences used for qPCR (10 µM stock).

Gene	Accession number	Primer forward sequence	Primer reverse sequence
16s rRNA	LN681572.1	CGGGGAGGGTCATTGGAAAC	GTTTACGGCGTGGACTACCA
gelE	NZ_KB944666.1	CCCTGTGTTATCCGTTCCGT	CCAACTGGTGACCCCGTATC
ebpA	NZ_KB944666.1	AGACGGTAGTGCACAATGGG	TGGTCTCCTGTACCGCCATA
ace	NZ_KB944666.1	CGGATTTCGGAACAGCAACG	TCTCCAGCCAAATCGCCTAC

4.1.18 Statistical analysis

GraphPad Prism 9 software (GraphPad, USA) was used for data analysis. Shapiro-Wilk test was performed to analyze the data distribution. For normally distributed data, means of two groups were compared with Student's t-test. For group analysis, one-way analysis of variance (ANOVA) followed by Dunnett's post hoc test was applied to compare every mean with the mean of control group. All data are presented as mean ± SD, and $p<0.05$ was considered significant. *$p<0.05$, **$p<0.01$, ***$p<0.001$, ****$p<0.0001$. Schematic illustration were made using BioRender.com.

4.2 Results

4.2.1 Finding the optimum medium for EV isolation

The experiments involving different media were conducted at various times (chronologically), with some options being introduced during later phases of the study. Consequently, not all experiments in this section included all media. The table below describes the options and the experiments in which they were investigated:

TABLE 4-5. Media options and experiments.

Options	Morphology	Endothelial characteristics (vWF)	Gene expression	EV production	RNA yield
10% FCS medium (Co)	✓	✓	✓	✓	×
2% EV-depleted FCS	✓	×	✓	✓	✓
10% EV-depleted FCS	✓	✓	✓	✓	✓
Endopan medium	✓	✓	✓	✓	×
EGM™ BulletKit™ (Lonza)	✓	×	×	✓	×
ITS-supplemented medium	✓	×	×	×	×
FCS-free medium	✓	×	×	×	×

4.2.1.1 Cell morphology

The experiment on morphology began by culturing HUVECs under static conditions with the hypothesis that if the cells remained stable in static culture first, then they could be examined under flow. HUVECs were subjected to various media for 72 hours, revealing normal morphology in 10% and 2% EV-depleted FCS medium, Endopan medium, and Lonza medium **(**Figure 4-4**)**. However, when grown in ITS-containing medium and serum-free medium, some cells were found to be partly detached. Consequently, the first four media were selected to be tested under flow conditions, revealing normal elongation of the cells in the direction of the flow for both EV-depleted FCS media and Endopan medium, while cells grown in Lonza medium detached under flow.

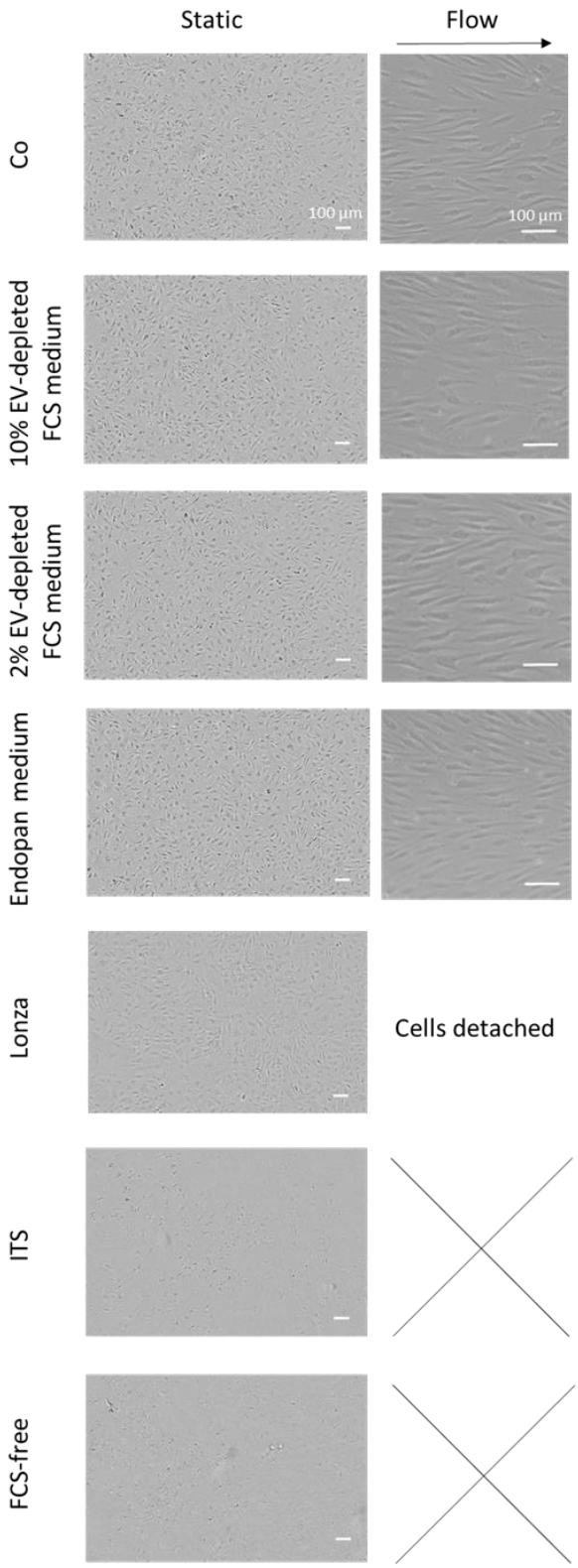

FIGURE 4-4**.** Morphology of HUVECs after 72 h culture in different media under static and 20 dynes cm^{-2} flow conditions. Scale bar=100 µm. Cells were a mix of two HUVEC donors with unknown sex, conducted in two independent experiments, each including one technical replicate.

4.2.1.2 Von Willebrand Factor

To make sure HUVECs keep their endothelial characteristics, we investigated the presence of von Willebrand Factor as an endothelial marker after incubation with different media under static and flow culture conditions **(**Figure 4-5**)**. The immunofluorescent staining detected the presence of vWF in HUVECs cultured in complete (Co), Endopan and 10% EV-depleted FCS medium in both culture conditions.

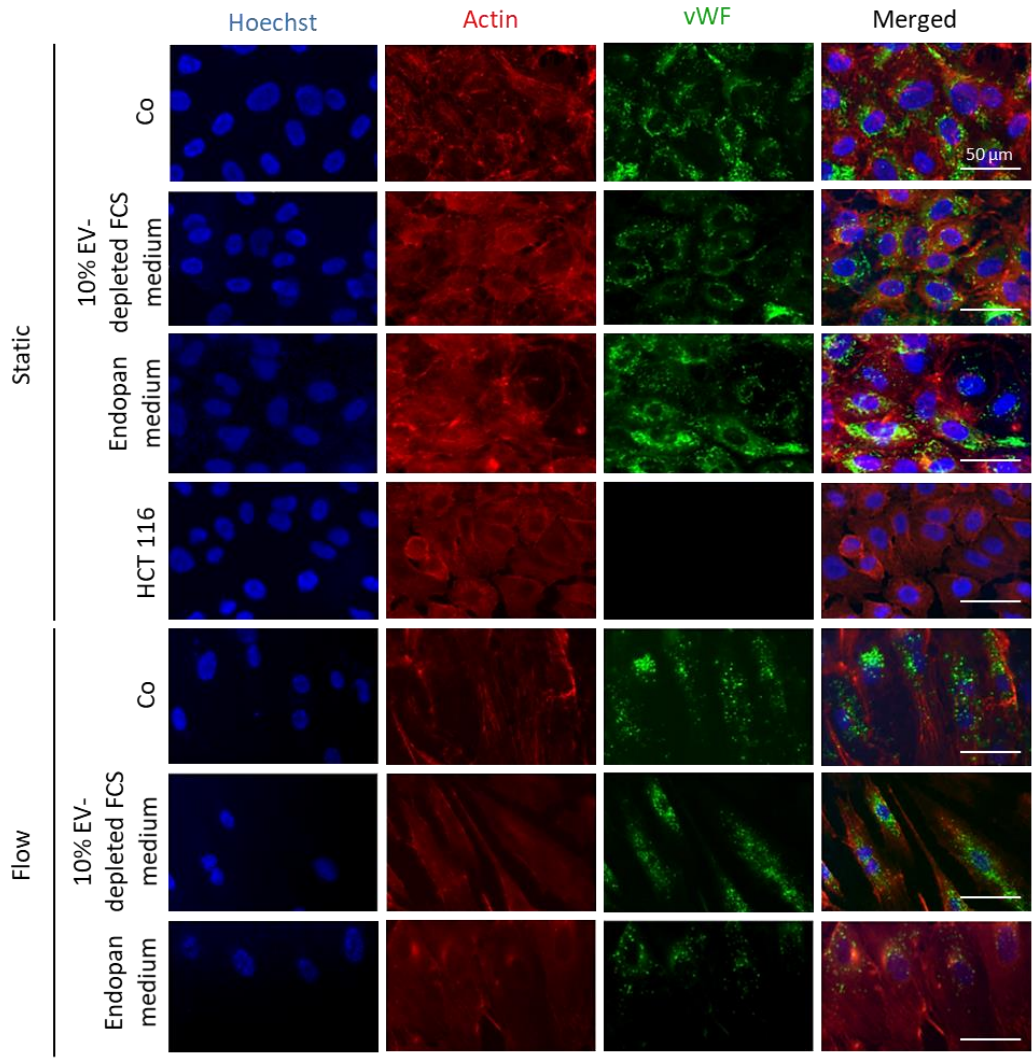

FIGURE 4-5. Fluorescence microscopy images of HUVECs cultured under static and under laminar flow conditions (20 dynes cm^{-2}) in 10% EV-depleted FCS medium and Endopan medium after 72 h. HCT116 cells were used as negative control. Blue: Hoechst, red: Actin, green: von Willebrand factor. Scale bar=50 µm. Cells were mix of two HUVEC donors with unknown sex, conducted in one experiment, including two technical replicates.

4.2.1.3 Gene expression

Additional investigations were conducted using qPCR to evaluate the impact of various media on HUVECs on the expression of genes known to be altered upon laminar flow. This was supposed to identify a medium that exhibits the least deviation in gene expression compared to the complete medium. Because laminar flow modulates the expression of adhesion molecules and anti-inflammatory factors,(Hahn et al. 2014; Pan 2009) the expression of relevant genes was examined in HUVECs cultured under laminar flow relative to static cultures. The data indicate a shift in gene expression that closely resembles the control condition when using a medium containing 2% EV-depleted FCS medium (Figure 4-6).

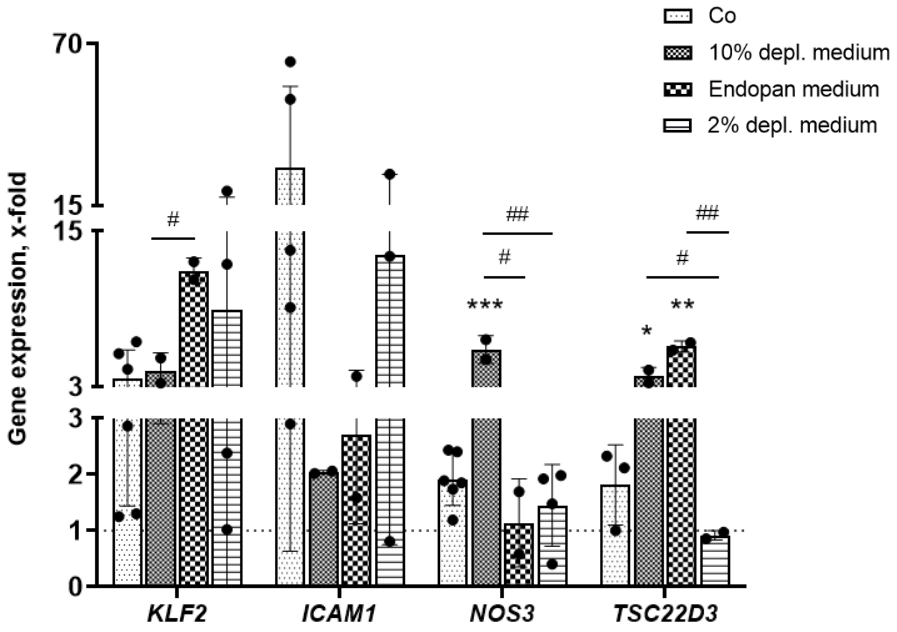

FIGURE 4-6. Gene expression of HUVECs incubated with different media under laminar flow conditions (20 dynes cm^{-2}) for 72 h. Data are normalised to static culture as control (dashed line), and shown as mean ± SD. Cells were a mix of two HUVEC donors with unknown sex. Dots show biological replicates, and each dot is the average of three technical replicates. Means of two groups were compared with Student's t-test. For group analysis, one-way analysis of variance (ANOVA) followed by Dunnett's post hoc test was applied to compare every mean with the mean of control group. # shows significant differences between groups. * indicates significant differences compared to the control (Co, indicated with the dashed line). $p<0.05$ is considered significant. $^{*}p<0.05$, $^{**}p<0.01$, $^{***}p<0.001$.

4.2.1.4 HUVECs produce different populations of EVs when cultured in different media

Next, our focus was directed towards investigating the potential impact of various media on the characteristics of the produced EVs in HUVECs. To achieve this, we first tested various media under static conditions before proceeding with the large-scale flow EV experiments. EVs were isolated from 72 h static cultures in control (Co), Endopan, 10% EV-depleted FCS, 2% EV-depleted FCS, and Lonza medium. A CD9+ EV population was detected by western blot analysis for EVs from HUVECs cultured in complete medium (Co), 10% EV-depleted FCS medium, and Endopan medium, while no signal for CD63 was recorded for neither of the conditions (Figure 4-7**)**. Interestingly, CD63 was present in EV samples from HUVECs cultured in 2% EV-depleted FCS medium and Lonza medium in addition to CD9 (full blots are provided in Figure S11).

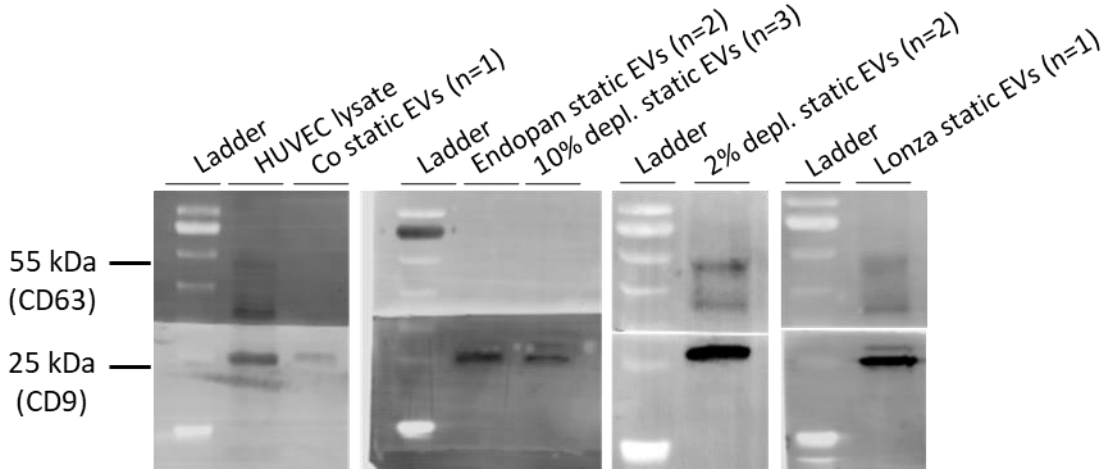

FIGURE 4-7. Western blot analysis of HUVEC EVs isolated form static cultures in different media after 72 h. Cells were a mix of two HUVEC donors with unknown sex. Number of biological replicates is shown in parenthesis.

4.2.1.5 RNA yield and EV markers

Given that the hollow fiber cartridge functions as a closed system, we aimed to ensure cell stability following the incubation period before progressing to large-scale EV collection. Attempts to image cells adhered to the fibers using scanning electron microscopy (SEM) were unsuccessful due to limitations in accessing the fibers. Consequently, our alternative approach involved assessing the RNA concentration of the cells. We hypothesized that if the cells remained adherent throughout the incubation period, it should be possible to isolate RNA in a concentration within an acceptable range relative to the initial cell seeding number. The RNA was less concentrated when incubated longer (72 h) in a low serum content (2% EV-depleted FCS medium), while the RNA extracted after shorter (48 h) incubation in the same medium had a higher concentration compared to when 10% EV-depleted FCS was used for 72 hours (n= 1, cells were a mix of 4 female HUVEC donors).

TABLE 4-6. RNA concentration of HUVECs

Medium	Flow incubation time	RNA C. ng μl^{-1}
2% EV-depleted FCS medium	72	19.5
2% EV-depleted FCS medium	48	67.5
10% EV-depleted FCS medium	72	40

In previous experiments, the presence of EV markers was investigated after 72 h of static incubation time. Since 48 h culture under laminar flow resulted in higher amounts of isolated RNA, we proceeded with large scale EV isolation from flow cultures, and performed western blot analysis with EVs isolated from conditioned media of cells used for RNA yield analysis to investigate whether lower incubation time would affect EV populations as well. Western blot analysis showed that CD63 and CD9 EV markers are detectable in samples after 48 h under static and flow cultures when 2% EV-depleted FCS medium is used, while no CD63 was present when cells were incubated in 10% EV-depleted FCS medium for 72 h (Figure 4-8).

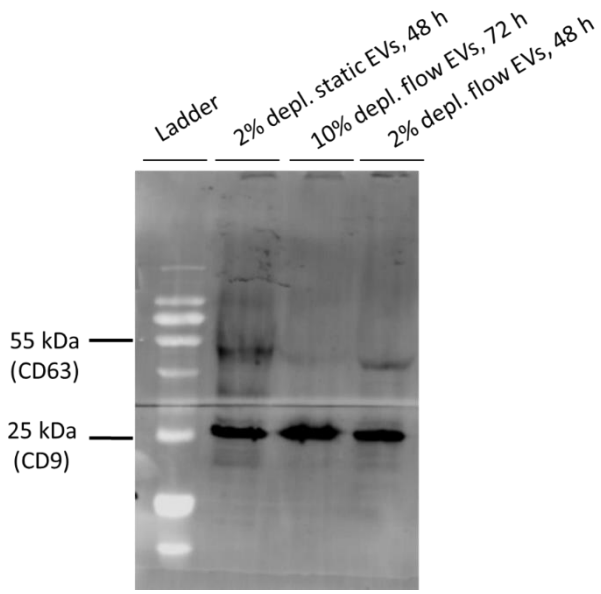

FIGURE 4-8. HUVEC EV marker analysis of static and flow cultures after 48 h. Mix of 4 female HUVEC donors was cultured in 2% EV-depleted FCS medium (under static, and under 20 dynes cm^{-2} laminar flow for 48 h), and in 10% EV-depleted FCS (under 20 dynes/cm^2 laminar flow for 72 h). Presence of EV markers (CD63, CD9) was examined using western blot. 30 µl of EVs were loaded into each pocket equal to 30 µg, 39 µg, 30 µg proteins from left to right (n=1).

Taken together, we decided to culture the cells for 48 h in 2% EV-depleted FCS medium under static and laminar flow conditions for further EV sample collection and analysis.

4.2.2 HUVEC EV isolation and characterization obtained from static and laminar flow cultures

4.2.2.1 EV characterization

Having identified the optimal medium for EV isolation suitable for both static and flow conditions, we proceeded with the main EV sample collection of both EV types with three biological replicates (while each biological replicate was a mix of three individual female donors), and their characterization. EVs were isolated using ultracentrifuge from HUVECs cultured in 2% EV-depleted FCS medium under static and laminar flow conditions (20 dynes cm^{-2}) for 48 h. The concentration of EVs was determined using NTA, revealing an average of $2.44\times10^{12} \pm 0.71\times10^{12}$ particles per milliliter for static EVs and $2.29\times10^{12} \pm 0.54\times10^{12}$ particles per milliliter for flow EVs. Furthermore, NTA showed 129 ± 3 nm and 134 ± 9 nm for the mode size of static and flow EVs respectively (Figure 4-9A, B). The morphology of the EVs was then verified through cryo-TEM, which confirmed their spherical structure for both EV types (Figure 4-9C, D). The zeta potential of the vesicles was negative, averaging from -10.9 ± 1.12 mV for static EVs to -10.2 ± 0.77 mV for flow EVs (Figure 4-9E). The average protein concentration was significantly higher in static EVs (Figure 4-9F).

TABLE 4-7. HUVEC EV characterization isolated from static and flow cultures from three individual EV isolations each measured in triplicates.

	Static EVs	**Flow EVs**
Particle c. **(particles per milliliter)**	$2.44\times10^{12} \pm 0.71\times10^{12}$	$2.29\times10^{12} \pm 0.54\times10^{12}$
Size **(nm)**	129 ± 3	134 ± 9
Zeta potential **(mv)**	-10.9 ± 1.12	-10.2 ± 0.77
Protein c. **(mg/ml)**	4.93 ± 1.8	3.1 ± 0.87

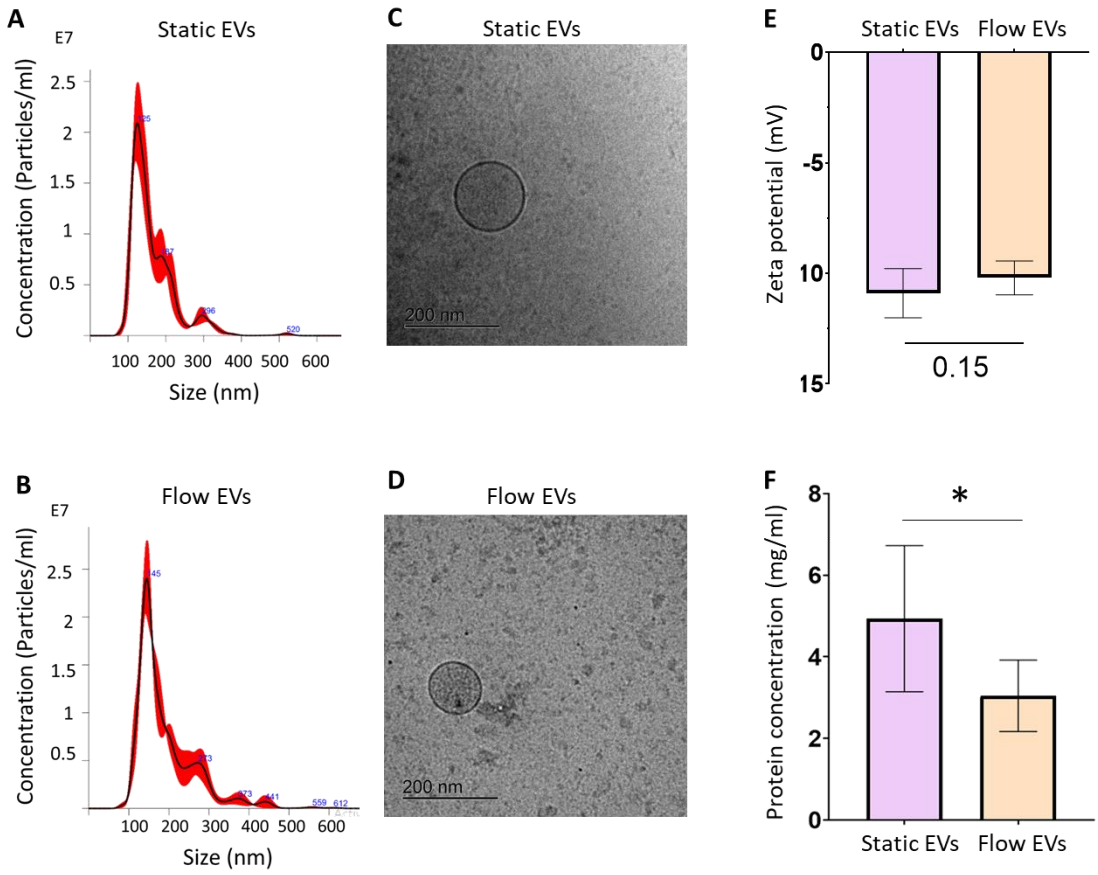

FIGURE 4-9. HUVEC EV characterization isolated from static and flow cultures. EVs were isolated using UC from HUVECs cultured in 2% EV-depleted FCS medium under static and laminar flow conditions (20 dynes cm^{-2}) for 48 h. **A, B)** Representative size distribution of particles by NanoSight particle tracking analysis of static and flow EVs, respectively. **C, D)** Representative cryo-TEM images of static and flow EVs, respectively, scale bar=200 nm. **E)** Zeta potential of the vesicles (n= three biological replicates, each replicate is a mix of three HUVEC female donors). **F)** Protein concentration of isolated EVs was assessed by BCA assay (n= six biological replicates, each replicate was a mix of three HUVEC female donors). Statistical differences were analyzed by Student's t-test. $^{*}p<0.05$.

4.2.2.2 MiRNA-seq profile of static and flow EVs

We performed miRNA-seq of both, cells and EVs. Principal component analysis (PCA) (Figure 4-10A, B) revealed a distinct separation between the biological replicates of the two conditions in parental cells and EVs. Figure 4-10C, D illustrates the differentially expressed miRNAs in a volcano plot for C) cells and D) EVs. Log2 fold change was plotted against -log10 p-value. Negative log2 fold change values represent abundancy under static condition, whereas positive values represent abundancy in flow condition. In cell samples, 11 miRNAs exhibited abundance under static conditions, whereas 16 were abundant in flow conditions. Regarding EVs, 3 miRNAs showed abundance in flow EVs, whereas 4 were abundant in static EVs. The differentially expressed miRNAs are shown in Figure 4-10E. Potential eukaryotic target genes, which might be affected by these significantly enriched miRNAs in EVs were identified using miRTarget Link 2.0. This revealed more target genes for flow EVs (Table 4-8) than static EVs (Table 4-9). Genes that might be affected by miRNAs from flow EVs play a role in phosphorylation, migration, cell motility, and signaling pathways according to GO biological processes analysis (Figure 4-10F); while predicted targets of miRNAs from static EVs are involved in cell differentiation and regulation of immune responses (Figure 4-10G).

To investigate the interaction between HUVEC EVs and *E. faecalis*, we first examined whether miRNAs abundant in static and flow EVs could target specific sites on the bacterial genome. Differentially expressed miRNA sequences abundant in EVs were retrieved from the miRBase database, while the sequences of virulence genes (*gelE, ebpA, ace*) of *E. faecalis* were obtained from the NCBI nucleotide database. The miRNA sequences were then subjected to *in silico* hybridization with the gene sequences using the RNAhybrid software. The hybridization analysis based on Minimum free energy (mfe) for likelyness of the hybridization revealed potential target sites within the *gelE*, *ebpA*, and *ace* sequences of *E. faecalis* (Figure 4-11).

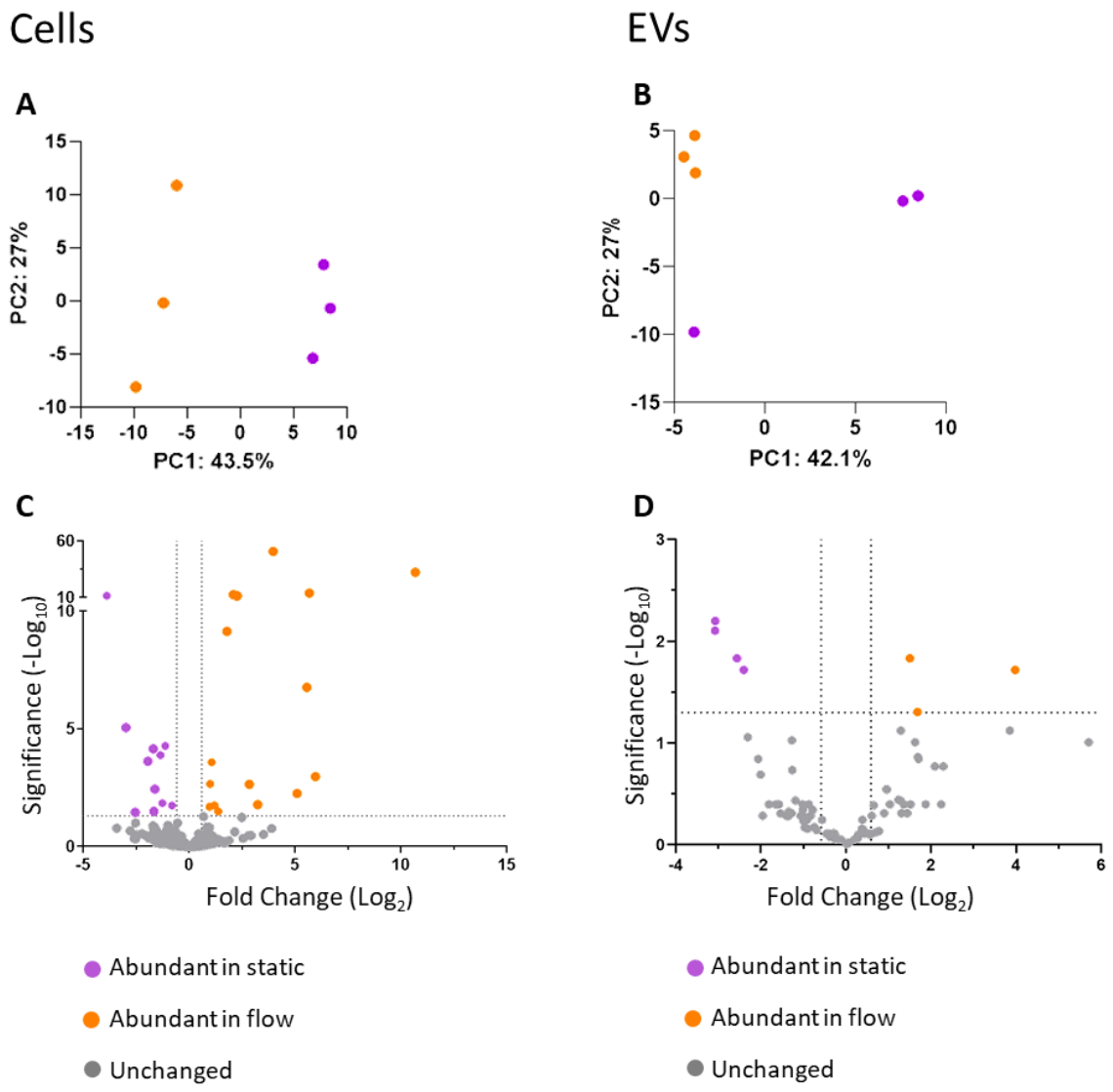
Cells
EVs
A
B
PC2: 27%
PC1: 43.5%
PC1: 42.1%
C
D
Significance (-Log10)
Fold Change (Log2)
Abundant in static
Abundant in flow
Unchanged

E

Cells

		F1	F2	F3	S1	S2	S3
Flow	hsa-miR-21-5p	9.95	9.97	10.43	2.21	2.19	2.31
	hsa-miR-122-5p	3.68	3.84	3.12	2.00	2.00	2.00
	hsa-miR-1290	5.94	6.27	6.36	2.70	2.19	2.31
	hsa-miR-451a	5.18	5.13	5.21	2.00	2.36	2.31
	hsa-miR-4516	3.50	3.84	3.57	2.00	2.00	2.31
	hsa-miR-3182	8.94	8.91	8.55	4.95	5.16	4.93
	hsa-miR-4485-3p	3.30	4.15	3.90	2.39	2.52	2.00
	hsa-miR-4448	4.53	4.33	4.30	2.84	2.19	2.96
	hsa-miR-199a-3p	7.19	7.87	7.15	5.40	5.29	5.21
	hsa-miR-199b-3p	7.19	7.85	7.12	5.40	5.29	5.21
	hsa-miR-23b-3p	8.00	8.18	8.17	5.68	6.09	6.48
	hsa-miR-23a-3p	8.33	8.61	8.59	6.25	6.85	7.11
	hsa-miR-139-5p	5.00	5.64	4.78	3.94	4.20	4.03
	hsa-miR-424-5p	6.27	6.56	5.43	5.27	5.06	4.88
	hsa-miR-221-3p	7.55	7.69	7.78	6.69	6.83	6.37
	hsa-miR-22-3p	7.88	7.47	8.11	6.70	7.08	6.83
	hsa-miR-26b-5p	7.13	6.89	7.13	5.92	5.74	6.64
Static	hsa-miR-20a-5p	7.16	7.62	7.30	8.48	7.84	8.13
	hsa-miR-17-5p	6.78	6.83	6.64	8.04	7.84	7.68
	hsa-miR-887-3p	4.53	4.81	5.67	6.53	6.16	5.97
	hsa-miR-671-5p	5.35	5.77	5.72	6.73	7.13	6.83
	hsa-miR-18a-5p	3.50	4.69	4.30	5.51	5.71	5.78
	hsa-miR-4301	3.68	3.59	4.41	5.53	4.29	5.76
	hsa-miR-92b-3p	5.24	4.69	5.01	6.11	6.89	6.57
	hsa-miR-193a-3p	3.84	4.05	5.53	6.23	6.58	6.48
	hsa-miR-1307-5p	2.79	3.10	2.00	4.73	4.33	3.53
	hsa-miR-10400-5p	3.30	2.90	3.75	6.25	5.37	5.25
	hsa-miR-12136	3.07	3.44	3.36	6.84	6.12	6.52

EVs

		F1	F2	F3	S1	S2	S3
Flow	hsa-miR-451a	7.25	7.74	7.70	6.21	6.53	6.02
	hsa-miR-4497	6.20	3.16	3.68	2.70	2.55	2.37
	hsa-miR-26b-5p	4.54	5.18	5.26	3.81	3.85	3.47
Static	hsa-miR-320a-3p	5.12	4.42	4.73	5.19	7.75	6.98
	hsa-miR-320b	4.96	4.11	4.56	5.19	7.68	6.86
	hsa-miR-320d	4.13	3.29	3.98	4.73	7.31	6.32
	hsa-miR-320c	4.28	3.41	4.22	4.86	7.54	6.63

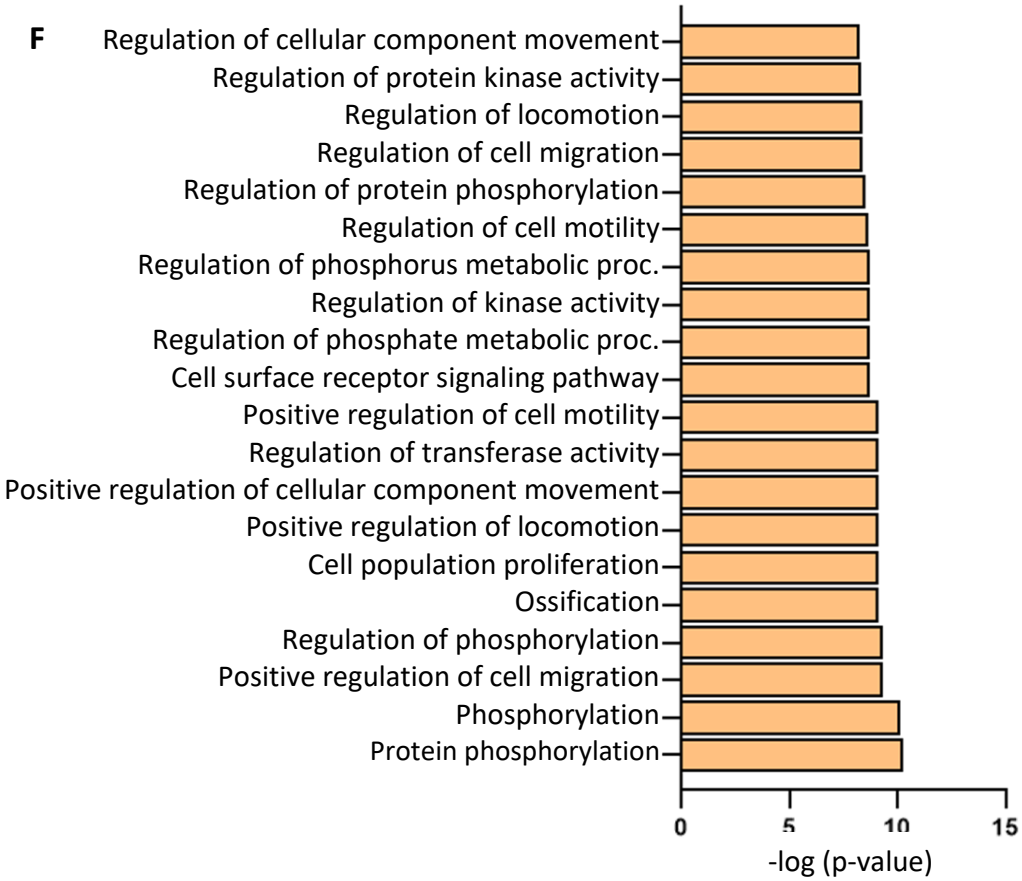
F
Regulation of cellular component movement
Regulation of protein kinase activity
Regulation of locomotion
Regulation of cell migration
Regulation of protein phosphorylation
Regulation of cell motility
Regulation of phosphorus metabolic proc.
Regulation of kinase activity
Regulation of phosphate metabolic proc.
Cell surface receptor signaling pathway
Positive regulation of cell motility
Regulation of transferase activity
Positive regulation of cellular component movement
Positive regulation of locomotion
Cell population proliferation
Ossification
Regulation of phosphorylation
Positive regulation of cell migration
Phosphorylation
Protein phosphorylation
0
5
10
15
-log (p-value)

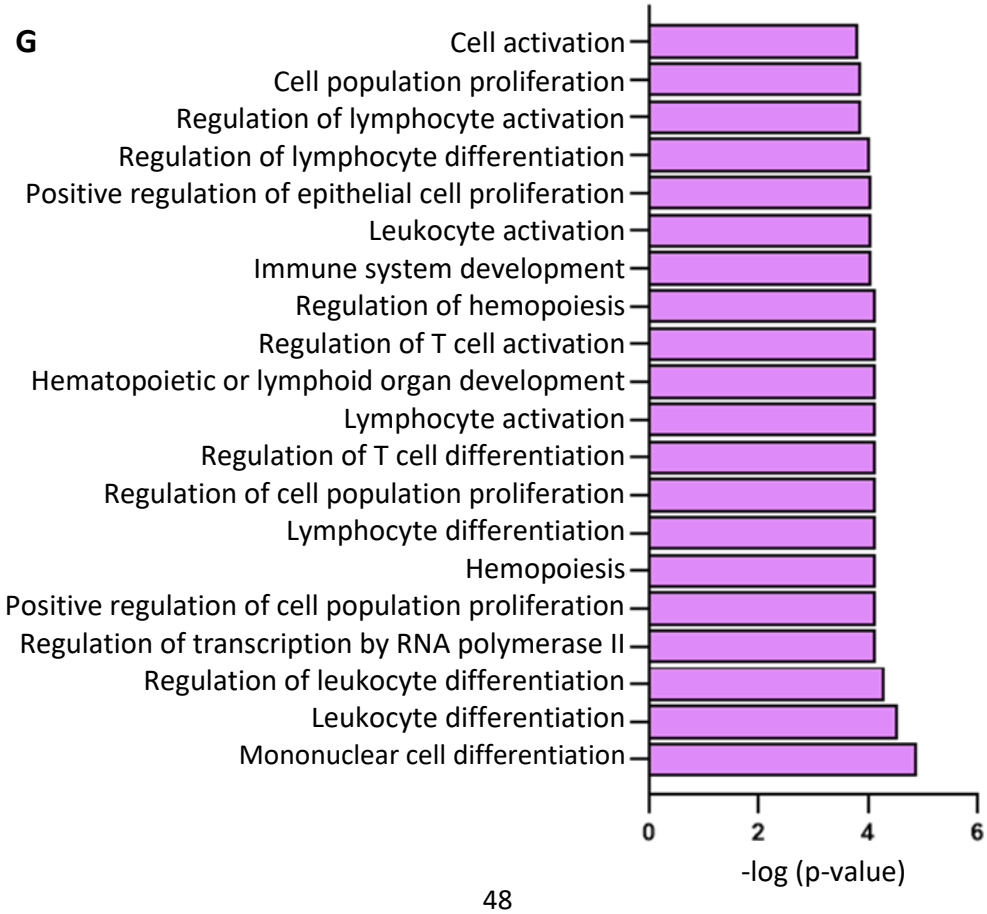
G
Cell activation
Cell population proliferation
Regulation of lymphocyte activation
Regulation of lymphocyte differentiation
Positive regulation of epithelial cell proliferation
Leukocyte activation
Immune system development
Regulation of hemopoiesis
Regulation of T cell activation
Hematopoietic or lymphoid organ development
Lymphocyte activation
Regulation of T cell differentiation
Regulation of cell population proliferation
Lymphocyte differentiation
Hemopoiesis
Positive regulation of cell population proliferation
Regulation of transcription by RNA polymerase II
Regulation of leukocyte differentiation
Leukocyte differentiation
Mononuclear cell differentiation
0
2
4
6
-log (p-value)

FIGURE 4-10**.** MiRNAseq data. **A, B)** PCA shows distinction between HUVEC parental cells **A)**, and static and flow EVs **B)**. **C, D)** Volcano plot representing the differential enrichment of miRNAs between cells **C)**, and EVs **D)**. Log_2 fold change (1.5) is plotted against $-log_{10}$ p-value (0.05). **E)** Distribution of differentially expressed miRNAs in static and flow EVs, and their parental cells. Transcripts per million (TPM) are shown (sorted by highest fold change) for all three independent preparations per condition (S: static EVs, F: flow EVs). N= three biological replicates, each replicate is a mix of three HUVEC female donors. Top 20 gene ontology (GO) biological processes for targets of miRNAs enriched in **F)** flow and **G)** static EVs derived from ShinyGO 0.80.

TABLE4-8. Validated targets of enriched miRNAs in flow EVs based on miRTarget Link 2.0.m

hsa-miR-4497 (weakly validated) (No strongly validated targets detected)		**hsa-miR-451a** (strongly validated)	**hsa-miR-26b-5p** (strongly validated)	
NPY4R	CAMK2N2	MIF	PTGS2	SMAD1
ATP13A4	MIPOL1	CAB39	EPHA2	MIEN1
TPM3	VEGFA	ABCB1	CDK6	COL1A2
SDF4	CASTOR2	AKT1	CCNE1	CTGF
ZNF490	CD226	MMP2	ABCA1	TLR4
NF2	CTTN	MMP9	ARL4C	HGF
CCNF	FBXL18	BCL2	GATA4	ST8SIA4
CCNY	IRX5	MYC	CHORDC1	PDE4A
LHFPL3	MTPAP	RAB14	NR2C2	FH
PRPS1L1	NAB2	TMED7	PLOD2	JAG1
APPBP2	ATP1B4	IKBKB	TAB1	IGF1
SH2B1	CBARP	IL6R	EZH2	LARP1
FAM83C	DSN1	DCBLD2	USP9X	
RAB22A	PRPS1	CPNE3	IGF1R	
BPNT1	SP140L	RAB5A	KPNA2	
FANCA	TBC1D24	ADAM10	RB1	
DUSP22	TMEM33	IL6	NAMPT	
RAB9A	PPAN	TSC1	PTEN	
HIST1H2AH	P2RY11	MAPK1	COX2	
LRRC27		OXTR	HAS2	
UGT8		CDKN2D	ULK2	
RUNX1		MAP3K1	TRAF5	

TABLE 4-9. Validated targets of enriched miRNAs in static EVs based on miRTarget Link 2.0.

hsa-miR-320a-3p (No target detected)	**hsa-miR-320b** (strongly validated)	**hsa-miR-320c** (strongly validated)	**hsa-miR-320d** (strongly validated)
-	NOD2	SMARCC1	RBFOX2
	MYC	GNAI1	GNAI1
	DLX5	PRDM1	
		XBP1	
		IRF4	
		EZH2	
		NOD2	

	gelE mRNA	*ebpA* mRNA	*ace* mRNA
hsa-mir-26b	target 5' G GUGU C 3' UUGUCC UUACUUGG GAUAGG AAUGAACU miRNA 3' UG ACUU U 5' mfe: -20.2 kcal/mol	target 5' G AA GUU C 3' CUAUC GAA CUUGGA GAUAG CUU GAACUU miRNA 3' UG GA AAU 5' mfe: -19.5 kcal/mol	target 5' A GA A 3' CCUGGA UACU GGACUU AUGA miRNA 3' UGGAUA A ACUU 5' mfe: -15.4 kcal/mol
hsa-mir-451a	target 5' C A UC A G 3' CU AGU UGG UAAUGGU GA UCA ACC AUUGCCA miRNA 3' UU G UU AA 5' mfe: -19.0 kcal/mol	target 5' U A A 3' ACUCA GUGACGGUU UGAGU CAUUGCCAA miRNA 3' CAUUAC A 5' mfe: -21.1 kcal/mol	target 5' U UUACUGU A 3' UUUAGUG UGGUAAUG GAGUCAU ACCAUUGC miRNA 3' UU U CAAA 5' mfe: -18.9 kcal/mol
hsa-mir-4497	target 5' U A U 3' GCCUA GUUCUGGA CGGGU CAGGGCCU miRNA 3' CGG C 5' mfe: -22.8 kcal/mol	target 5' U UGACUGG A 3' CUUAGUCGU UCCGGA GGGUCGGCA GGGCCU miRNA 3' C C 5' mfe: -24 kcal/mol	target 5' A AA AU U U 3' CCAG GUCC G G GGUC CAGG C C miRNA 3' CG GG GC U 5' mfe: -21.0 kcal/mol
hsa-mir-320a	target 5' G AU A C 3' UGCUUUUUCA GCCUA GUU GCGGGAGAGU UGGGU CGA miRNA 3' A AAA 5' mfe: -23.3 kcal/mol	target 5' U CAAA C 3' UCGCUU CAGCUCAGC AGCGGG GUUGGGUCG miRNA 3' AGA AAAA 5' mfe: -25.2 kcal/mol	target 5' A UAUCACCAAUAG G A 3' CGCU UUCUCAACC A GCGG GAGAGUUGG U miRNA 3' A G CGAAAA 5' mfe: -22.3 kcal/mol
hsa-mir-320b	target 5' G AU A C 3' UGCUUUUUCA GCCUA GUU ACGGGAGAGU UGGGU CGA miRNA 3' A AAA 5' mfe: -24 kcal/mol	target 5' A AAACAG A 3' UCUUCUCAACC AGC GGGAGAGUUGG UCG miRNA 3' AAC G AAAA 5' mfe: -24.5 kcal/mol	target 5' C UAUCACCAAUAG G A 3' GCU UUCUCAACC A CGG GAGAGUUGG U miRNA 3' AA G CGAAAA 5' mfe: -20.3 kcal/mol
hsa-mir-320c	target 5' U UAGCUCCGAU A 3' AUCCUCUU UCCAGC UGGGAGAG GGGUCG miRNA 3' UU AAAA 5' mfe: -23.5 kcal/mol	target 5' A AAACAG A 3' AUCUUCUCAACC AGC UGGGAGAGUUGG UCG miRNA 3' G AAAA 5' mfe: -25.4 kcal/mol	target 5' G G A 3' UUCUCAACC A GAGAGUUGG U miRNA 3' GG G CGAAAA 5' mfe: -18.9 kcal/mol
hsa-mir-320d	target 5' U UAGCUCCGAU A 3' CCUCUU UCCAGC GGAGAG GGGUCG miRNA 3' UU AAAA 5' mfe: -20.5 kcal/mol	target 5' U AAACAG A 3' CUUCUCAACC AGC GGAGAGUUGG UCG miRNA 3' G AAAA 5' mfe: -22.3 kcal/mol	target 5' G G A 3' UUCUCAACC A GAGAGUUGG U miRNA 3' AG G CGAAAA 5' mfe: -18.9 kcal/mol

FIGURE 4-11. Hybridization of the significant abundant miRNAs in static and flow EVs with *E. faecalis* mRNA. Minimum free energy (mfe) is shown for each duplex.

4.2.2.3 Proteomics analysis of static and flow EVs

A total of 3268 proteins were detected including 664 proteins unique in static EVs and 520 proteins in flow EVs with 2084 proteins common in both types (Figure 4-12A). PCA revealed a distinct separation between static and flow EVs, with biological replicates within each category demonstrating similarity (Figure 4-12B). Fold changes were calculated using the unique spectrum counts of flow EVs/static EVs. Figure 4-12C illustrates the differentially expressed proteins in a volcano plot, i.e. $\log_2$ fold change was plotted against $-\log_{10}$ p-value. Negative $\log_2$ fold change values represent proteins more abundant in static EVs, whereas positive values represent abundant proteins in flow EVs. Cellular component analysis showed that the significantly enriched proteins in both EV types are annotated with exosomal and cytosolic spaces (Figure S12). Interestingly, within the significant gene ontology (GO) cellular component terms of flow EV proteins, mitochondrial origin was also observed. Next, we analysed the biological processes that these significant proteins are associated with. Figure 4-12D shows that the proteins significantly enriched in flow EVs play a role in localization, transport, and respiration. Biological processes associated with enriched proteins in static EVs are shown in Figure 4-12E, suggesting a role in cellular metabolism, and translation. Based on the mitochondrial origin of flow EV-enriched proteins as indicated by cellular component terms, and considering their involvement in cellular respiration, proton transport, and energy processes, we conducted a detailed analysis of these proteins. Specifically, we examined their abundance and presence in static EVs as well. Figure 4-12F illustrates the unique spectrum counts of mitochondrial proteins significantly present in flow EVs, alongside their counts in static EVs. Notably, it demonstrates either an absence or reduced presence of mitochondrial proteins in static EVs. Gene ontology analysis also showed involvement of the mitochondrial proteins in biological processes, such as respiration, oxidative phosphorylation, and ion transport (Figure 4-12G).

Exclusive, unique spectrum count raw data of a series of EV marker proteins (Mashayekhi et al. 2024; Hoppstädter et al. 2019; van Niel, D'Angelo, and Raposo 2018) are shown in Figure S13 for the independent preparations per condition. Overall, the EV-specific protein distribution was quite similar in both conditions. Only milk fat globule-epidermal growth factor-factor 8 (MFG-E8) was highly expressed in static EVs compared to the low expression in flow EVs.

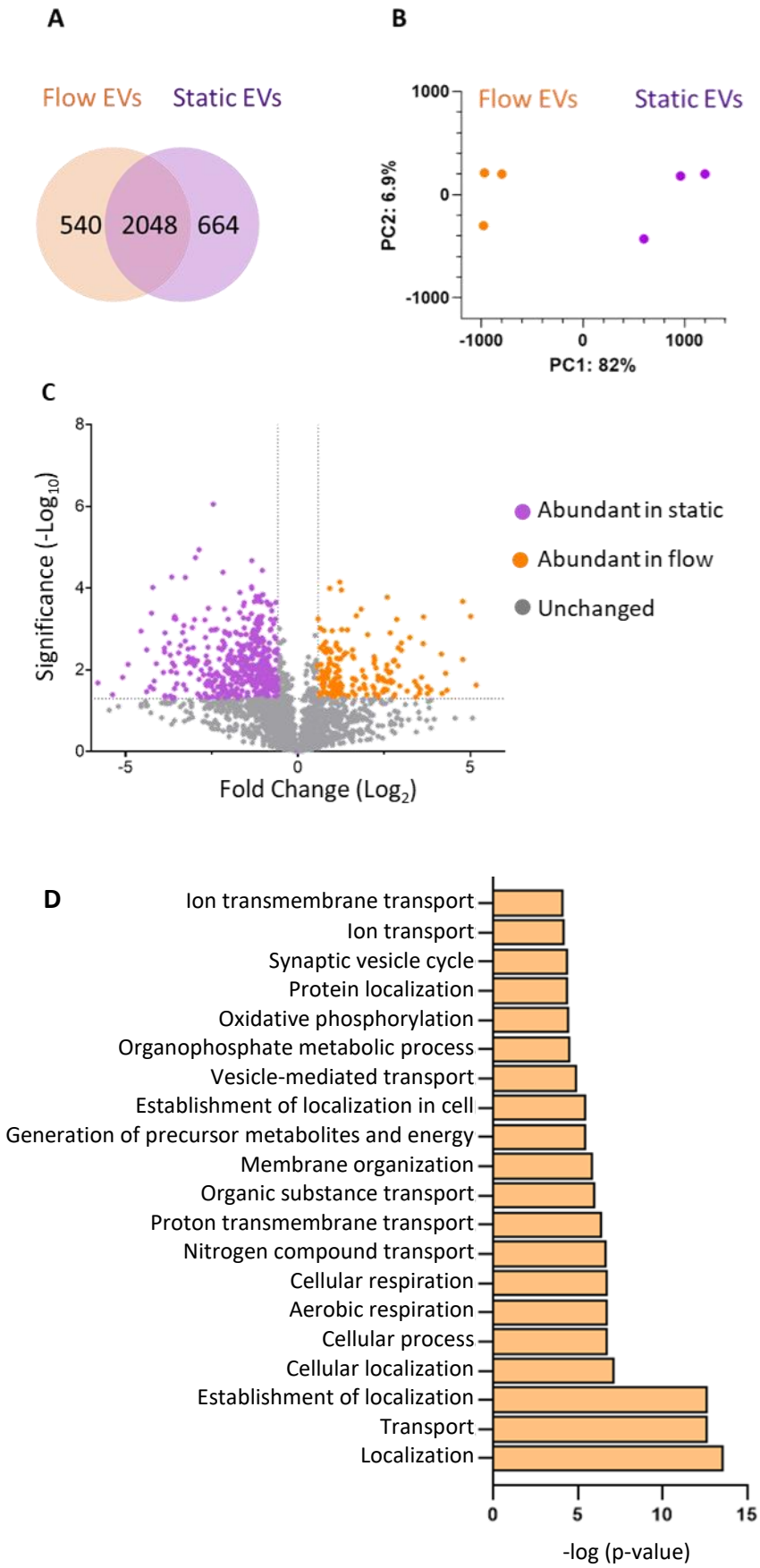
A
Flow EVs
Static EVs
540
2048
664
B
Flow EVs
Static EVs
1000
0
-1000
PC2: 6.9%
-1000
0
1000
PC1: 82%
C
Significance (-Log10)
8
6
4
2
0
-5
0
5
Fold Change (Log2)
Abundant in static
Abundant in flow
Unchanged
D
Ion transmembrane transport
Ion transport
Synaptic vesicle cycle
Protein localization
Oxidative phosphorylation
Organophosphate metabolic process
Vesicle-mediated transport
Establishment of localization in cell
Generation of precursor metabolites and energy
Membrane organization
Organic substance transport
Proton transmembrane transport
Nitrogen compound transport
Cellular respiration
Aerobic respiration
Cellular process
Cellular localization
Establishment of localization
Transport
Localization
0
5
10
15
-log (p-value)

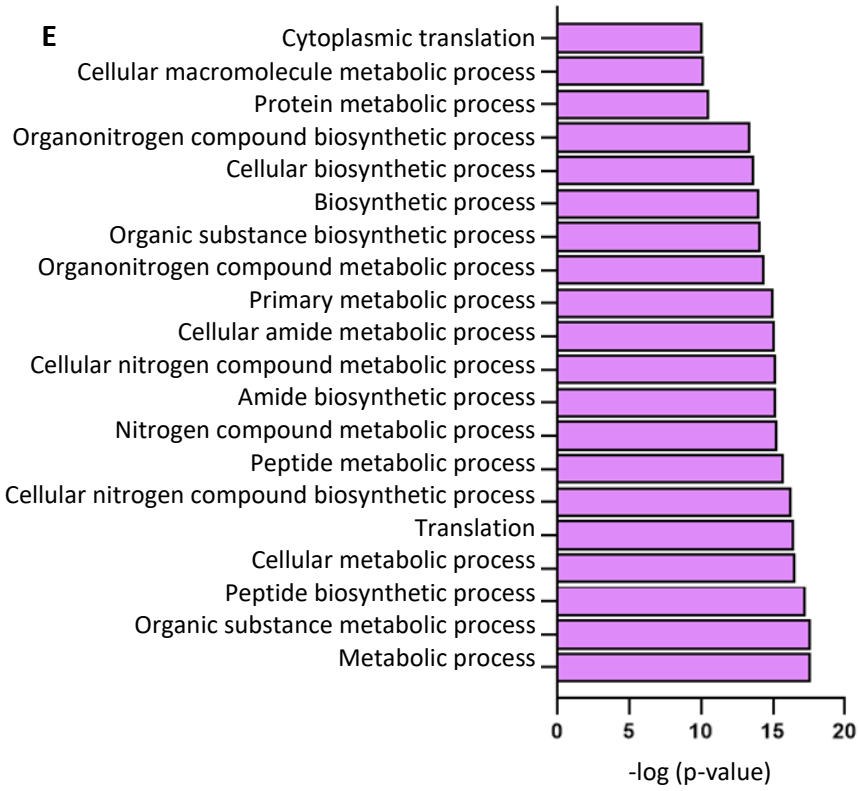
E
Cytoplasmic translation
Cellular macromolecule metabolic process
Protein metabolic process
Organonitrogen compound biosynthetic process
Cellular biosynthetic process
Biosynthetic process
Organic substance biosynthetic process
Organonitrogen compound metabolic process
Primary metabolic process
Cellular amide metabolic process
Cellular nitrogen compound metabolic process
Amide biosynthetic process
Nitrogen compound metabolic process
Peptide metabolic process
Cellular nitrogen compound biosynthetic process
Translation
Cellular metabolic process
Peptide biosynthetic process
Organic substance metabolic process
Metabolic process
0
5
10
15
20
-log (p-value)

F

	F1	F2	F3	S1	S2	S3
ACADS	3	3	3	3	2	2
AK3	8	5	6	0	2	0
ANK2	23	30	27	18	9	11
ATP5F1A	53	55	61	53	39	37
ATP5F1B	156	135	148	139	119	115
ATP5ME	7	4	6	2	0	0
ATP5PB	11	5	9	2	0	0
CISD2	5	4	4	3	2	2
CKMT1	13	15	14	12	6	5
COX4I1	10	5	8	2	0	0
CRYM	6	6	6	4	5	4
CYC1	17	11	13	7	0	0
DNAJC5	11	10	14	12	9	8
FAM49B	27	23	23	12	12	11
FIS1	6	6	6	4	5	4
GLOD4	3	4	4	2	2	2
HEBP2	5	4	3	0	2	0
HSPA5	58	39	43	38	25	23
IDH3B	17	18	16	11	11	8
IDH3G	14	12	15	12	8	7
LRRC59	8	6	5	3	3	2
NAXD	2	3	2	2	2	2
NDUFA12	6	4	5	3	2	2
PC	17	14	21	8	0	0
PCCB	27	28	26	23	23	15
PDE2A	5	5	4	2	0	0
PDHB	7	4	6	2	0	0
PHB	23	15	21	12	3	4
PHB2	22	15	19	11	3	3
RAP1GDS1	5	5	4	2	0	0
SCCPDH	4	3	4	2	0	0
SDHA	10	7	9	4	4	2
SDHB	4	2	2	2	2	2
SEPTIN4	13	12	12	10	9	4
SFXN1	17	10	13	4	2	0
SH3GLB1	2	2	2	0	2	0
SLC25A11	17	15	16	8	4	4
SLC25A12	24	23	25	4	0	0
SLC25A3	19	12	14	10	0	3
SLC25A4	2	3	2	2	0	0
SLC25A5	29	21	22	14	4	5
SLC25A6	12	12	10	8	0	2
SLC44A2	16	17	13	10	13	10
SNAP23	18	13	10	12	7	6
SUCLA2	18	21	25	18	8	9
SYNJ2BP	10	4	6	3	0	0
UQCRB	6	4	4	3	0	0
UQCRC1	16	10	9	4	0	0
VDAC1	54	32	38	17	10	13
VDAC2	17	14	16	8	3	3
VDAC3	16	9	7	5	0	0
YKT6	5	8	5	6	4	5

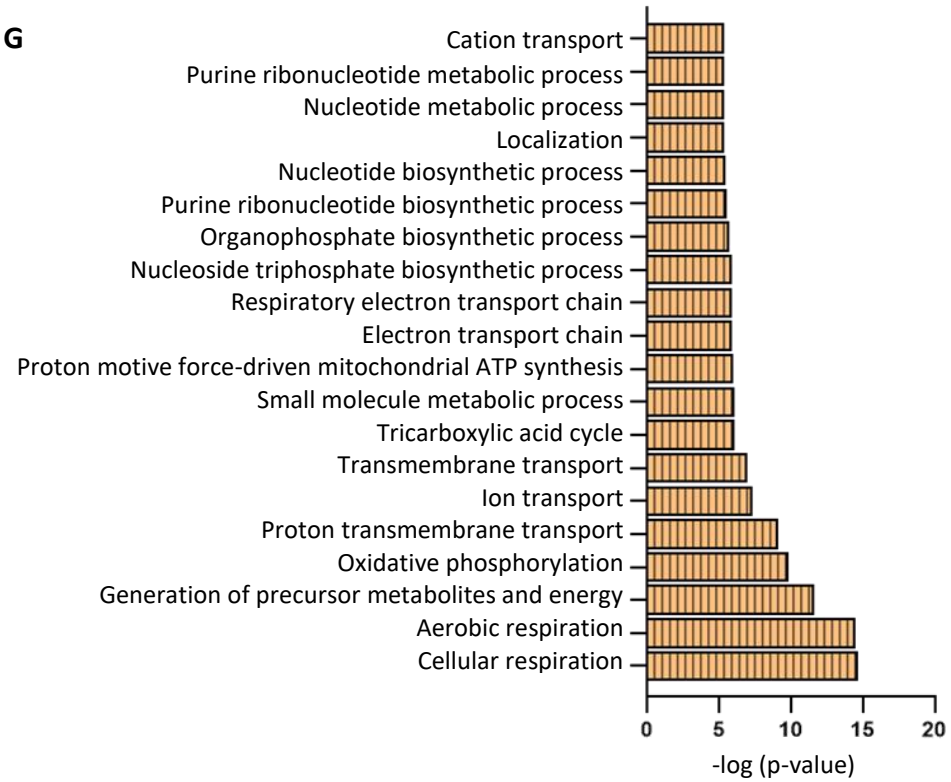

FIGURE 4-12. Proteomics data of static and flow EVs. **A)** Number of detected proteins. **B)** PCA shows a clear distinction between static and flow EVs (n=3). **C)** Volcano plot representing the differential enrichment between the two EV types. Log_2 fold change (1.5) is plotted against $-log_{10}$ p-value (0.05). Top 20 gene ontology (GO) biological processes for proteins significantly enriched in **D)** flow EVs and **E)** static EVs according to the STRING database. **F)** Abundant mitochondrial proteins in static and flow EVs and their distribution. Exclusive unique spectrum count raw data are shown for all three independent preparations per condition (S: static EVs, F: flow EVs). **G)** Top 20 gene ontology (GO) biological processes for mitochondrial proteins significantly enriched in flow EVs according to the STRING database. N= three biological replicates, each replicate is a mix of three HUVEC female donors.

4.2.3 Modulation of bacterial gene expression by HUVEC EVs

Modulation of virulence genes in *E. faecalis* in response to HUVEC EVs prepared from three biological replicates while each biological replicate was a mix of three individual female donors (the EV stock used for RNAseq and proteomics studies) was analyzed by real-time quantitative PCR (Figure 4-13). Both static and flow EVs upregulated gelatinase (*gelE*) in a dose-dependent manner, while the upregulation observed in flow EVs was more pronounced. Furthermore, both types of EVs elevated the expression of endocarditis and biofilm-associated pili (*ebpA*) in a dose-dependent manner. The expression of collagen adhesion (*ace*) exhibited an increase in response to static EVs, but a reduction when exposed to flow EVs.

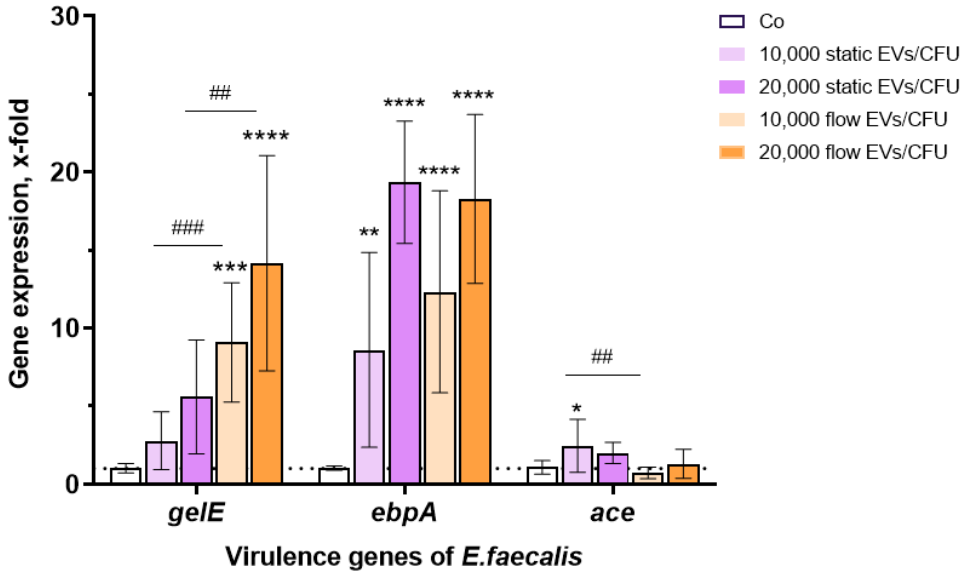

FIGURE 4-13. Expression of virulence-associated genes in *E. faecalis* by qRT-PCR after incubation with HUVEC EVs. Data are normalised to medium-treated bacteria as control (dashed line). Data shown as mean ± SD. EVs from three biological replicates were used, and qPCR was performed in three technical replicates.

4.3 Discussion

In the first step, it was necessary to find an approach to prevent FCS-derived EV contaminants (Urzì, Bagge, and Crescitelli 2022). Although some protocols simply proceed with serum-free medium for EV isolation from human cell lines (Q. Zhang et al. 2023; F. Wang, Cerione, and Antonyak 2021), the utilization of primary endothelial cells in this work, which were intended to be cultured under flow conditions, prevented us from removing FCS from our setting. During the primary setup experiments, these cells were observed to be detached when grown in FCS-free medium under static culture conditions, leading us to conclude that they would not maintain adherence under the mechanical force of shear flow in serum-free medium. Consequently, our approach involved an effort to deplete EVs from FCS, aiming to address this critical aspect of our experimental setup.

Shelke et al. compared the centrifugation of FCS for a short (1.5 h) and a long period (18 h) to test the efficiency of these two EV depletion protocols. They found that 18 h centrifugation reduced FCS-derived EV RNA content by 95%; however, it does not completely eliminate EV contaminants from FCS (Shelke et al. 2014). Later, a study on the effects of serum dilution on the depletion efficiency suggested that the amount of RNA in the EV-depleted supernatant was reduced in diluted FCS compared to non-diluted condition, and thus recommended to dilute the FCS to 30% prior to EV depletion (Driedonks, Nijen Twilhaar, and Nolte-‘t Hoen 2018). Therefore, in this study, a medium containing 30% FCS was ultracentrifuged and then utilized to formulate the primary culture medium for EV production during the incubation period.

One study on the impact of different media on EV production has previously reported that EVs produced from N2a mouse neuroblastoma cells in Opti-MEM (reduced-serum medium) were greater in quantity than EVs produced in DMEM-containing serum (J. Li et al. 2015). Later, the same group attempted to identify specific media components affecting EV production. They found higher levels of EV surface markers (CD9, CD63, and CD81) from HEK293T cells cultured in serum-free Opti-MEM compared to serum-including conditions. Interestingly, a CD81+ EV population was not detectable by western blot analysis when complete medium was used to harvest EVs (Bost et al. 2022). Also comparing the enrichment levels of genes comprising a certain gene ontology term between the different media conditions, in which cells were cultured for EV production, Bost et al. found that the sphingolipid and ceramide pathways influencing exosome production (Verderio, Gabrielli, and Giussani 2018), were upregulated in the Opti-MEM samples compared to the serum-containing media. CD63 functions in ESCRT-independent vesicle formation (van Niel et al. 2011), and ESCRT-independent exosome formation relies on ceramide generation by neutral sphingomyelinase (Elsherbini and Bieberich 2018). This could explain the presence of CD63 marker in HUVEC-derived EVs when low serum amount was employed.

In this work, in addition to static culture condition, we also characterized vesicles isolated from HUVECs subjected to laminar flow trying to simulate the physiological conditions. Several fluid shear stress models have been used in the literature. Parallel-plate flow chambers like the one we used for set up experiments allow the cell layer to be observed with a microscope (Sun, Zhang, and Xia 2021). Cone-and-plate systems are used to analyze the shear responses of cells to flow independent of hydrostatic pressure (Franzoni et al. 2016). The orbital shaker method is able to generate a larger disturbed flow (Fernandes et al. 2022). In recent years, microfluidic systems have been often, allowing the creation of constant or active shear flow with external equipment, like pumps, which dynamically adjust fluid shear stress by altering the inlet flow (Mohammed et al. 2019; Tovar-Lopez et al. 2019; Takahashi et al. 2023). However, the choice of a specific model depends on the downstream analysis requirements. Here we used a hollow fiber cartridge system (Ebrahim et al. 2019) that allowed for larger-scale cell cultivation compared to other commercially available *in vitro* settings. This made it possible to isolate EVs from a

large volume of conditioned medium required for downstream processing; therefore, reducing the number of batches needed for multiple analysis and improving the consistency of the data generated.

Commonly used EV isolation methods including ultracentrifugation, density gradient centrifugation, size exclusion chromatography, and polymer-based precipitation, vary in EV yield, the depletion of protein contaminants, labour-intensity, and cost of the procedure. Utilizing a combination of two or more methods has the potential to enhance the removal of protein contaminants; however, it comes at the cost of reducing the overall number of EVs (Brennan et al. 2020). Therefore, the choice of EV isolation method used should depend on the amount of starting material together with the downstream application. Although commercial EV separation kits have been used to isolate EVs from HUVECs (Jeon, Kang, and Lee 2020; Hosseinkhani et al. 2020), differential centrifugation has been the most widely used method (Maiullari et al. 2021; Jeon, Kang, and Lee 2020; Mensà et al. 2020; Hosseinkhani et al. 2018; Lamichhane et al. 2017; Jeon et al. 2017; Lin et al. 2016). In our research, we isolated vesicles from the culture medium using ultracentrifugation, without additional purification steps. This decision was due to the noticeable sample loss observed during trial runs of size exclusion chromatography to purify the isolated EVs.

Definitive characterization of biogenesis-based EV subtypes is challenging, as there are no universal molecular markers for ectosomes (also known as microvesicle or microparticle; refers to EVs originating from the cell surface), exosomes (refers to EVs originating from internal compartments of the cell, released *via* MVBs), or other EV subtypes (Welsh et al. 2024). In our work, we examined a series of EV protein markers based on previous reports (Mashayekhi et al. 2024; Hoppstädter et al. 2019; van Niel, D'Angelo, and Raposo 2018) irrespective of the biogenesis routes. A genome-wide association study for coronary artery disease involving over a million participants identified MFG-E8 as one of the risk variants and genes associated with cardiovascular diseases (Aragam et al. 2022) positioning it as a potential prognostic biomarker for vascular diseases (Ni, Zhan, and Liu 2020). An *in vivo* study on endothelial–vascular smooth muscle cell (VSMC) interactions in mice further highlighted the role of MFG-E8 in driving the pro-inflammatory phenotypic shift of VSMCs (Chiang, Chu, and Lee 2019). Dysregulated EC-VSMC communication was shown to potentially contribute to the development of atherosclerosis (M. Li et al. 2018). Among the more abundant proteins in flow EVs, we observed a variety of mitochondrial proteins that were either absent or less prominent in static EVs. This observation aligns with previous reports documenting the presence of mitochondrial proteins in EVs from mouse embryonic fibroblasts and monocyte-derived dendritic cells (Todkar et al. 2021; Kowal et al. 2016). Vascular endothelial cells sense shear stress generated by flowing blood and transmit this information into the cell interior (Ando and Yamamoto 2021). Previous data have shown a role of mitochondria in the EC mechanotransduction of fluid shear stress (Scheitlin et al. 2016; Yamamoto et al. 2023). A recent study suggests that changes in the magnitude and pattern of fluid shear stress alter the mitochondrial content, shape, and intracellular distribution in different vessel regions of a mouse model *in vivo* and in primary mouse aortic endothelial cells *in vitro* (Hong et al. 2022). It has been shown that unidirectional flow induces an elevation of oxidative phosphorylation-dependent ATP generation (Yamamoto, Imamura, and Ando 2018; Yamamoto et al. 2020; Han et al. 2021). On the other hand, exposing HUVECs to laminar flow (20 dynes cm^{-2}) for 24 h decreases glycolysis pathway (Basehore et al. 2021). In line with these findings, we saw an increase in ATP synthase subunits (ATP5MF, ATP5F1A, ATP5F1B, ATP5ME, ATP5PB) and other respiratory chain members (CYC1 (Cytochrome c1. heme protein), UQCRC1 (Cytochrome b-c1 complex subunit 1), and COX4I1 (Cytochrome c oxidase subunit 4 isoform 1)) in flow EVs. Furthermore, PDP1 (Pyruvate dehydrogenase phosphatase 1), a mediator of glycolysis pathway (X. Wang et al. 2021), was not detected in any of the flow EV replicates.

Intracellular miRNA expression profiles of ECs adapt to diverse flow patterns and impact endothelial biology (Mitić and Caporali 2023; X. Zhang et al. 2023; X. Xu et al. 2021; Rashad et al. 2020). Cellular culture conditions are not only reflected in exosomal proteins but also in miRNA contents. Therefore, we hypothesized that the miRNA content of ECs is also regulated by shear stress. To test this, we performed miRNA sequencing with EVs and cells.

MiRNA-451a was among the significantly enriched miRNAs in both flow EVs and parental cells, with lower abundance in static samples. It is also reported to be downregulated in EVs derived from shear stress culture of ±5 dyne cm^{-2} compared to when 20 dyne cm^{-2} was applied on HUVECs for 24 h in a cone and plate system (Chung et al. 2022). Patients with atherosclerosis showed significantly lower circulating miRNA-451a than healthy controls (Hu et al. 2021), consistent with our results in static conditions that mimic pro-atherosclerotic environments. The same group showed miRNA-451a upregulation could stimulate HUVECs proliferation and apoptosis by directly targeting macrophage migration inhibitory factor (MIF), suggesting miRNA-451a contribution in regulating atherosclerosis.

MiR-21-5p was significantly abundant in the flow cells. MiRNA-21 expression in endothelial cells has been found to be significantly upregulated by shear stress treatment (Shah et al. 2018), causing an anti-apoptotic effect by directly targeting the PTEN tumor suppressor gene. Further analysis revealed that PTEN, a known target of miR-21, was downregulated in HUVECs exposed to unidirectional shear stress (15 dynes cm^{-2}) or transfected with pre-miR-21. HUVECs overexpressing miR-21 exhibited decreased apoptosis and increased eNOS phosphorylation and nitric oxide (NO) production (Weber et al. 2010). Another significant miRNA in flow cells was miR-1290, which has been shown to increase monocytic THP-1 cells adhesion to HUVECs by regulating ICAM-1 and VCAM-1 (Hongxin Xu et al. 2022).

On the EV side, we saw a significant abundance of miR-320 family in static EVs. MiR-320a, a key regulator of atherogenesis, has been shown to promote this process by enhancing multiple risk factors associated with coronary artery disease (CAD) (C. Chen et al. 2015). Knockdown of miR-320a led to increased proliferation and suppressed apoptosis in cultured endothelial cells. Conversely, the overexpression of miR-320a intensified apoptosis *in vitro* and enhanced vessel abnormalities in the heart, leading to subsequent cardiac dysfunction in mice (Yin et al. 2016). On the other hand, miR-26b was among the most abundant miRs in flow EVs, and has been shown to be an essential mediator for inhibiting endothelial apoptosis both *in vivo* and *in vitro* by directly targeting TRPC6 (Y. Zhang et al. 2015). Another study highlighted the role of miR-26b in endothelial cell growth, survival, and angiogenesis. MiR-26b overexpression enhanced EC proliferation, migration, and tube formation, while inhibition of miR-26b suppressed the proliferative and angiogenic capacity of ECs (Martello et al. 2018).

In chapter one, we studied the effect of bacterial-derived EVs on host cells. This chapter delves deeper into the interaction between the host and microbiome by investigating the influence of host-derived EVs on bacteria, focusing on endothelial derived EVs. Unlike chapter one, the use of DiI dye for labelling EVs and studying their uptake in bacteria was not feasible. Unpurified EVs contain impurities that could disrupt the accuracy of a lipid-incorporating dye like DiI, potentially leading to false positives in uptake studies. We tried an alternative dye that did not require extensive removal steps due to limited material availability. CFSE (carboxyfluorescein succinimidyl ester) is an amine-reactive dye, and fluoresces upon cleavage by esterases (Dehghani and Gaborski 2020). However, since bacterial cells fluoresced when incubated with the dye (data not shown), its use would still lead to false positives without prior removal of non-incorporated dye in the EVs. Therefore, we proceeded with gene expression study. Host-derived EVs are mainly studied with the primary focus on understanding their antiviral and antibacterial effects on pathogens or other host cells (Brakhage et al. 2021). While Enterococci are among contributors to infections in the bloodstream (Suppli et al. 2011), our understanding of how environmental stimuli in the bloodstream impact *Enterococcai* remains relatively limited.

Our data showed changes in gene expression of *E. faecalis* after incubation with HUVEC-derived EVs. Human microRNAs have been identified as important players in the regulation of gene expression during host-pathogen interactions. It has been discovered that human microRNAs can translocate to the pathogen *via* extracellular vesicles, which in turn impact the pathogen's capacity to form biofilms (Koeppen et al. 2021). Thus, non-coding RNAs originating from the bacterial pathogen and the human host are thought to be involved in a phenomenon known as trans-kingdom signaling. These RNAs affect both the pathogen's and the host's gene expression and are crucial for the development of disease as well as the immune system's response to it. Recent reports suggest that certain miRNAs released by mammalian cells can regulate bacterial gene expression (Shirong Liu et al. 2016; 2019; Santos et al. 2020). We also showed miRNAs abundant in either static or flow EVs could target regions of bacterial mRNA. Our results revealed significant abundance of miR-320c in static EVs, and subsequent qPCR data indicated a lower abundance of its potential target, *gelE* mRNA. This pattern was also seen for significantly abundant miRNAs in flow EVs, miR-26b and miR-451a, which the expression of *ace* mRNA as their potential target site was less abundant after incubation with flow EVs. Future investigations need to be conducted to explore the extent to which host miRNA and culture conditions affect virulence.

Here, we identified the optimal media for isolating EVs from primary HUVEC cells, suitable for both static and laminar flow culture conditions. To mimic physiological conditions, we utilized a hollow fiber cartridge to apply laminar shear stress to HUVECs. Additionally, we characterized EVs from static and flow cultures based on morphology, particle size, and content. Our findings revealed an abundance of mitochondrial proteins in EVs isolated from laminar flow cultures. Furthermore, we demonstrated that incubation with EVs derived from HUVECs modulate the gene expression of *E. faecalis*. Further investigations would expand the findings of this study, particularly concerning the internalization mechanisms and regulatory effects at the interface of host EVs and the microbiome.

5 References

Abat, Cédric, Michael Huart, Vincent Garcia, Grégory Dubourg, and Didier Raoult. 2016. "Enterococcus Faecalis Urinary-Tract Infections: Do They Have a Zoonotic Origin?" *Journal of Infection* 73 (4): 305–13. https://doi.org/10.1016/j.jinf.2016.07.012.

Afonina, Irina, Brenda Tien, Zeus Nair, Artur Matysik, Ling Ning Lam, Mark Veleba, Augustine Koh Jing Jie, et al. 2021. "The Composition and Function of Enterococcus Faecalis Membrane Vesicles." *microLife* 2 (January):uqab002. https://doi.org/10.1093/femsml/uqab002.

Al-Fityan, Salma, Britta Diesel, Thorben Fischer, Emmanuel Ampofo, Annika Schomisch, Vida Mashayekhi, Marc Schneider, and Alexandra K. Kiemer. 2023. "Nanostructured Microparticles Repolarize Macrophages and Induce Cell Death in an In Vitro Model of Tumour-Associated Macrophages." *Pharmaceutics* 15 (7): 1895. https://doi.org/10.3390/pharmaceutics15071895.

Ando, Joji, and Kimiko Yamamoto. 2021. "Hemodynamic Forces, Endothelial Mechanotransduction, and Vascular Diseases." *Magnetic Resonance in Medical Sciences* 21 (2): 258–66. https://doi.org/10.2463/mrms.rev.2021-0018.

Aragam, Krishna G., Tao Jiang, Anuj Goel, Stavroula Kanoni, Brooke N. Wolford, Deepak S. Atri, Elle M. Weeks, et al. 2022. "Discovery and Systematic Characterization of Risk Variants and Genes for Coronary Artery Disease in over a Million Participants." *Nature Genetics* 54 (12): 1803–15. https://doi.org/10.1038/s41588-022-01233-6.

Barnes, Aaron M. T., Jennifer L. Dale, Yuqing Chen, Dawn A. Manias, Kerryl E. Greenwood Quaintance, Melissa K. Karau, Purna C. Kashyap, Robin Patel, Carol L. Wells, and Gary M. Dunny. 2016. "Enterococcus Faecalis Readily Colonizes the Entire Gastrointestinal Tract and Forms Biofilms in a Germ-Free Mouse Model." *Virulence* 8 (3): 282–96. https://doi.org/10.1080/21505594.2016.1208890.

Barnes, Aaron M. T., Kristi L. Frank, and Gary M. Dunny. 2021. "Enterococcal Endocarditis: Hiding in Plain Sight." *Frontiers in Cellular and Infection Microbiology* 11. https://www.frontiersin.org/articles/10.3389/fcimb.2021.722482.

Basehore, Sarah E., Samantha Bohlman, Callie Weber, Swathi Swaminathan, Yuji Zhang, Cholsoon Jang, Zoltan Arany, and Alisa Morss Clyne. 2021. "Laminar Flow on Endothelial Cells Suppresses eNOS O-GlcNAcylation to Promote eNOS Activity." *Circulation Research* 129 (11): 1054–66. https://doi.org/10.1161/CIRCRESAHA.121.318982.

Bastounis, Effie E., Prathima Radhakrishnan, Christopher K. Prinz, and Julie A. Theriot. 2022. "Mechanical Forces Govern Interactions of Host Cells with Intracellular Bacterial Pathogens." *Microbiology and Molecular Biology Reviews* 86 (2): e00094-20. https://doi.org/10.1128/mmbr.00094-20.

Baxter, Amy A., Thanh Kha Phan, Eric Hanssen, Michael Liem, Mark D. Hulett, Suresh Mathivanan, and Ivan K. H. Poon. 2019. "Analysis of Extracellular Vesicles Generated from Monocytes under Conditions of Lytic Cell Death." *Scientific Reports* 9 (1): 7538. https://doi.org/10.1038/s41598-019-44021-9.

Bebien, Magali, Mary E. Hensler, Suzel Davanture, Li-Chung Hsu, Michael Karin, Jin Mo Park, Lena Alexopoulou, George Y. Liu, Victor Nizet, and Toby Lawrence. 2012. "The Pore-Forming Toxin β Hemolysin/Cytolysin Triggers P38 MAPK-Dependent IL-10 Production in Macrophages and Inhibits Innate Immunity." *PLOS Pathogens* 8 (7): e1002812. https://doi.org/10.1371/journal.ppat.1002812.

Beganovic, Maya, Megan K Luther, Louis B Rice, Cesar A Arias, Michael J Rybak, and Kerry L LaPlante. 2018. "A Review of Combination Antimicrobial Therapy for Enterococcus Faecalis Bloodstream Infections and Infective Endocarditis." *Clinical Infectious Diseases: An Official Publication of the Infectious Diseases Society of America* 67 (2): 303–9. https://doi.org/10.1093/cid/ciy064.

Bergenhenegouwen, Jeroen van, Theo S. Plantinga, Leo A. B. Joosten, Mihai G. Netea, Gert Folkerts, Aletta D. Kraneveld, Johan Garssen, and Arjan P. Vos. 2013. "TLR2 & Co: A Critical Analysis of the Complex Interactions between TLR2 and Coreceptors." *Journal of Leukocyte Biology* 94 (5): 885–902. https://doi.org/10.1189/jlb.0113003.

Berumen Sánchez, Greg, Kaitlyn E. Bunn, Heather H. Pua, and Marjan Rafat. 2021. "Extracellular Vesicles: Mediators of Intercellular Communication in Tissue Injury and Disease." *Cell Communication and Signaling* 19 (1): 104. https://doi.org/10.1186/s12964-021-00787-y.

Billington, E. O., S. H. Phang, D. B. Gregson, J. D. D. Pitout, T. Ross, D. L. Church, K. B. Laupland, and M. D. Parkins. 2014. "Incidence, Risk Factors, and Outcomes for Enterococcus Spp. Blood Stream Infections: A Population-Based Study." *International Journal of Infectious Diseases* 26 (September):76–82. https://doi.org/10.1016/j.ijid.2014.02.012.

Bitto, Natalie J., Ross Chapman, Sacha Pidot, Adam Costin, Camden Lo, Jasmine Choi, Tanya D'Cruze, et al. 2017. "Bacterial Membrane Vesicles Transport Their DNA Cargo into Host Cells." *Scientific Reports* 7 (1): 7072. https://doi.org/10.1038/s41598-017-07288-4.

Bitto, Natalie J., Lesley Cheng, Ella L. Johnston, Rishi Pathirana, Thanh Kha Phan, Ivan K. H. Poon, Neil M. O'Brien-Simpson, Andrew F. Hill, Timothy P. Stinear, and Maria Kaparakis-Liaskos. 2021. "Staphylococcus Aureus Membrane Vesicles Contain Immunostimulatory DNA, RNA and Peptidoglycan That Activate Innate Immune Receptors and Induce Autophagy." *Journal of Extracellular Vesicles* 10 (6): e12080. https://doi.org/10.1002/jev2.12080.

Bost, Jeremy P., Osama Saher, Daniel Hagey, Doste R. Mamand, Xiuming Liang, Wenyi Zheng, Giulia Corso, et al. 2022. "Growth Media Conditions Influence the Secretion Route and Release Levels of Engineered Extracellular Vesicles." *Advanced Healthcare Materials* 11 (5): 2101658. https://doi.org/10.1002/adhm.202101658.

Brakhage, Axel A, Ann-Kathrin Zimmermann, Flora Rivieccio, Corissa Visser, and Matthew G Blango. 2021. "Host-Derived Extracellular Vesicles for Antimicrobial Defense." *microLife* 2 (January):uqab003. https://doi.org/10.1093/femsml/uqab003.

Brandt, Karim J., Céline Fickentscher, Egbert K. O. Kruithof, and Philippe de Moerloose. 2013. "TLR2 Ligands Induce NF-κB Activation from Endosomal Compartments of Human Monocytes." *PLOS ONE* 8 (12): e80743. https://doi.org/10.1371/journal.pone.0080743.

Brennan, K., K. Martin, S. P. FitzGerald, J. O'Sullivan, Y. Wu, A. Blanco, C. Richardson, and M. M. Mc Gee. 2020. "A Comparison of Methods for the Isolation and Separation of Extracellular Vesicles from Protein and Lipid Particles in Human Serum." *Scientific Reports* 10 (1): 1039. https://doi.org/10.1038/s41598-020-57497-7.

Brown, Lisa, Julie M. Wolf, Rafael Prados-Rosales, and Arturo Casadevall. 2015. "Through the Wall: Extracellular Vesicles in Gram-Positive Bacteria, Mycobacteria and Fungi." *Nature Reviews Microbiology* 13 (10): 620–30. https://doi.org/10.1038/nrmicro3480.

Cao, Zhirui, Naoki Sugimura, Elke Burgermeister, Matthias P. Ebert, Tao Zuo, and Ping Lan. 2022. "The Gut Virome: A New Microbiome Component in Health and Disease." *eBioMedicine* 81 (July). https://doi.org/10.1016/j.ebiom.2022.104113.

Chen, Chen, Yan Wang, Shenglan Yang, Huaping Li, Gang Zhao, Feng Wang, Lei Yang, and Dao Wen Wang. 2015. "MiR-320a Contributes to Atherogenesis by Augmenting Multiple Risk Factors and down-Regulating SRF." *Journal of Cellular and Molecular Medicine* 19 (5): 970–85. https://doi.org/10.1111/jcmm.12483.

Chen, Shanze, Abdullah F. U. H. Saeed, Quan Liu, Qiong Jiang, Haizhao Xu, Gary Guishan Xiao, Lang Rao, and Yanhong Duo. 2023. "Macrophages in Immunoregulation and Therapeutics." *Signal Transduction and Targeted Therapy* 8 (1): 1–35. https://doi.org/10.1038/s41392-023-01452-1.

Chen, Shuang, Michelle H. Wong, Danica J. Schulte, Moshe Arditi, and Kathrin S. Michelsen. 2007. "Differential Expression of Toll-like Receptor 2 (TLR2) and Responses to TLR2 Ligands between

Human and Murine Vascular Endothelial Cells." *Journal of Endotoxin Research* 13 (5): 281–96. https://doi.org/10.1177/0968051907085096.

Chiang, Hou-Yu, Pao-Hsien Chu, and Ting-Hein Lee. 2019. "MFG-E8 Mediates Arterial Aging by Promoting the Proinflammatory Phenotype of Vascular Smooth Muscle Cells." *Journal of Biomedical Science* 26 (1): 61. https://doi.org/10.1186/s12929-019-0559-0.

Chow, J. W., L. A. Thal, M. B. Perri, J. A. Vazquez, S. M. Donabedian, D. B. Clewell, and M. J. Zervos. 1993. "Plasmid-Associated Hemolysin and Aggregation Substance Production Contribute to Virulence in Experimental Enterococcal Endocarditis." *Antimicrobial Agents and Chemotherapy* 37 (11): 2474–77. https://doi.org/10.1128/AAC.37.11.2474.

Christovich, Anna, and Xin M. Luo. 2022. "Gut Microbiota, Leaky Gut, and Autoimmune Diseases." *Frontiers in Immunology* 13 (June). https://doi.org/10.3389/fimmu.2022.946248.

Chung, Jihwa, Kyoung Hwa Kim, Namhee Yu, Shung Hyun An, Sanghyuk Lee, and Kihwan Kwon. 2022. "Fluid Shear Stress Regulates the Landscape of microRNAs in Endothelial Cell-Derived Small Extracellular Vesicles and Modulates the Function of Endothelial Cells." *International Journal of Molecular Sciences* 23 (3): 1314. https://doi.org/10.3390/ijms23031314.

Cicchese, Joseph M., Stephanie Evans, Caitlin Hult, Louis R. Joslyn, Timothy Wessler, Jess A. Millar, Simeone Marino, et al. 2018. "Dynamic Balance of Pro- and Anti-Inflammatory Signals Controls Disease and Limits Pathology." *Immunological Reviews* 285 (1): 147–67. https://doi.org/10.1111/imr.12671.

Clos-Sansalvador, Marta, Marta Monguió-Tortajada, Santiago Roura, Marcella Franquesa, and Francesc E. Borràs. 2022. "Commonly Used Methods for Extracellular Vesicles' Enrichment: Implications in Downstream Analyses and Use." *European Journal of Cell Biology* 101 (3): 151227. https://doi.org/10.1016/j.ejcb.2022.151227.

Coburn, Phillip S., and Michael S. Gilmore. 2003. "The Enterococcus Faecalis Cytolysin: A Novel Toxin Active against Eukaryotic and Prokaryotic Cells." *Cellular Microbiology* 5 (10): 661–69. https://doi.org/10.1046/j.1462-5822.2003.00310.x.

Cocucci, Emanuele, Gabriella Racchetti, and Jacopo Meldolesi. 2009. "Shedding Microvesicles: Artefacts No More." *Trends in Cell Biology* 19 (2): 43–51. https://doi.org/10.1016/j.tcb.2008.11.003.

Costantini, Paolo E., Christophe Vanpouille, Andrea Firrincieli, Martina Cappelletti, Leonid Margolis, and Rogers A. Ñahui Palomino. 2022. "Extracellular Vesicles Generated by Gram-Positive Bacteria Protect Human Tissues Ex Vivo From HIV-1 Infection." *Frontiers in Cellular and Infection Microbiology* 11 (January):822882. https://doi.org/10.3389/fcimb.2021.822882.

Dahl, Anders, Kasper Iversen, Niels Tonder, Nis Hoest, Magnus Arpi, Morten Dalsgaard, Mahtab Chehri, et al. 2019. "Prevalence of Infective Endocarditis in Enterococcus Faecalis Bacteremia." *Journal of the American College of Cardiology* 74 (2): 193–201. https://doi.org/10.1016/j.jacc.2019.04.059.

Dahlem, Charlotte, Wei Xiong Siow, Maria Lopatniuk, William K. F. Tse, Sonja M. Kessler, Susanne H. Kirsch, Jessica Hoppstädter, et al. 2020. "Thioholgamide A, a New Anti-Proliferative Anti-Tumor Agent, Modulates Macrophage Polarization and Metabolism." *Cancers* 12 (5): 1288. https://doi.org/10.3390/cancers12051288.

Dauros Singorenko, Priscila, Vanessa Chang, Alana Whitcombe, Denis Simonov, Jiwon Hong, Anthony Phillips, Simon Swift, and Cherie Blenkiron. 2017. "Isolation of Membrane Vesicles from Prokaryotes: A Technical and Biological Comparison Reveals Heterogeneity." *Journal of Extracellular Vesicles* 6 (1): 1324731. https://doi.org/10.1080/20013078.2017.1324731.

Davies, Peter F. 1995. "Flow-Mediated Endothelial Mechanotransduction." *Physiological Reviews* 75 (3): 519–60.

De Santis, Stefania, Elisabetta Cavalcanti, Mauro Mastronardi, Emilio Jirillo, and Marcello Chieppa. 2015. "Nutritional Keys for Intestinal Barrier Modulation." *Frontiers in Immunology* 6 (December):612. https://doi.org/10.3389/fimmu.2015.00612.

Dehghani, Mehdi, and Thomas R. Gaborski. 2020. "Chapter Two - Fluorescent Labeling of Extracellular Vesicles." In *Methods in Enzymology*, edited by Sheila Spada and Lorenzo Galluzzi, 645:15–42. Extracellular Vesicles. Academic Press. https://doi.org/10.1016/bs.mie.2020.09.002.

Di Vincenzo, Federica, Angelo Del Gaudio, Valentina Petito, Loris Riccardo Lopetuso, and Franco Scaldaferri. 2024. "Gut Microbiota, Intestinal Permeability, and Systemic Inflammation: A Narrative Review." *Internal and Emergency Medicine* 19 (2): 275–93. https://doi.org/10.1007/s11739-023-03374-w.

Diesel, Britta, Nadège Ripoche, Rebecca T. Risch, Sascha Tierling, Jörn Walter, and Alexandra K. Kiemer. 2012. "Inflammation-Induced up-Regulation of TLR2 Expression in Human Endothelial Cells Is Independent of Differential Methylation in the TLR2 Promoter CpG Island." *Innate Immunity* 18 (1): 112–23. https://doi.org/10.1177/1753425910394888.

Dong, Liang, Chung-Ying Huang, Eric J. Johnson, Lei Yang, Richard C. Zieren, Kengo Horie, Chi-Ju Kim, et al. 2021. "High-Throughput Simultaneous mRNA Profiling Using nCounter Technology Demonstrates That Extracellular Vesicles Contain Different mRNA Transcripts Than Their Parental Prostate Cancer Cells." *Analytical Chemistry* 93 (8): 3717–25. https://doi.org/10.1021/acs.analchem.0c03185.

Drage, Michael G., Nicole D. Pecora, Amy G. Hise, Maria Febbraio, Roy L. Silverstein, Douglas T. Golenbock, W. Henry Boom, and Clifford V. Harding. 2009. "TLR2 and Its Co-Receptors Determine Responses of Macrophages and Dendritic Cells to Lipoproteins of Mycobacterium Tuberculosis." *Cellular Immunology* 258 (1): 29–37. https://doi.org/10.1016/j.cellimm.2009.03.008.

Driedonks, Tom A. P., Maarten K. Nijen Twilhaar, and Esther N. M. Nolte-'t Hoen. 2018. "Technical Approaches to Reduce Interference of Fetal Calf Serum Derived RNA in the Analysis of Extracellular Vesicle RNA from Cultured Cells." *Journal of Extracellular Vesicles* 8 (1): 1552059. https://doi.org/10.1080/20013078.2018.1552059.

Ebrahim, Abdul Shukkur, Thomas W. Carion, Eliisa Strand, Laura A. Young, Haoshen Shi, and Elizabeth A. Berger. 2019. "Application of a Flow-Based Hollow-Fiber Co-Culture System to Study Cellular Influences under Hyperglycemic Conditions." *Scientific Reports* 9 (1): 3771. https://doi.org/10.1038/s41598-019-40555-0.

Effah, Clement Yaw, Xianfei Ding, Emmanuel Kwateng Drokow, Xiang Li, Ran Tong, and Tongwen Sun. 2024. "Bacteria-Derived Extracellular Vesicles: Endogenous Roles, Therapeutic Potentials and Their Biomimetics for the Treatment and Prevention of Sepsis." *Frontiers in Immunology* 15 (February). https://doi.org/10.3389/fimmu.2024.1296061.

EL Andaloussi, Samir, Imre Mäger, Xandra O. Breakefield, and Matthew J. A. Wood. 2013. "Extracellular Vesicles: Biology and Emerging Therapeutic Opportunities." *Nature Reviews Drug Discovery* 12 (5): 347–57. https://doi.org/10.1038/nrd3978.

Elsherbini, Ahmed, and Erhard Bieberich. 2018. "Ceramide and Exosomes: A Novel Target in Cancer Biology and Therapy." *Advances in Cancer Research* 140:121–54. https://doi.org/10.1016/bs.acr.2018.05.004.

Escolà-Vergé, Laura, Nuria Fernández-Hidalgo, María Nieves Larrosa, Ruben Fernandez-Galera, and Benito Almirante. 2021. "Secular Trends in the Epidemiology and Clinical Characteristics of Enterococcus Faecalis Infective Endocarditis at a Referral Center (2007–2018)." *European Journal of Clinical Microbiology & Infectious Diseases* 40 (6): 1137–48. https://doi.org/10.1007/s10096-020-04117-x.

Fakharian, Farzaneh, Siva Thirugnanam, David A. Welsh, Woong-Ki Kim, Jay Rappaport, Kyle Bittinger, and Namita Rout. 2023. "The Role of Gut Dysbiosis in the Loss of Intestinal Immune Cell

Functions and Viral Pathogenesis." *Microorganisms* 11 (7): 1849. https://doi.org/10.3390/microorganisms11071849.

Fecher-Trost, Claudia, Ulrich Wissenbach, Andreas Beck, Pascal Schalkowsky, Christof Stoerger, Janka Doerr, Anna Dembek, et al. 2013. "The in Vivo TRPV6 Protein Starts at a Non-AUG Triplet, Decoded as Methionine, Upstream of Canonical Initiation at AUG." *The Journal of Biological Chemistry* 288 (23): 16629–44. https://doi.org/10.1074/jbc.M113.469726.

Fehlmann, Tobias, Fabian Kern, Omar Laham, Christina Backes, Jeffrey Solomon, Pascal Hirsch, Carsten Volz, Rolf Müller, and Andreas Keller. 2021. "miRMaster 2.0: Multi-Species Non-Coding RNA Sequencing Analyses at Scale." *Nucleic Acids Research* 49 (W1): W397–408. https://doi.org/10.1093/nar/gkab268.

Feng, Du, Wen-Long Zhao, Yun-Ying Ye, Xiao-Chen Bai, Rui-Qin Liu, Lei-Fu Chang, Qiang Zhou, and Sen-Fang Sui. 2010. "Cellular Internalization of Exosomes Occurs Through Phagocytosis." *Traffic* 11 (5): 675–87. https://doi.org/10.1111/j.1600-0854.2010.01041.x.

Fernandes, Andreia, Vahid Hosseini, Viola Vogel, and Robert D. Lovchik. 2022. "Engineering Solutions for Biological Studies of Flow-Exposed Endothelial Cells on Orbital Shakers." *PLOS ONE* 17 (1): e0262044. https://doi.org/10.1371/journal.pone.0262044.

Fitzgerald, Katherine A., and Jonathan C. Kagan. 2020. "Toll-like Receptors and the Control of Immunity." *Cell* 180 (6): 1044–66. https://doi.org/10.1016/j.cell.2020.02.041.

Flo, Trude H., Øyvind Halaas, Sverre Torp, Liv Ryan, Egil Lien, Brit Dybdahl, Anders Sundan, and Terje Espevik. 2001. "Differential Expression of Toll-like Receptor 2 in Human Cells." *Journal of Leukocyte Biology* 69 (3): 474–81. https://doi.org/10.1189/jlb.69.3.474.

Flores-Mireles, Ana L., Jennifer N. Walker, Michael Caparon, and Scott J. Hultgren. 2015. "Urinary Tract Infections: Epidemiology, Mechanisms of Infection and Treatment Options." *Nature Reviews Microbiology* 13 (5): 269–84. https://doi.org/10.1038/nrmicro3432.

Frangos, J. A., L. V. McIntire, and S. G. Eskin. 1988. "Shear Stress Induced Stimulation of Mammalian Cell Metabolism." *Biotechnology and Bioengineering* 32 (8): 1053–60. https://doi.org/10.1002/bit.260320812.

Franzoni, Marco, Irene Cattaneo, Bogdan Ene-Iordache, Alberto Oldani, Paolo Righettini, and Andrea Remuzzi. 2016. "Design of a Cone-and-Plate Device for Controlled Realistic Shear Stress Stimulation on Endothelial Cell Monolayers." *Cytotechnology* 68 (5): 1885–96. https://doi.org/10.1007/s10616-015-9941-2.

Freedberg, Daniel E., Margaret J. Zhou, Margot E. Cohen, Medini K. Annavajhala, Sabrina Khan, Dagmara I. Moscoso, Christian Brooks, et al. 2018. "Pathogen Colonization of the Gastrointestinal Microbiome at Intensive Care Unit Admission and Risk for Subsequent Death or Infection." *Intensive Care Medicine* 44 (8): 1203–11. https://doi.org/10.1007/s00134-018-5268-8.

Furuyama, Noemi, and Marcelo Palma Sircili. 2021. "Outer Membrane Vesicles (OMVs) Produced by Gram-Negative Bacteria: Structure, Functions, Biogenesis, and Vaccine Application." *BioMed Research International* 2021 (March):1490732. https://doi.org/10.1155/2021/1490732.

Ge, Steven Xijin, Eun Wo Son, and Runan Yao. 2018. "iDEP: An Integrated Web Application for Differential Expression and Pathway Analysis of RNA-Seq Data." *BMC Bioinformatics* 19 (1): 534. https://doi.org/10.1186/s12859-018-2486-6.

Greening, David W., Rong Xu, Shashi K. Gopal, Alin Rai, and Richard J. Simpson. 2017. "Proteomic Insights into Extracellular Vesicle Biology – Defining Exosomes and Shed Microvesicles." *Expert Review of Proteomics* 14 (1): 69–95. https://doi.org/10.1080/14789450.2017.1260450.

Guerardel, Yann, Irina Sadovskaya, Emmanuel Maes, Sylviane Furlan, Marie-Pierre Chapot-Chartier, Stéphane Mesnage, Lionel Rigottier-Gois, and Pascale Serror. 2020. "Complete Structure of the Enterococcal Polysaccharide Antigen (EPA) of Vancomycin-Resistant Enterococcus Faecalis V583 Reveals That EPA Decorations Are Teichoic Acids Covalently Linked to a

Rhamnopolysaccharide Backbone." *mBio* 11 (2): e00277-20. https://doi.org/10.1128/mBio.00277-20.

Guilliams, Martin, and Freya R. Svedberg. 2021. "Does Tissue Imprinting Restrict Macrophage Plasticity?" *Nature Immunology* 22 (2): 118–27. https://doi.org/10.1038/s41590-020-00849-2.

Guiton, Pascale S., Thomas J. Hannan, Bradley Ford, Michael G. Caparon, and Scott J. Hultgren. 2013. "Enterococcus Faecalis Overcomes Foreign Body-Mediated Inflammation To Establish Urinary Tract Infections." *Infection and Immunity* 81 (1): 329–39. https://doi.org/10.1128/IAI.00856-12.

Hahn, Rebecca T., Jessica Hoppstädter, Kerstin Hirschfelder, Nina Hachenthal, Britta Diesel, Sonja M. Kessler, Hanno Huwer, and Alexandra K. Kiemer. 2014. "Downregulation of the Glucocorticoid-Induced Leucine Zipper (GILZ) Promotes Vascular Inflammation." *Atherosclerosis* 234 (2): 391–400. https://doi.org/10.1016/j.atherosclerosis.2014.03.028.

Han, Yue, Ming He, Traci Marin, Hui Shen, Wei-Ting Wang, Tzong-Yi Lee, Hsiao-Chin Hong, et al. 2021. "Roles of KLF4 and AMPK in the Inhibition of Glycolysis by Pulsatile Shear Stress in Endothelial Cells." *Proceedings of the National Academy of Sciences of the United States of America* 118 (21): e2103982118. https://doi.org/10.1073/pnas.2103982118.

Hancock, Lynn E., Barbara E. Murray, and Jouko Sillanpää. 2014. "Enterococcal Cell Wall Components and Structures." In *Enterococci: From Commensals to Leading Causes of Drug Resistant Infection*, edited by Michael S. Gilmore, Don B. Clewell, Yasuyoshi Ike, and Nathan Shankar. Boston: Massachusetts Eye and Ear Infirmary. http://www.ncbi.nlm.nih.gov/books/NBK190431/.

Heinrich, Eilien, Olga Hartwig, Christine Walt, Arefeh Kardani, Marcus Koch, Leila Pourtalebi Jahromi, Jessica Hoppstädter, et al. 2023. "Cell-Derived Vesicles for Antibiotic Delivery—Understanding the Challenges of a Biogenic Carrier System." *Small* 19 (25): 2207479. https://doi.org/10.1002/smll.202207479.

Hickey, Christina A., Kristine A. Kuhn, David L. Donermeyer, Nathan T. Porter, Chunsheng Jin, Elizabeth A. Cameron, Haerin Jung, et al. 2015. "Colitogenic Bacteroides Thetaiotaomicron Antigens Access Host Immune Cells in a Sulfatase-Dependent Manner via Outer Membrane Vesicles." *Cell Host & Microbe* 17 (5): 672–80. https://doi.org/10.1016/j.chom.2015.04.002.

Hong, Soon-Gook, Junchul Shin, Soo Young Choi, Jeffery C. Powers, Benjamin M. Meister, Jacqueline Sayoc, Jun Seok Son, et al. 2022. "Flow Pattern–Dependent Mitochondrial Dynamics Regulates the Metabolic Profile and Inflammatory State of Endothelial Cells." *JCI Insight* 7 (18). https://doi.org/10.1172/jci.insight.159286.

Hoppstädter, Jessica, Anna Dembek, Rebecca Linnenberger, Charlotte Dahlem, Ahmad Barghash, Claudia Fecher-Trost, Gregor Fuhrmann, et al. 2019. "Toll-Like Receptor 2 Release by Macrophages: An Anti-Inflammatory Program Induced by Glucocorticoids and Lipopolysaccharide." *Frontiers in Immunology* 10 (July):1634. https://doi.org/10.3389/fimmu.2019.01634.

Hosseinkhani, Baharak, Nynke M.S. van den Akker, Daniel G.M. Molin, and Luc Michiels. 2020. "(Sub)Populations of Extracellular Vesicles Released by TNF-α –Triggered Human Endothelial Cells Promote Vascular Inflammation and Monocyte Migration." *Journal of Extracellular Vesicles* 9 (1): 1801153. https://doi.org/10.1080/20013078.2020.1801153.

Hosseinkhani, Baharak, Sören Kuypers, Nynke M. S. van den Akker, Daniel G. M. Molin, and Luc Michiels. 2018. "Extracellular Vesicles Work as a Functional Inflammatory Mediator Between Vascular Endothelial Cells and Immune Cells." *Frontiers in Immunology* 9 (August). https://doi.org/10.3389/fimmu.2018.01789.

Hou, Kaijian, Zhuo-Xun Wu, Xuan-Yu Chen, Jing-Quan Wang, Dongya Zhang, Chuanxing Xiao, Dan Zhu, et al. 2022. "Microbiota in Health and Diseases." *Signal Transduction and Targeted Therapy* 7 (1): 1–28. https://doi.org/10.1038/s41392-022-00974-4.

Hu, Hongxia, Ping Guo, Qian Zhao, Haoran Li, Hualei Liu, and Caihong Ma. 2021. "Upregulation of microRNA-451a Improves Endothelial Cell Function in Atherosclerosis by Direct Targeting of Macrophage Migration Inhibitory Factor." *BIOCELL* 45 (4): 995–1004. https://doi.org/10.32604/biocell.2021.012851.

Huttenhower, Curtis, Dirk Gevers, Rob Knight, Sahar Abubucker, Jonathan H. Badger, Asif T. Chinwalla, Heather H. Creasy, et al. 2012. "Structure, Function and Diversity of the Healthy Human Microbiome." *Nature* 486 (7402): 207–14. https://doi.org/10.1038/nature11234.

Huycke, M. M., C. A. Spiegel, and M. S. Gilmore. 1991. "Bacteremia Caused by Hemolytic, High-Level Gentamicin-Resistant Enterococcus Faecalis." *Antimicrobial Agents and Chemotherapy* 35 (8): 1626–34. https://doi.org/10.1128/AAC.35.8.1626.

Ike, Y., H. Hashimoto, and D. B. Clewell. 1984. "Hemolysin of Streptococcus Faecalis Subspecies Zymogenes Contributes to Virulence in Mice." *Infection and Immunity* 45 (2): 528–30. https://doi.org/10.1128/iai.45.2.528-530.1984.

Jeon, Hyungtaek, Su-Kyung Kang, and Myung-Shin Lee. 2020. "Effects of Different Separation Methods on the Physical and Functional Properties of Extracellular Vesicles." *PLOS ONE* 15 (7): e0235793. https://doi.org/10.1371/journal.pone.0235793.

Jeon, Hyungtaek, Seung-Min Yoo, Hyo Sun Choi, Ji Young Mun, Hee-Gyoo Kang, Jiyeong Lee, Jinsung Park, Shou-Jiang Gao, and Myung-Shin Lee. 2017. "Extracellular Vesicles from KSHV-Infected Endothelial Cells Activate the Complement System." *Oncotarget* 8 (59): 99841–60. https://doi.org/10.18632/oncotarget.21668.

Jeong, Dokyung, Min Jeong Kim, Yejin Park, Jinkyoung Chung, Hee-Seok Kweon, Nae-Gyu Kang, Seung Jin Hwang, Sung Hun Youn, Bo Kyoung Hwang, and Doory Kim. 2022. "Visualizing Extracellular Vesicle Biogenesis in Gram-Positive Bacteria Using Super-Resolution Microscopy." *BMC Biology* 20 (1): 270. https://doi.org/10.1186/s12915-022-01472-3.

Jett, B. D., H. G. Jensen, R. E. Nordquist, and M. S. Gilmore. 1992. "Contribution of the pAD1-Encoded Cytolysin to the Severity of Experimental Enterococcus Faecalis Endophthalmitis." *Infection and Immunity* 60 (6): 2445–52. https://doi.org/10.1128/iai.60.6.2445-2452.1992.

Jiang, Yuyun, Xi Liu, Jixian Ye, Yongbin Ma, Jiahui Mao, Dingqi Feng, and Xuefeng Wang. 2023. "Migrasomes, a New Mode of Intercellular Communication." *Cell Communication and Signaling* 21 (1): 105. https://doi.org/10.1186/s12964-023-01121-4.

Kakarla, Ramesh, Jaehark Hur, Yeon Ji Kim, Jaeyoung Kim, and Yong-Joon Chwae. 2020. "Apoptotic Cell-Derived Exosomes: Messages from Dying Cells." *Experimental & Molecular Medicine* 52 (1): 1–6. https://doi.org/10.1038/s12276-019-0362-8.

Kalra, Hina, Gregor P. C. Drummen, and Suresh Mathivanan. 2016. "Focus on Extracellular Vesicles: Introducing the Next Small Big Thing." *International Journal of Molecular Sciences* 17 (2): 170. https://doi.org/10.3390/ijms17020170.

Kawasaki, Takumi, and Taro Kawai. 2014. "Toll-Like Receptor Signaling Pathways." *Frontiers in Immunology* 5. https://www.frontiersin.org/articles/10.3389/fimmu.2014.00461.

Khalil, Maha A., Jamal A. Alorabi, Lamya M. Al-Otaibi, Sameh S. Ali, and Sobhy E. Elsilk. 2023. "Antibiotic Resistance and Biofilm Formation in Enterococcus Spp. Isolated from Urinary Tract Infections." *Pathogens* 12 (1): 34. https://doi.org/10.3390/pathogens12010034.

Kim, Ji Hyun, Jaewook Lee, Jaesung Park, and Yong Song Gho. 2015. "Gram-Negative and Gram-Positive Bacterial Extracellular Vesicles." *Seminars in Cell & Developmental Biology* 40 (April):97–104. https://doi.org/10.1016/j.semcdb.2015.02.006.

Kline, Kimberly A., and Amanda L. Lewis. 2016. "Gram-Positive Uropathogens, Polymicrobial Urinary Tract Infection, and the Emerging Microbiota of the Urinary Tract." *Microbiology Spectrum* 4 (2): 10.1128/microbiolspec.uti-0012–2012. https://doi.org/10.1128/microbiolspec.uti-0012-2012.

Koeppen, Katja, Amanda Nymon, Roxanna Barnaby, Laura Bashor, Zhongyou Li, Thomas H. Hampton, Amanda E. Liefeld, et al. 2021. "Let-7b-5p in Vesicles Secreted by Human Airway Cells Reduces Biofilm Formation and Increases Antibiotic Sensitivity of P. Aeruginosa." *Proceedings of the National Academy of Sciences* 118 (28): e2105370118. https://doi.org/10.1073/pnas.2105370118.

Kowal, Joanna, Guillaume Arras, Marina Colombo, Mabel Jouve, Jakob Paul Morath, Bjarke Primdal-Bengtson, Florent Dingli, Damarys Loew, Mercedes Tkach, and Clotilde Théry. 2016. "Proteomic Comparison Defines Novel Markers to Characterize Heterogeneous Populations of Extracellular Vesicle Subtypes." *Proceedings of the National Academy of Sciences* 113 (8): E968–77. https://doi.org/10.1073/pnas.1521230113.

Lamichhane, Tek N., Christopher A. Leung, Lampouguin Yenkoidiok Douti, and Steven M. Jay. 2017. "Ethanol Induces Enhanced Vascularization Bioactivity of Endothelial Cell-Derived Extracellular Vesicles via Regulation of MicroRNAs and Long Non-Coding RNAs." *Scientific Reports* 7 (1): 13794. https://doi.org/10.1038/s41598-017-14356-2.

Larsson, Erik, Valentina Tremaroli, Ying Shiuan Lee, Omry Koren, Intawat Nookaew, Ashwana Fricker, Jens Nielsen, Ruth E. Ley, and Fredrik Bäckhed. 2012. "Analysis of Gut Microbial Regulation of Host Gene Expression along the Length of the Gut and Regulation of Gut Microbial Ecology through MyD88." *Gut* 61 (8): 1124–31. https://doi.org/10.1136/gutjnl-2011-301104.

Laskin, D. L., R. A. Soltys, R. A. Berg, and D. J. Riley. 1994. "Activation of Alveolar Macrophages by Native and Synthetic Collagen-like Polypeptides." *American Journal of Respiratory Cell and Molecular Biology* 10 (1): 58–64. https://doi.org/10.1165/ajrcmb.10.1.8292381.

Leendertse, Masja, Rob J. L. Willems, Roelof Flierman, Alex F. de Vos, Marc J. M. Bonten, and Tom van der Poll. 2010. "The Complement System Facilitates Clearance of Enterococcus Faecium during Murine Peritonitis." *The Journal of Infectious Diseases* 201 (4): 544–52. https://doi.org/10.1086/650341.

Leendertse, Masja, Rob J. L. Willems, Ida A. J. Giebelen, Joris J. T. H. Roelofs, Marc J. M. Bonten, and Tom van der Poll. 2009. "Neutrophils Are Essential for Rapid Clearance of Enterococcus Faecium in Mice." *Infection and Immunity* 77 (1): 485–91. https://doi.org/10.1128/IAI.00863-08.

Leendertse, Masja, Rob J.L. Willems, Ida A.J. Giebelen, Joris J.T.H. Roelofs, Nico van Rooijen, Marc J.M. Bonten, and Tom van der Poll. 2009. "Peritoneal Macrophages Are Important for the Early Containment of Enterococcus Faecium Peritonitis in Mice." *Innate Immunity* 15 (1): 3–12. https://doi.org/10.1177/1753425908100238.

Lehrich, Brandon M., Yaxuan Liang, and Massimo S. Fiandaca. 2021. "Foetal Bovine Serum Influence on in Vitro Extracellular Vesicle Analyses." *Journal of Extracellular Vesicles* 10 (3). https://doi.org/10.1002/jev2.12061.

Li, Danyang, and Minghua Wu. 2021. "Pattern Recognition Receptors in Health and Diseases." *Signal Transduction and Targeted Therapy* 6 (1): 1–24. https://doi.org/10.1038/s41392-021-00687-0.

Li, Jinghuan, Yi Lee, Henrik J. Johansson, Imre Mäger, Pieter Vader, Joel Z. Nordin, Oscar P. B. Wiklander, Janne Lehtiö, Matthew J. A. Wood, and Samir EL Andaloussi. 2015. "Serum-Free Culture Alters the Quantity and Protein Composition of Neuroblastoma-Derived Extracellular Vesicles." *Journal of Extracellular Vesicles* 4. https://doi.org/10.3402/jev.v4.26883.

Li, Manna, Ming Qian, Kathy Kyler, and Jian Xu. 2018. "Endothelial–Vascular Smooth Muscle Cells Interactions in Atherosclerosis." *Frontiers in Cardiovascular Medicine* 5 (October). https://doi.org/10.3389/fcvm.2018.00151.

Liao, Sumei, Marlise I. Klein, Kyle P. Heim, Yuwei Fan, Jacob P. Bitoun, San-Joon Ahn, Robert A. Burne, Hyun Koo, L. Jeannine Brady, and Zezhang T. Wen. 2014. "Streptococcus Mutans Extracellular DNA Is Upregulated during Growth in Biofilms, Actively Released via Membrane Vesicles, and

Influenced by Components of the Protein Secretion Machinery." *Journal of Bacteriology* 196 (13): 2355–66. https://doi.org/10.1128/jb.01493-14.

Lin, Xiao, Yu He, Xue Hou, Zhenming Zhang, Rui Wang, and Qiong Wu. 2016. "Endothelial Cells Can Regulate Smooth Muscle Cells in Contractile Phenotype through the miR-206/ARF6&NCX1/Exosome Axis." *PLOS ONE* 11 (3): e0152959. https://doi.org/10.1371/journal.pone.0152959.

Linden, Peter. 2003. "Can Enterococcal Infections Initiate Sepsis Syndrome?" *Current Infectious Disease Reports* 5 (5): 372–78. https://doi.org/10.1007/s11908-003-0016-8.

Liu, Shirong, Andre Pires da Cunha, Rafael M. Rezende, Ron Cialic, Zhiyun Wei, Lynn Bry, Laurie E. Comstock, Roopali Gandhi, and Howard L. Weiner. 2016. "The Host Shapes the Gut Microbiota via Fecal microRNA." *Cell Host & Microbe* 19 (1): 32–43. https://doi.org/10.1016/j.chom.2015.12.005.

Liu, Shirong, Rafael M. Rezende, Thais G. Moreira, Stephanie K. Tankou, Laura M. Cox, Meng Wu, Anya Song, et al. 2019. "Oral Administration of miR-30d from Feces of MS Patients Suppresses MS-like Symptoms in Mice by Expanding Akkermansia Muciniphila." *Cell Host & Microbe* 26 (6): 779-794.e8. https://doi.org/10.1016/j.chom.2019.10.008.

Liu, Shu, André Hossinger, Sarah Göbbels, and Ina M. Vorberg. 2017. "Prions on the Run: How Extracellular Vesicles Serve as Delivery Vehicles for Self-Templating Protein Aggregates." *Prion* 11 (2): 98–112. https://doi.org/10.1080/19336896.2017.1306162.

Liu, Ya-Juan, and Cheng Wang. 2023. "A Review of the Regulatory Mechanisms of Extracellular Vesicles-Mediated Intercellular Communication." *Cell Communication and Signaling* 21 (1): 77. https://doi.org/10.1186/s12964-023-01103-6.

Luo, Rongjin, Yanmin Chang, Huaizhen Liang, Weifeng Zhang, Yu Song, Gaocai Li, and Cao Yang. 2023. "Interactions between Extracellular Vesicles and Microbiome in Human Diseases: New Therapeutic Opportunities." *iMeta* 2 (2): e86. https://doi.org/10.1002/imt2.86.

Ma, Liang, Ying Li, Junya Peng, Danni Wu, Xiaoxin Zhao, Yitong Cui, Lilian Chen, Xiaojun Yan, Yanan Du, and Li Yu. 2015. "Discovery of the Migrasome, an Organelle Mediating Release of Cytoplasmic Contents during Cell Migration." *Cell Research* 25 (1): 24–38. https://doi.org/10.1038/cr.2014.135.

Machata, Silke, Svetlin Tchatalbachev, Walid Mohamed, Lothar Jänsch, Torsten Hain, and Trinad Chakraborty. 2008. "Lipoproteins of Listeria Monocytogenes Are Critical for Virulence and TLR2-Mediated Immune Activation1." *The Journal of Immunology* 181 (3): 2028–35. https://doi.org/10.4049/jimmunol.181.3.2028.

Maiullari, Fabio, Maila Chirivì, Marco Costantini, Anna Maria Ferretti, Sandro Recchia, Silvia Maiullari, Marika Milan, et al. 2021. "In Vivo Organized Neovascularization Induced by 3D Bioprinted Endothelial-Derived Extracellular Vesicles." *Biofabrication* 13 (3): 035014. https://doi.org/10.1088/1758-5090/abdacf.

Mäkinen, P. L., D. B. Clewell, F. An, and K. K. Mäkinen. 1989. "Purification and Substrate Specificity of a Strongly Hydrophobic Extracellular Metalloendopeptidase ('gelatinase') from Streptococcus Faecalis (Strain 0G1-10)." *The Journal of Biological Chemistry* 264 (6): 3325–34.

Maredia, Reshma, Navya Devineni, Peter Lentz, Shatha F. Dallo, JiehJuen Yu, Neal Guentzel, James Chambers, Bernard Arulanandam, William E. Haskins, and Tao Weitao. 2012. "Vesiculation from *Pseudomonas Aeruginosa* under SOS." *The Scientific World Journal* 2012 (February):e402919. https://doi.org/10.1100/2012/402919.

Martello, Andrea, David Mellis, Marco Meloni, Alison Howarth, Daniel Ebner, Andrea Caporali, and Ayman Al Haj Zen. 2018. "Phenotypic miRNA Screen Identifies miR-26b to Promote the Growth and Survival of Endothelial Cells." *Molecular Therapy. Nucleic Acids* 13 (December):29–43. https://doi.org/10.1016/j.omtn.2018.08.006.

Mashayekhi, Vida, Annika Schomisch, Sari Rasheed, Ernesto Aparicio-Puerta, Timo Risch, Daniela Yildiz, Marcus Koch, et al. 2024. "The RNA Binding Protein IGF2BP2/IMP2 Alters the Cargo of Cancer Cell-Derived Extracellular Vesicles Supporting Tumor-Associated Macrophages." *Cell Communication and Signaling : CCS* 22 (June):344. https://doi.org/10.1186/s12964-024-01701-y.

Mateescu, Bogdan, Emma J. K. Kowal, Bas W. M. van Balkom, Sabine Bartel, Suvendra N. Bhattacharyya, Edit I. Buzás, Amy H. Buck, et al. 2017. "Obstacles and Opportunities in the Functional Analysis of Extracellular Vesicle RNA – an ISEV Position Paper." *Journal of Extracellular Vesicles* 6 (1): 1286095. https://doi.org/10.1080/20013078.2017.1286095.

McQueen, Anna, and Christina M. Warboys. 2023. "Mechanosignalling Pathways That Regulate Endothelial Barrier Function." *Current Opinion in Cell Biology* 84 (October):102213. https://doi.org/10.1016/j.ceb.2023.102213.

McWhorter, Frances Y., Tingting Wang, Phoebe Nguyen, Thanh Chung, and Wendy F. Liu. 2013. "Modulation of Macrophage Phenotype by Cell Shape." *Proceedings of the National Academy of Sciences of the United States of America* 110 (43): 17253–58. https://doi.org/10.1073/pnas.1308887110.

Mehanny, Mina, Marcus Koch, Claus-Michael Lehr, and Gregor Fuhrmann. 2020. "Streptococcal Extracellular Membrane Vesicles Are Rapidly Internalized by Immune Cells and Alter Their Cytokine Release." *Frontiers in Immunology* 11 (February). https://doi.org/10.3389/fimmu.2020.00080.

Mensà, Emanuela, Michele Guescini, Angelica Giuliani, Maria Giulia Bacalini, Deborah Ramini, Giacomo Corleone, Manuela Ferracin, et al. 2020. "Small Extracellular Vesicles Deliver miR-21 and miR-217 as pro-Senescence Effectors to Endothelial Cells." *Journal of Extracellular Vesicles* 9 (1). https://doi.org/10.1080/20013078.2020.1725285.

Minciacchi, Valentina R., Michael R. Freeman, and Dolores Di Vizio. 2015. "Extracellular Vesicles in Cancer: Exosomes, Microvesicles and the Emerging Role of Large Oncosomes." *Seminars in Cell & Developmental Biology* 40 (April):41–51. https://doi.org/10.1016/j.semcdb.2015.02.010.

Mitić, Tijana, and Andrea Caporali. 2023. "Emerging Roles of Non-Coding RNAs in Endothelial Cell Function." *Current Opinion in Physiology* 34 (August):100672. https://doi.org/10.1016/j.cophys.2023.100672.

Moellering, R. C. 1992. "Emergence of Enterococcus as a Significant Pathogen." *Clinical Infectious Diseases* 14 (6): 1173–78. https://doi.org/10.1093/clinids/14.6.1173.

Mohamed Elashiry, Mohamed, Fucong Tian, Mahmoud Elashiry, Rana Zeitoun, Ranya Elsayed, Matthew L. Andrews, Brian E. Bergeon, Christopher Cutler, and Franklin Tay. 2021. "Enterococcus Faecalis Shifts Macrophage Polarization toward M1-like Phenotype with an Altered Cytokine Profile." *Journal of Oral Microbiology* 13 (1): 1868152. https://doi.org/10.1080/20002297.2020.1868152.

Mohammad, Majd, Abukar Ali, Minh-Thu Nguyen, Friedrich Götz, Rille Pullerits, and Tao Jin. 2022. "Staphylococcus Aureus Lipoproteins in Infectious Diseases." *Frontiers in Microbiology* 13. https://www.frontiersin.org/articles/10.3389/fmicb.2022.1006765.

Mohammed, Mokhaled, Peter Thurgood, Christopher Gilliam, Ngan Nguyen, Elena Pirogova, Karlheinz Peter, Khashayar Khoshmanesh, and Sara Baratchi. 2019. "Studying the Response of Aortic Endothelial Cells under Pulsatile Flow Using a Compact Microfluidic System." *Analytical Chemistry* 91 (18): 12077–84. https://doi.org/10.1021/acs.analchem.9b03247.

Mulcahy, Laura Ann, Ryan Charles Pink, and David Raul Francisco Carter. 2014. "Routes and Mechanisms of Extracellular Vesicle Uptake." *Journal of Extracellular Vesicles* 3 (1): 24641. https://doi.org/10.3402/jev.v3.24641.

Muraca, Maurizio, Lorenza Putignani, Alessandra Fierabracci, Anna Teti, and Giorgio Perilongo. 2015. "Gut Microbiota-Derived Outer Membrane Vesicles: Under-Recognized Major Players in Health and Disease?" *Discovery Medicine* 19 (106): 343–48.

Muralidharan-Chari, Vandhana, James Clancy, Carolyn Plou, Maryse Romao, Philippe Chavrier, Graca Raposo, and Crislyn D'Souza-Schorey. 2009. "ARF6-Regulated Shedding of Tumor Cell-Derived Plasma Membrane Microvesicles." *Current Biology* 19 (22): 1875–85. https://doi.org/10.1016/j.cub.2009.09.059.

Nagpal, Ravinder, and Hariom Yadav. 2017. "Bacterial Translocation from the Gut to the Distant Organs: An Overview." *Annals of Nutrition and Metabolism* 71 (Suppl. 1): 11–16. https://doi.org/10.1159/000479918.

Nallapareddy, Sreedhar R., and Barbara E. Murray. 2008. "Role Played by Serum, a Biological Cue, in the Adherence of Enterococcus Faecalis to Extracellular Matrix Proteins, Collagen, Fibrinogen, and Fibronectin." *The Journal of Infectious Diseases* 197 (12): 1728–36. https://doi.org/10.1086/588143.

Nallapareddy, Sreedhar R., Kavindra V. Singh, Jouko Sillanpää, Danielle A. Garsin, Magnus Höök, Stanley L. Erlandsen, and Barbara E. Murray. 2006. "Endocarditis and Biofilm-Associated Pili of *Enterococcus Faecalis*." *The Journal of Clinical Investigation* 116 (10): 2799–2807. https://doi.org/10.1172/JCI29021.

Nallapareddy, Sreedhar R., Kavindra V. Singh, Jouko Sillanpää, Meng Zhao, and Barbara E. Murray. 2011. "Relative Contributions of Ebp Pili and the Collagen Adhesin Ace to Host Extracellular Matrix Protein Adherence and Experimental Urinary Tract Infection by Enterococcus Faecalis OG1RF." *Infection and Immunity* 79 (7): 2901–10. https://doi.org/10.1128/iai.00038-11.

Nguyen, Minh-Thu, Julia Uebele, Nimerta Kumari, Hiroshi Nakayama, Lena Peter, Olga Ticha, Anne-Kathrin Woischnig, et al. 2017. "Lipid Moieties on Lipoproteins of Commensal and Non-Commensal Staphylococci Induce Differential Immune Responses." *Nature Communications* 8 (1): 2246. https://doi.org/10.1038/s41467-017-02234-4.

Ni, Yu-Qing, Jun-Kun Zhan, and You-Shuo Liu. 2020. "Roles and Mechanisms of MFG-E8 in Vascular Aging-Related Diseases." *Ageing Research Reviews* 64 (December):101176. https://doi.org/10.1016/j.arr.2020.101176.

Niel, Guillaume van, David R. F. Carter, Aled Clayton, Daniel W. Lambert, Graça Raposo, and Pieter Vader. 2022. "Challenges and Directions in Studying Cell–Cell Communication by Extracellular Vesicles." *Nature Reviews Molecular Cell Biology* 23 (5): 369–82. https://doi.org/10.1038/s41580-022-00460-3.

Niel, Guillaume van, Stéphanie Charrin, Sabrina Simoes, Maryse Romao, Leila Rochin, Paul Saftig, Michael S. Marks, Eric Rubinstein, and Graça Raposo. 2011. "The Tetraspanin CD63 Regulates ESCRT-Independent and Dependent Endosomal Sorting during Melanogenesis." *Developmental Cell* 21 (4): 708–21. https://doi.org/10.1016/j.devcel.2011.08.019.

Niel, Guillaume van, Gisela D'Angelo, and Graça Raposo. 2018. "Shedding Light on the Cell Biology of Extracellular Vesicles." *Nature Reviews Molecular Cell Biology* 19 (4): 213–28. https://doi.org/10.1038/nrm.2017.125.

Nielsen, Hailyn V., Pascale S. Guiton, Kimberly A. Kline, Gary C. Port, Jerome S. Pinkner, Fabrice Neiers, Staffan Normark, Birgitta Henriques-Normark, Michael G. Caparon, and Scott J. Hultgren. 2012. "The Metal Ion-Dependent Adhesion Site Motif of the Enterococcus Faecalis EbpA Pilin Mediates Pilus Function in Catheter-Associated Urinary Tract Infection." *mBio* 3 (4): 10.1128/mbio.00177-12. https://doi.org/10.1128/mbio.00177-12.

Oli, Ajay Kumar, Palaksha K. Javaregowda, Apoorva Jain, Chandrakanth R. Kelmani, Ajay Kumar Oli, Palaksha K. Javaregowda, Apoorva Jain, and Chandrakanth R. Kelmani. 2022. "Mechanism Involved in Biofilm Formation of Enterococcus Faecalis</Em>." In *Focus on Bacterial Biofilms*. IntechOpen. https://doi.org/10.5772/intechopen.103949.

Oliviera Nascimento, Laura de, Paola Massari, and Lee Wetzler. 2012. "The Role of TLR2 in Infection and Immunity." *Frontiers in Immunology* 3. https://www.frontiersin.org/articles/10.3389/fimmu.2012.00079.

Orsi, G. B., and V. Ciorba. 2013. "Vancomycin Resistant Enterococci Healthcare Associated Infections." *Annali Di Igiene: Medicina Preventiva E Di Comunita* 25 (6): 485–92. https://doi.org/10.7416/ai.2013.1948.

Ortega Quesada, Braulio Andrés, Jonathan Cuccia, Rachael Coates, Blake Nassar, Ethan Littlefield, Elizabeth C. Martin, and Adam T. Melvin. 2024. "A Modular Microfluidic Platform to Study How Fluid Shear Stress Alters Estrogen Receptor Phenotype in ER+ Breast Cancer Cells." *Microsystems & Nanoengineering* 10 (1): 1–13. https://doi.org/10.1038/s41378-024-00653-0.

Öztürk, Recep, and Ahmet Murt. 2020. "Epidemiology of Urological Infections: A Global Burden." *World Journal of Urology* 38 (11): 2669–79. https://doi.org/10.1007/s00345-019-03071-4.

Pan, Shi. 2009. "Molecular Mechanisms Responsible for the Atheroprotective Effects of Laminar Shear Stress." *Antioxidants & Redox Signaling* 11 (7): 1669–82. https://doi.org/10.1089/ars.2009.2487.

Park, Ok-Jin, Ji Young Han, Jung Eun Baik, Jun Ho Jeon, Seok-Seong Kang, Cheol-Heui Yun, Jong-Won Oh, Ho Seong Seo, and Seung Hyun Han. 2013. "Lipoteichoic Acid of Enterococcus Faecalis Induces the Expression of Chemokines via TLR2 and PAFR Signaling Pathways." *Journal of Leukocyte Biology* 94 (6): 1275–84. https://doi.org/10.1189/jlb.1012522.

Pathirana, Rishi D., and Maria Kaparakis-Liaskos. 2016. "Bacterial Membrane Vesicles: Biogenesis, Immune Regulation and Pathogenesis." *Cellular Microbiology* 18 (11): 1518–24. https://doi.org/10.1111/cmi.12658.

Postlethwaite, A. E., and A. H. Kang. 1976. "Collagen-and Collagen Peptide-Induced Chemotaxis of Human Blood Monocytes." *The Journal of Experimental Medicine* 143 (6): 1299–1307. https://doi.org/10.1084/jem.143.6.1299.

Prados-Rosales, Rafael, Andres Baena, Luis R. Martinez, Jose Luque-Garcia, Rainer Kalscheuer, Usha Veeraraghavan, Carmen Camara, et al. 2011. "Mycobacteria Release Active Membrane Vesicles That Modulate Immune Responses in a TLR2-Dependent Manner in Mice." *The Journal of Clinical Investigation* 121 (4): 1471–83. https://doi.org/10.1172/JCI44261.

Qu, Mingjuan, Hongwei Zhu, and Xingxiao Zhang. 2022. "Extracellular Vesicle-Mediated Regulation of Macrophage Polarization in Bacterial Infections." *Frontiers in Microbiology* 13. https://www.frontiersin.org/articles/10.3389/fmicb.2022.1039040.

Rai, Anand Kumar, and Patricia J. Johnson. 2019. "Trichomonas Vaginalis Extracellular Vesicles Are Internalized by Host Cells Using Proteoglycans and Caveolin-Dependent Endocytosis." *Proceedings of the National Academy of Sciences* 116 (43): 21354–60. https://doi.org/10.1073/pnas.1912356116.

Rakoff-Nahoum, Seth, Michael J. Coyne, and Laurie E. Comstock. 2014. "An Ecological Network of Polysaccharide Utilization among Human Intestinal Symbionts." *Current Biology* 24 (1): 40–49. https://doi.org/10.1016/j.cub.2013.10.077.

Ramos, Yusibeska, Stephanie Sansone, and Diana K. Morales. 2021. "Sugarcoating It: Enterococcal Polysaccharides as Key Modulators of Host–Pathogen Interactions." *PLoS Pathogens* 17 (9): e1009822. https://doi.org/10.1371/journal.ppat.1009822.

Rashad, Sherif, Xiaobo Han, Khalid Saqr, Simon Tupin, Makoto Ohta, Kuniyasu Niizuma, and Teiji Tominaga. 2020. "Epigenetic Response of Endothelial Cells to Different Wall Shear Stress Magnitudes: A Report of New Mechano-miRNAs." *Journal of Cellular Physiology* 235 (11): 7827–39. https://doi.org/10.1002/jcp.29436.

Rescigno, Maria. 2011. "The Intestinal Epithelial Barrier in the Control of Homeostasis and Immunity." *Trends in Immunology* 32 (6): 256–64. https://doi.org/10.1016/j.it.2011.04.003.

Rey-Giraud, Flora, Mathias Hafner, and Carola H. Ries. 2012. "In Vitro Generation of Monocyte-Derived Macrophages under Serum-Free Conditions Improves Their Tumor Promoting Functions." *PLOS ONE* 7 (8): e42656. https://doi.org/10.1371/journal.pone.0042656.

Riley, D. J., R. A. Berg, R. A. Soltys, J. S. Kerr, H. N. Guss, S. F. Curran, and D. L. Laskin. 1988. "Neutrophil Response Following Intratracheal Instillation of Collagen Peptides into Rat Lungs." *Experimental Lung Research* 14 (4): 549–63. https://doi.org/10.3109/01902148809087827.

Robbins, Paul D., Akaitz Dorronsoro, and Cori N. Booker. 2016. "Regulation of Chronic Inflammatory and Immune Processes by Extracellular Vesicles." *The Journal of Clinical Investigation* 126 (4): 1173–80. https://doi.org/10.1172/JCI81131.

Rodrigues, Meryl, Jia Fan, Christopher Lyon, Meihua Wan, and Ye Hu. 2018. "Role of Extracellular Vesicles in Viral and Bacterial Infections: Pathogenesis, Diagnostics, and Therapeutics." *Theranostics* 8 (10): 2709–21. https://doi.org/10.7150/thno.20576.

Rojas-González, Diana M., Aaron Babendreyer, Andreas Ludwig, and Petra Mela. 2023. "Analysis of Flow-Induced Transcriptional Response and Cell Alignment of Different Sources of Endothelial Cells Used in Vascular Tissue Engineering." *Scientific Reports* 13 (1): 14384. https://doi.org/10.1038/s41598-023-41247-6.

Rompikuntal, Pramod Kumar, Bernard Thay, Muhammad Khanzeb Khan, Jonna Alanko, Anna-Maija Penttinen, Sirkka Asikainen, Sun Nyunt Wai, and Jan Oscarsson. 2012. "Perinuclear Localization of Internalized Outer Membrane Vesicles Carrying Active Cytolethal Distending Toxin from Aggregatibacter Actinomycetemcomitans." *Infection and Immunity* 80 (1): 31–42. https://doi.org/10.1128/iai.06069-11.

Roux, Etienne, Pauline Bougaran, Pascale Dufourcq, and Thierry Couffinhal. 2020. "Fluid Shear Stress Sensing by the Endothelial Layer." *Frontiers in Physiology* 11 (July). https://doi.org/10.3389/fphys.2020.00861.

Rumbo, Carlos, Esteban Fernández-Moreira, María Merino, Margarita Poza, Jose Antonio Mendez, Nelson C. Soares, Alejandro Mosquera, Fernando Chaves, and Germán Bou. 2011. "Horizontal Transfer of the OXA-24 Carbapenemase Gene via Outer Membrane Vesicles: A New Mechanism of Dissemination of Carbapenem Resistance Genes in Acinetobacter Baumannii." *Antimicrobial Agents and Chemotherapy* 55 (7): 3084–90. https://doi.org/10.1128/aac.00929-10.

Santos, André A., Marta B. Afonso, Ricardo S. Ramiro, David Pires, Madalena Pimentel, Rui E. Castro, and Cecília M.P. Rodrigues. 2020. "Host miRNA-21 Promotes Liver Dysfunction by Targeting Small Intestinal Lactobacillus in Mice." *Gut Microbes* 12 (1): 1840766. https://doi.org/10.1080/19490976.2020.1840766.

Satta, Nathalie, Egbert K. O. Kruithof, Guido Reber, and Philippe de Moerloose. 2008. "Induction of TLR2 Expression by Inflammatory Stimuli Is Required for Endothelial Cell Responses to Lipopeptides." *Molecular Immunology* 46 (1): 145–57. https://doi.org/10.1016/j.molimm.2008.07.017.

Scalise, Anna Agata, Nikolaos Kakogiannos, Federica Zanardi, Fabio Iannelli, and Monica Giannotta. 2021. "The Blood–Brain and Gut–Vascular Barriers: From the Perspective of Claudins." *Tissue Barriers* 9 (3): 1926190. https://doi.org/10.1080/21688370.2021.1926190.

Scheitlin, Christopher G., Justin A. Julian, Santhanam Shanmughapriya, Muniswamy Madesh, Nikolaos M. Tsoukias, and B. Rita Alevriadou. 2016. "Endothelial Mitochondria Regulate the Intracellular Ca2+ Response to Fluid Shear Stress." *American Journal of Physiology. Cell Physiology* 310 (6): C479-490. https://doi.org/10.1152/ajpcell.00171.2015.

Schenk, Mirjam, John T. Belisle, and Robert L. Modlin. 2009. "TLR2 Looks at Lipoproteins." *Immunity* 31 (6): 847–49. https://doi.org/10.1016/j.immuni.2009.11.008.

Șchiopu, Pavel, Dan Alexandru Toc, Ioana Alina Colosi, Carmen Costache, Giuseppe Ruospo, George Berar, Ștefan-Gabriel Gălbău, et al. 2023. "An Overview of the Factors Involved in Biofilm

Production by the Enterococcus Genus." *International Journal of Molecular Sciences* 24 (14): 11577. https://doi.org/10.3390/ijms241411577.

Schulz, Eilien, Anna Karagianni, Marcus Koch, and Gregor Fuhrmann. 2020. "Hot EVs – How Temperature Affects Extracellular Vesicles." *European Journal of Pharmaceutics and Biopharmaceutics* 146 (January):55–63. https://doi.org/10.1016/j.ejpb.2019.11.010.

Schwechheimer, Carmen, and Meta J. Kuehn. 2015. "Outer-Membrane Vesicles from Gram-Negative Bacteria: Biogenesis and Functions." *Nature Reviews Microbiology* 13 (10): 605–19. https://doi.org/10.1038/nrmicro3525.

Sender, Ron, Shai Fuchs, and Ron Milo. 2016. "Revised Estimates for the Number of Human and Bacteria Cells in the Body." *PLoS Biology* 14 (8): e1002533. https://doi.org/10.1371/journal.pbio.1002533.

Shah, Ravi, Olivia Ziegler, Ashish Yeri, Xiaojun Liu, Venkatesh Murthy, Dustin Rabideau, Chun Yang Xiao, et al. 2018. "MicroRNAs Associated With Reverse Left Ventricular Remodeling in Humans Identify Pathways of Heart Failure Progression." *Circulation. Heart Failure* 11 (2): e004278. https://doi.org/10.1161/CIRCHEARTFAILURE.117.004278.

Shamsul, Haque M, Akira Hasebe, Mitsuhiro Iyori, Makoto Ohtani, Kazuto Kiura, Diya Zhang, Yasunori Totsuka, and Ken- ichiro Shibata. 2010. "The Toll-like Receptor 2 (TLR2) Ligand FSL-1 Is Internalized via the Clathrin-Dependent Endocytic Pathway Triggered by CD14 and CD36 but Not by TLR2." *Immunology* 130 (2): 262–72. https://doi.org/10.1111/j.1365-2567.2009.03232.x.

Sharma, Shivani, Michael LeClaire, James Wohlschlegel, and James Gimzewski. 2020. "Impact of Isolation Methods on the Biophysical Heterogeneity of Single Extracellular Vesicles." *Scientific Reports* 10 (August):13327. https://doi.org/10.1038/s41598-020-70245-1.

Shelke, Ganesh Vilas, Cecilia Lässer, Yong Song Gho, and Jan Lötvall. 2014. "Importance of Exosome Depletion Protocols to Eliminate Functional and RNA-Containing Extracellular Vesicles from Fetal Bovine Serum." *Journal of Extracellular Vesicles* 3 (1): 24783. https://doi.org/10.3402/jev.v3.24783.

Shen, Kuan-Yin, Ying-Chyi Song, I-Hua Chen, Chih-Hsiang Leng, Hsin-Wei Chen, Hui-Ju Li, Pele Chong, and Shih-Jen Liu. 2014. "Molecular Mechanisms of TLR2-Mediated Antigen Cross-Presentation in Dendritic Cells." *The Journal of Immunology* 192 (9): 4233–41. https://doi.org/10.4049/jimmunol.1302850.

Shkoporov, Andrey N., and Colin Hill. 2019. "Bacteriophages of the Human Gut: The 'Known Unknown' of the Microbiome." *Cell Host & Microbe* 25 (2): 195–209. https://doi.org/10.1016/j.chom.2019.01.017.

Sillanpää, Jouko, Chungyu Chang, Kavindra V. Singh, Maria Camila Montealegre, Sreedhar R. Nallapareddy, Barrett R. Harvey, Hung Ton-That, and Barbara E. Murray. 2013. "Contribution of Individual Ebp Pilus Subunits of Enterococcus Faecalis OG1RF to Pilus Biogenesis, Biofilm Formation and Urinary Tract Infection." *PLOS ONE* 8 (7): e68813. https://doi.org/10.1371/journal.pone.0068813.

Singh, K. V., X. Qin, G. M. Weinstock, and B. E. Murray. 1998. "Generation and Testing of Mutants of Enterococcus Faecalis in a Mouse Peritonitis Model." *The Journal of Infectious Diseases* 178 (5): 1416–20. https://doi.org/10.1086/314453.

Singh, Kavindra V., Sreedhar R. Nallapareddy, and Barbara E. Murray. 2007. "Importance of the Ebp (Endocarditisand Biofilm-Associated Pilus) Locus in the Pathogenesis of Enterococcus Faecalis Ascending Urinary Tract Infection." *The Journal of Infectious Diseases* 195 (11): 1671–77. https://doi.org/10.1086/517524.

Sjöström, Annika E., Linda Sandblad, Bernt Eric Uhlin, and Sun Nyunt Wai. 2015. "Membrane Vesicle-Mediated Release of Bacterial RNA." *Scientific Reports* 5. https://doi.org/10.1038/srep15329.

Stam, Janine, Sabine Bartel, Rainer Bischoff, and Justina C. Wolters. 2021. “Isolation of Extracellular Vesicles with Combined Enrichment Methods.” *Journal of Chromatography B* 1169 (April):122604. https://doi.org/10.1016/j.jchromb.2021.122604.

Steck, Natalie, Micha Hoffmann, Irina G. Sava, Sandra C. Kim, Hannes Hahne, Susan L. Tonkonogy, Katrin Mair, et al. 2011. “Enterococcus Faecalis Metalloprotease Compromises Epithelial Barrier and Contributes to Intestinal Inflammation.” *Gastroenterology* 141 (3): 959–71. https://doi.org/10.1053/j.gastro.2011.05.035.

Stevens, S. X., H. G. Jensen, B. D. Jett, and M. S. Gilmore. 1992. “A Hemolysin-Encoding Plasmid Contributes to Bacterial Virulence in Experimental Enterococcus Faecalis Endophthalmitis.” *Investigative Ophthalmology & Visual Science* 33 (5): 1650–56.

Suetens, Carl, Katrien Latour, Tommi Kärki, Enrico Ricchizzi, Pete Kinross, Maria Luisa Moro, Béatrice Jans, et al. 2018. “Prevalence of Healthcare-Associated Infections, Estimated Incidence and Composite Antimicrobial Resistance Index in Acute Care Hospitals and Long-Term Care Facilities: Results from Two European Point Prevalence Surveys, 2016 to 2017.” *Eurosurveillance* 23 (46): 1800516. https://doi.org/10.2807/1560-7917.ES.2018.23.46.1800516.

Sun, Yuqing, Bo Zhang, and Lianghua Xia. 2021. “Effect of Low Wall Shear Stress on the Morphology of Endothelial Cells and Its Evaluation Indicators.” *Computer Methods and Programs in Biomedicine* 208 (September):106082. https://doi.org/10.1016/j.cmpb.2021.106082.

Suppli, M., R. Aabenhus, Z. B. Harboe, L. P. Andersen, M. Tvede, and J. -U. S. Jensen. 2011. “Mortality in Enterococcal Bloodstream Infections Increases with Inappropriate Antimicrobial Therapy.” *Clinical Microbiology and Infection* 17 (7): 1078–83. https://doi.org/10.1111/j.1469-0691.2010.03394.x.

Surbatovic, Maja, Nada Popovic, Danilo Vojvodic, Ivan Milosevic, Gordana Acimovic, Milan Stojicic, Milic Veljovic, Jasna Jevdjic, Dragan Djordjevic, and Sonja Radakovic. 2015. “Cytokine Profile in Severe Gram-Positive and Gram-Negative Abdominal Sepsis.” *Scientific Reports* 5 (1): 11355. https://doi.org/10.1038/srep11355.

Takahashi, Naoyuki, Daisuke Yoshino, Ryuji Sugahara, Satomi Hirose, Kazuki Sone, Jean-Paul Rieu, and Kenichi Funamoto. 2023. “Microfluidic Platform for the Reproduction of Hypoxic Vascular Microenvironments.” *Scientific Reports* 13 (1): 5428. https://doi.org/10.1038/s41598-023-32334-9.

Tamburini, Sabrina, Nan Shen, Han Chih Wu, and Jose C. Clemente. 2016. “The Microbiome in Early Life: Implications for Health Outcomes.” *Nature Medicine* 22 (7): 713–22. https://doi.org/10.1038/nm.4142.

Tanaka, Keiichiro, Divyesh Joshi, Sushma Timalsina, and Martin A. Schwartz. 2021. “Early Events in Endothelial Flow Sensing.” *Cytoskeleton* 78 (6): 217–31. https://doi.org/10.1002/cm.21652.

Tedesco, Serena, Federica De Majo, Jieun Kim, Annalisa Trenti, Lucia Trevisi, Gian Paolo Fadini, Chiara Bolego, Peter W. Zandstra, Andrea Cignarella, and Libero Vitiello. 2018. “Convenience versus Biological Significance: Are PMA-Differentiated THP-1 Cells a Reliable Substitute for Blood-Derived Macrophages When Studying in Vitro Polarization?” *Frontiers in Pharmacology* 9 (February):71. https://doi.org/10.3389/fphar.2018.00071.

Théry, Clotilde, Sebastian Amigorena, Graça Raposo, and Aled Clayton. 2006a. “Isolation and Characterization of Exosomes from Cell Culture Supernatants and Biological Fluids.” *Current Protocols in Cell Biology* 30 (1): 3.22.1-3.22.29. https://doi.org/10.1002/0471143030.cb0322s30.

———. 2006b. “Isolation and Characterization of Exosomes from Cell Culture Supernatants and Biological Fluids.” *Current Protocols in Cell Biology* 30 (1). https://doi.org/10.1002/0471143030.cb0322s30.

Thompson, Alexander G., Elizabeth Gray, Sabrina M. Heman-Ackah, Imre Mäger, Kevin Talbot, Samir El Andaloussi, Matthew J. Wood, and Martin R. Turner. 2016. "Extracellular Vesicles in Neurodegenerative Disease — Pathogenesis to Biomarkers." *Nature Reviews Neurology* 12 (6): 346–57. https://doi.org/10.1038/nrneurol.2016.68.

Thriene, Kerstin, and Karin B. Michels. 2023. "Human Gut Microbiota Plasticity throughout the Life Course." *International Journal of Environmental Research and Public Health* 20 (2). https://doi.org/10.3390/ijerph20021463.

Tkach, Mercedes, and Clotilde Théry. 2016. "Communication by Extracellular Vesicles: Where We Are and Where We Need to Go." *Cell* 164 (6): 1226–32. https://doi.org/10.1016/j.cell.2016.01.043.

Todkar, Kiran, Lilia Chikhi, Véronique Desjardins, Firas El-Mortada, Geneviève Pépin, and Marc Germain. 2021. "Selective Packaging of Mitochondrial Proteins into Extracellular Vesicles Prevents the Release of Mitochondrial DAMPs." *Nature Communications* 12 (1): 1971. https://doi.org/10.1038/s41467-021-21984-w.

Torre-Escudero, Eduardo de la, Jared Q. Gerlach, Adam P. S. Bennett, Krystyna Cwiklinski, Heather L. Jewhurst, Kathryn M. Huson, Lokesh Joshi, et al. 2019. "Surface Molecules of Extracellular Vesicles Secreted by the Helminth Pathogen Fasciola Hepatica Direct Their Internalisation by Host Cells." *PLOS Neglected Tropical Diseases* 13 (1): e0007087. https://doi.org/10.1371/journal.pntd.0007087.

Tovar-Lopez, Francisco, Peter Thurgood, Christopher Gilliam, Ngan Nguyen, Elena Pirogova, Khashayar Khoshmanesh, and Sara Baratchi. 2019. "A Microfluidic System for Studying the Effects of Disturbed Flow on Endothelial Cells." *Frontiers in Bioengineering and Biotechnology* 7. https://www.frontiersin.org/articles/10.3389/fbioe.2019.00081.

Toyofuku, Masanori, Nobuhiko Nomura, and Leo Eberl. 2019. "Types and Origins of Bacterial Membrane Vesicles." *Nature Reviews Microbiology* 17 (1): 13–24. https://doi.org/10.1038/s41579-018-0112-2.

Triantafilou, Martha, Maria Manukyan, Alan Mackie, Siegfried Morath, Thomas Hartung, Holger Heine, and Kathy Triantafilou. 2004. "Lipoteichoic Acid and Toll-like Receptor 2 Internalization and Targeting to the Golgi Are Lipid Raft-Dependent *." *Journal of Biological Chemistry* 279 (39): 40882–89. https://doi.org/10.1074/jbc.M400466200.

Tun, Win M., Choon Hwai Yap, Shier Nee Saw, Joanna L. James, and Alys R. Clark. 2019. "Differences in Placental Capillary Shear Stress in Fetal Growth Restriction May Affect Endothelial Cell Function and Vascular Network Formation." *Scientific Reports* 9 (1): 9876. https://doi.org/10.1038/s41598-019-46151-6.

Turnbull, Lynne, Masanori Toyofuku, Amelia L. Hynen, Masaharu Kurosawa, Gabriella Pessi, Nicola K. Petty, Sarah R. Osvath, et al. 2016. "Explosive Cell Lysis as a Mechanism for the Biogenesis of Bacterial Membrane Vesicles and Biofilms." *Nature Communications* 7 (1): 11220. https://doi.org/10.1038/ncomms11220.

Twardowska, Agata, Adam Makaro, Agata Binienda, Jakub Fichna, and Maciej Salaga. 2022. "Preventing Bacterial Translocation in Patients with Leaky Gut Syndrome: Nutrition and Pharmacological Treatment Options." *International Journal of Molecular Sciences* 23 (6): 3204. https://doi.org/10.3390/ijms23063204.

Ubeda, Carles, Ying Taur, Robert R. Jenq, Michele J. Equinda, Tammy Son, Miriam Samstein, Agnes Viale, et al. 2010. "Vancomycin-Resistant *Enterococcus* Domination of Intestinal Microbiota Is Enabled by Antibiotic Treatment in Mice and Precedes Bloodstream Invasion in Humans." *The Journal of Clinical Investigation* 120 (12): 4332–41. https://doi.org/10.1172/JCI43918.

Urzì, Ornella, Roger Olofsson Bagge, and Rossella Crescitelli. 2022. "The Dark Side of Foetal Bovine Serum in Extracellular Vesicle Studies." *Journal of Extracellular Vesicles* 11 (10): 12271. https://doi.org/10.1002/jev2.12271.

Vagner, Tatyana, Andrew Chin, Javier Mariscal, Serguei Bannykh, David M. Engman, and Dolores Di Vizio. 2019. "Protein Composition Reflects Extracellular Vesicle Heterogeneity." *PROTEOMICS* 19 (8): 1800167. https://doi.org/10.1002/pmic.201800167.

Valadi, Hadi, Karin Ekström, Apostolos Bossios, Margareta Sjöstrand, James J. Lee, and Jan O. Lötvall. 2007. "Exosome-Mediated Transfer of mRNAs and microRNAs Is a Novel Mechanism of Genetic Exchange between Cells." *Nature Cell Biology* 9 (6): 654–59. https://doi.org/10.1038/ncb1596.

Verderio, Claudia, Martina Gabrielli, and Paola Giussani. 2018. "Role of Sphingolipids in the Biogenesis and Biological Activity of Extracellular Vesicles." *Journal of Lipid Research* 59 (8): 1325–40. https://doi.org/10.1194/jlr.R083915.

Walsby, Elisabeth, Andrea Buggins, Stephen Devereux, Ceri Jones, Guy Pratt, Paul Brennan, Chris Fegan, and Chris Pepper. 2014. "Development and Characterization of a Physiologically Relevant Model of Lymphocyte Migration in Chronic Lymphocytic Leukemia." *Blood* 123 (23): 3607–17. https://doi.org/10.1182/blood-2013-12-544569.

Wang, Fangyu, Richard A. Cerione, and Marc A. Antonyak. 2021. "Isolation and Characterization of Extracellular Vesicles Produced by Cell Lines." *STAR Protocols* 2 (1): 100295. https://doi.org/10.1016/j.xpro.2021.100295.

Wang, Xiuxiu, Xiaoyue Shen, Yuting Yan, and Hongmin Li. 2021. "Pyruvate Dehydrogenase Kinases (PDKs): An Overview toward Clinical Applications." *Bioscience Reports* 41 (4): BSR20204402. https://doi.org/10.1042/BSR20204402.

Weber, Martina, Meredith B. Baker, Jeffrey P. Moore, and Charles D. Searles. 2010. "MiR-21 Is Induced in Endothelial Cells by Shear Stress and Modulates Apoptosis and eNOS Activity." *Biochemical and Biophysical Research Communications* 393 (4): 643–48. https://doi.org/10.1016/j.bbrc.2010.02.045.

Wei, Zhiyun, Arsen O. Batagov, David R. F. Carter, and Anna M. Krichevsky. 2016. "Fetal Bovine Serum RNA Interferes with the Cell Culture Derived Extracellular RNA." *Scientific Reports* 6 (1): 31175. https://doi.org/10.1038/srep31175.

Weiner, Lindsey M., Amy K. Webb, Brandi Limbago, Margaret A. Dudeck, Jean Patel, Alexander J. Kallen, Jonathan R. Edwards, and Dawn M. Sievert. 2016. "Antimicrobial-Resistant Pathogens Associated With Healthcare-Associated Infections: Summary of Data Reported to the National Healthcare Safety Network at the Centers for Disease Control and Prevention, 2011–2014." *Infection Control and Hospital Epidemiology* 37 (11): 1288–1301. https://doi.org/10.1017/ice.2016.174.

Welsh, Joshua A., Deborah C. I. Goberdhan, Lorraine O'Driscoll, Edit I. Buzas, Cherie Blenkiron, Benedetta Bussolati, Houjian Cai, et al. 2024. "Minimal Information for Studies of Extracellular Vesicles (MISEV2023): From Basic to Advanced Approaches." *Journal of Extracellular Vesicles* 13 (2): e12404. https://doi.org/10.1002/jev2.12404.

Wheeler, Richard, Paulo André Dias Bastos, Olivier Disson, Aline Rifflet, Ilana Gabanyi, Julia Spielbauer, Marion Bérard, Marc Lecuit, and Ivo Gomperts Boneca. 2023. "Microbiota-Induced Active Translocation of Peptidoglycan across the Intestinal Barrier Dictates Its within-Host Dissemination." *Proceedings of the National Academy of Sciences* 120 (4): e2209936120. https://doi.org/10.1073/pnas.2209936120.

Wolf, Peter. 1967. "The Nature and Significance of Platelet Products in Human Plasma." *British Journal of Haematology* 13 (3): 269–88. https://doi.org/10.1111/j.1365-2141.1967.tb08741.x.

Xu, Hongxin, Ying Cui, Xianwei Liu, Xiao Zheng, Jiaqing Liu, Xinxin Hu, Fuhua Gao, et al. 2022. "miR-1290 Promotes IL-8-Mediated Vascular Endothelial Cell Adhesion by Targeting GSK-3β." *Molecular Biology Reports* 49 (3): 1871–82. https://doi.org/10.1007/s11033-021-06998-3.

Xu, Hui, Xiang Wang, Wenke Feng, Qi Liu, Shanshan Zhou, Quan Liu, and Lu Cai. 2020. "The Gut Microbiota and Its Interactions with Cardiovascular Disease." *Microbial Biotechnology* 13 (3): 637–56. https://doi.org/10.1111/1751-7915.13524.

Xu, Minxue, Jie Ji, Dandan Jin, Yue Wu, Tong Wu, Renjie Lin, Shengze Zhu, et al. 2023. "The Biogenesis and Secretion of Exosomes and Multivesicular Bodies (MVBs): Intercellular Shuttles and Implications in Human Diseases." *Genes & Diseases* 10 (5): 1894–1907. https://doi.org/10.1016/j.gendis.2022.03.021.

Xu, Xiangshan, Yang Yang, Guofeng Wang, Yu Yin, Shuo Han, Donghan Zheng, Shaobo Zhou, Yuanyuan Zhao, Yong Chen, and Yuanzhe Jin. 2021. "Low Shear Stress Regulates Vascular Endothelial Cell Pyroptosis through miR-181b-5p/STAT-3 Axis." *Journal of Cellular Physiology* 236 (1): 318–27. https://doi.org/10.1002/jcp.29844.

Yamamoto, Kimiko, Hiromi Imamura, and Joji Ando. 2018. "Shear Stress Augments Mitochondrial ATP Generation That Triggers ATP Release and Ca2+ Signaling in Vascular Endothelial Cells." *American Journal of Physiology. Heart and Circulatory Physiology* 315 (5): H1477–85. https://doi.org/10.1152/ajpheart.00204.2018.

Yamamoto, Kimiko, Yoshitsugu Nogimori, Hiromi Imamura, and Joji Ando. 2020. "Shear Stress Activates Mitochondrial Oxidative Phosphorylation by Reducing Plasma Membrane Cholesterol in Vascular Endothelial Cells." *Proceedings of the National Academy of Sciences of the United States of America* 117 (52): 33660–67. https://doi.org/10.1073/pnas.2014029117.

Yamamoto, Kimiko, Yuji Shimogonya, Ryohei Maeno, Kenshiroh Kawabe, and Joji Ando. 2023. "Endothelial Cells Differentially Sense Laminar and Disturbed Flows by Altering the Lipid Order of Their Plasma and Mitochondrial Membranes." *American Journal of Physiology-Cell Physiology* 325 (6): C1532–44. https://doi.org/10.1152/ajpcell.00393.2023.

Yáñez-Mó, María, Pia R.-M. Siljander, Zoraida Andreu, Apolonija Bedina Zavec, Francesc E. Borràs, Edit I. Buzas, Krisztina Buzas, et al. 2015. "Biological Properties of Extracellular Vesicles and Their Physiological Functions." *Journal of Extracellular Vesicles* 4 (1): 27066. https://doi.org/10.3402/jev.v4.27066.

Yang, Jinho, Tae-Seop Shin, Jong Seong Kim, Young-Koo Jee, and Yoon-Keun Kim. 2022. "A New Horizon of Precision Medicine: Combination of the Microbiome and Extracellular Vesicles." *Experimental & Molecular Medicine* 54 (4): 466–82. https://doi.org/10.1038/s12276-022-00748-6.

Yin, Zhongwei, Yanru Zhao, Huaping Li, Mengwen Yan, Ling Zhou, Chen Chen, and Dao Wen Wang. 2016. "miR-320a Mediates Doxorubicin-Induced Cardiotoxicity by Targeting VEGF Signal Pathway." *Aging (Albany NY)* 8 (1): 192–207.

Yoo, Ji Youn, Maureen Groer, Samia Valeria Ozorio Dutra, Anujit Sarkar, and Daniel Ian McSkimming. 2020. "Gut Microbiota and Immune System Interactions." *Microorganisms* 8 (10). https://doi.org/10.3390/microorganisms8101587.

Zhang, Qin, Dennis K. Jeppesen, James N. Higginbotham, Jeffrey L. Franklin, and Robert J. Coffey. 2023. "Comprehensive Isolation of Extracellular Vesicles and Nanoparticles." *Nature Protocols* 18 (5): 1462–87. https://doi.org/10.1038/s41596-023-00811-0.

Zhang, Xiaoyan, Jiaxing Sun, Peiran Zhang, Ting Wen, Ruonan Wang, Liang Liang, Ziyan Yang, et al. 2023. "miR-342-5p Downstream to Notch Enhances Arterialization of Endothelial Cells in Response to Shear Stress by Repressing MYC." *Molecular Therapy - Nucleic Acids* 32 (June):343–58. https://doi.org/10.1016/j.omtn.2023.03.022.

Zhang, Yong, Wei Qin, Longyin Zhang, Xianxian Wu, Ning Du, Yingying Hu, Xiaoguang Li, et al. 2015. "MicroRNA-26a Prevents Endothelial Cell Apoptosis by Directly Targeting TRPC6 in the Setting of Atherosclerosis." *Scientific Reports* 5 (1): 9401. https://doi.org/10.1038/srep09401.

Zheng, Danping, Timur Liwinski, and Eran Elinav. 2020. “Interaction between Microbiota and Immunity in Health and Disease.” *Cell Research* 30 (6): 492–506. https://doi.org/10.1038/s41422-020-0332-7.

Zhou, Xiaoxue, Feng Xie, Lin Wang, Long Zhang, Suping Zhang, Meiyu Fang, and Fangfang Zhou. 2020. “The Function and Clinical Application of Extracellular Vesicles in Innate Immune Regulation.” *Cellular & Molecular Immunology* 17 (4): 323–34. https://doi.org/10.1038/s41423-020-0391-1.

Zou, Jun, and Nathan Shankar. 2016. “Surface Protein Esp Enhances Pro-Inflammatory Cytokine Expression through NF-κB Activation during Enterococcal Infection.” *Innate Immunity* 22 (1): 31–39. https://doi.org/10.1177/1753425915611237.

6 Appendix

6.1 Abbreviations

ACTB	Actin beta
APC	Antigen-presenting cells
BCA	Bicinchoninic acid
BHI	Brain heart infusion
CCL8	Chemokine C-C motif ligand 8
CD	Cluster of differentiation
cDNA	Complementary DNA
CFU	Colony forming unit
DAMP	Damage-associated molecular patterns
DMSO	Dimethyl sulfoxide
EC	Endothelial cells
ECM	Extracellular matrix
EDTA	Ethylenediamine tetraacetic acid
eNOS	Endothelial nitric oxide synthase
EV	Extracellular vesicle
FACS	Fluorescence-activated cell sorting
FCS	Fetal calf serum
FITC	Fluorescein isothiocyanate
GILZ	Glucocorticoid-induced leucine zipper
HEK	Human embryonic kidney
HMDM	Human monocyte-derived macrophage
HUVEC	Human umbilical vein endothelial cell
ICAM-1	Intercellular adhesion molecule-1
IL	Interleukin
ITS	Insulin-transferrin-selenium
KLF2	Krüppel-like Factor 2
LPS	Lipopolysaccharide
MCP1	Monocyte chemoattractant protein-1
M-CSF	Macrophage colony-stimulating factor
MFI	Median fluorescence intensity
MTT	3-(4,5-dimethylthiazol-2-yl)-2,5-diphenyltetrazolium bromide
MVB	Multivesicular bodies
NF-κB	Nuclear factor kappa-light-chain-enhancer of activated B cells
NTA	Nanoparticle tracking analysis
OD	Optical density
OM	outer membrane
OMV	Outer membrane vesicles
PAMP	pathogen-associated molecular patterns
PBM	Peripheral blood mononuclear cell
PBS	Phosphate buffer saline
PFA	Paraformaldehyde
PG	Peptidoglycan
PI	Propidium iodide
PRR	Pattern recognition receptors
PVDF	Polyvinylidene difluoride
qPCR	Quantitative polymerase chain reaction
RPMI	Roswell Park Memorial Institute
SD	Standard deviation
SDS-PAGE	Sodium dodecyl sulfate-polyacrylamide gel electrophoresis

SEAP	Secreted embryonic alkaline phosphatase
TEM	Transmission electron microscopy
TL	Toll-like receptor
TNF	Tumor necrosis factor
UC	Ultracentrifugation
UTI	Urinary tract infections
VCAM-1	Vascular cell adhesion molecule-1
VEGFA	Vascular endothelial growth factor
vWF	von Willebrand Factor

6.2 List of figures

6.3 List of tables

6.4 Supplements

6.4.1 Growth curve of *Enterococcus faecalis*

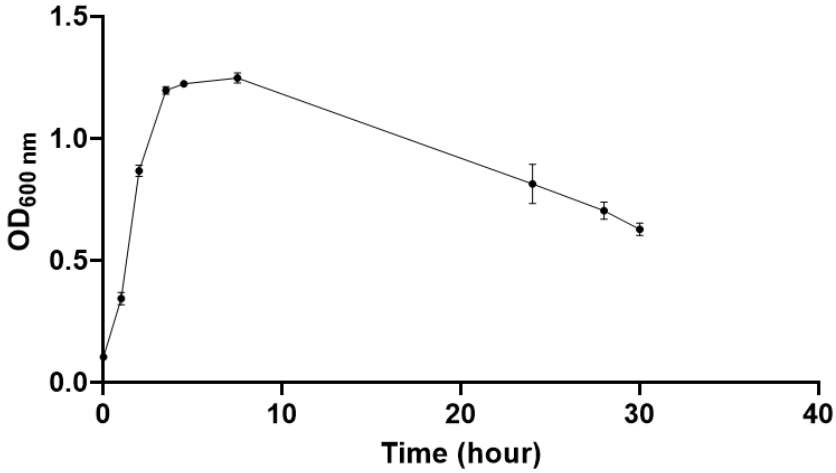

FIGURE S 1. Growth curve of *Enterococcus faecalis*. The optical density (OD) from three replicates was measured for cultures in BHI medium under static conditions at 37 °C.

6.4.2 Protein concentration of SEC fractions analyzed by BCA assay

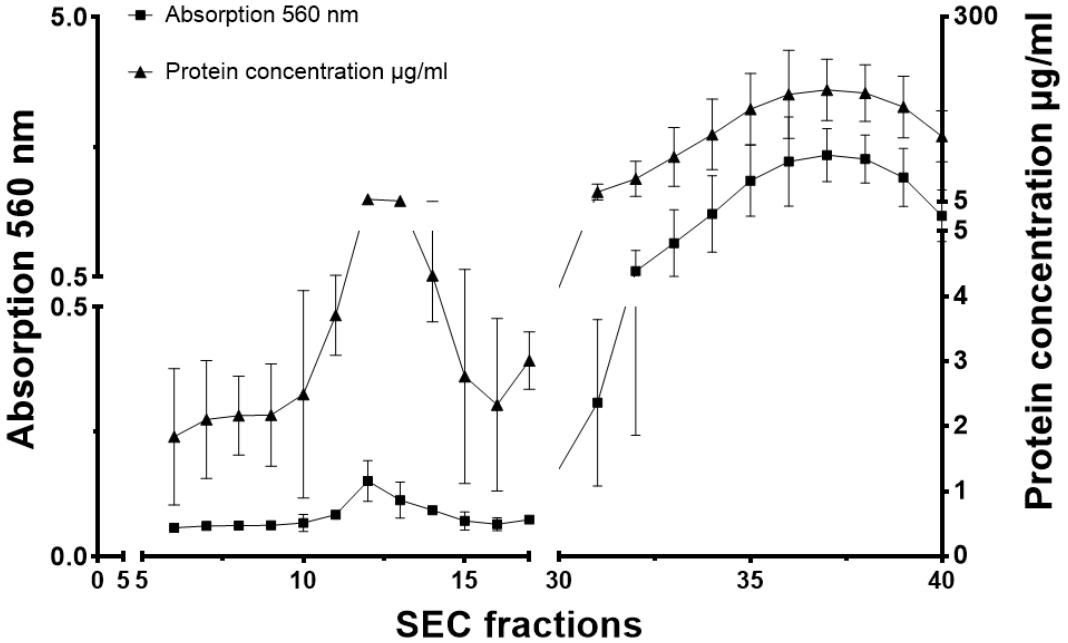

FIGURE S 2. Protein concentration of SEC fractions analyzed by BCA assay, and measured absorptions at 560 nm (n=2, two individual preparations).

6.4.3 Gene expression of HMDM individual donors

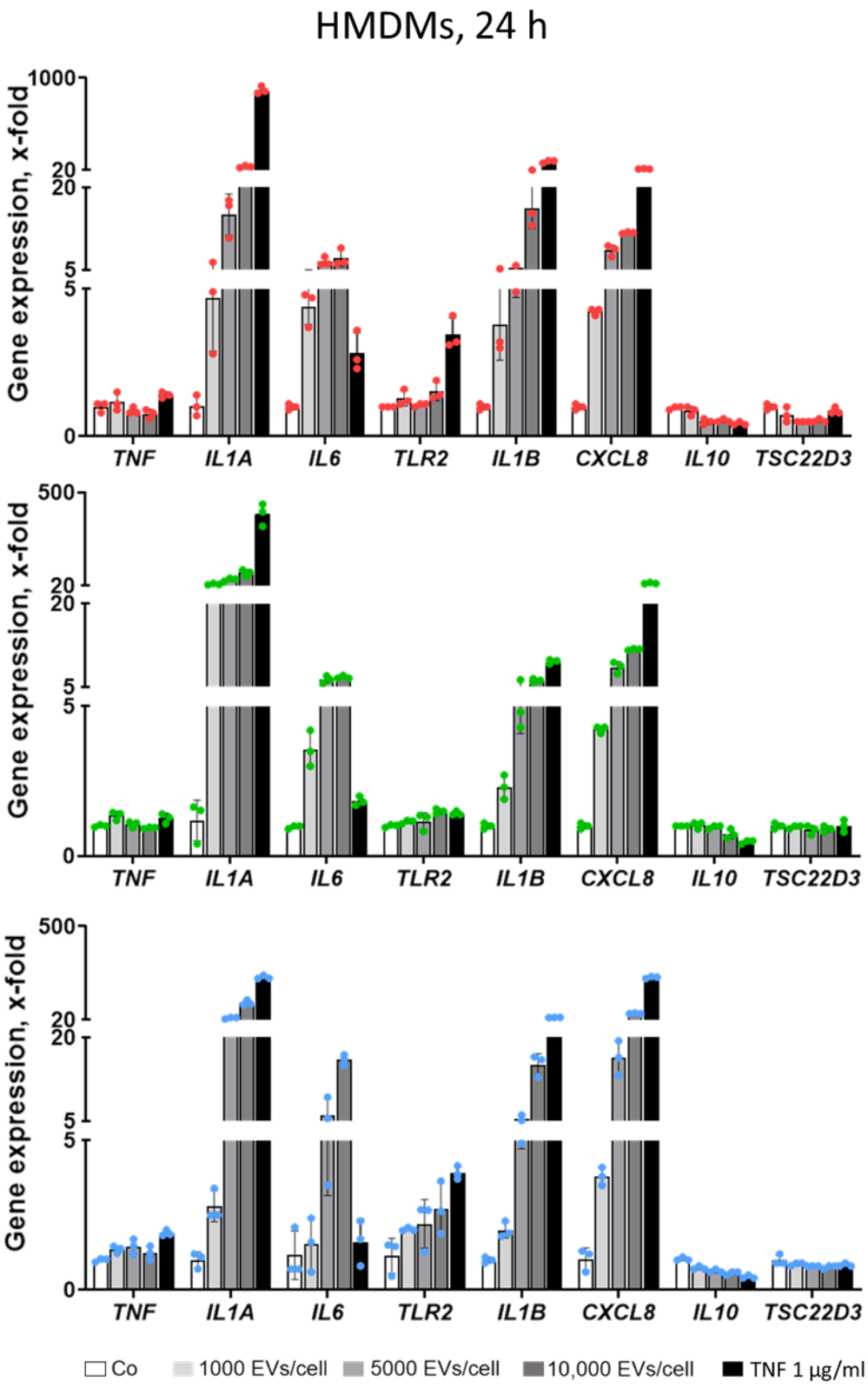

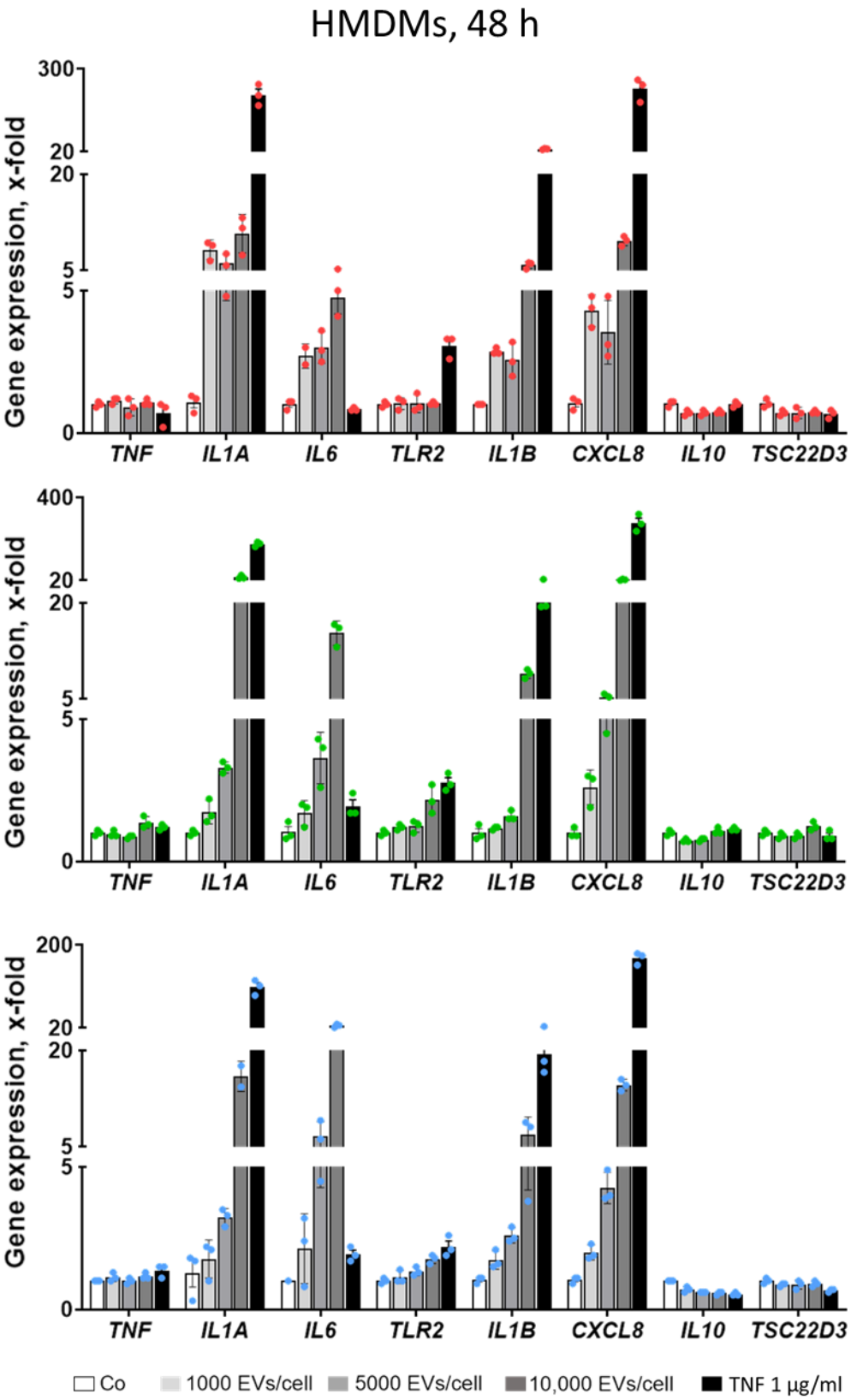
HMDMs, 48 h
Gene expression, x-fold
300
20
20
5
5
0
TNF
IL1A
IL6
TLR2
IL1B
CXCL8
IL10
TSC22D3
400
200
Co
1000 EVs/cell
5000 EVs/cell
10,000 EVs/cell
TNF 1 µg/ml

FIGURE S 3. Gene expression of HMDM individual donors after 24 h and 48 h incubation with bacterial EVs at different EV per cell ratios (1000, 5000, and 10,000 EVs/cell).

6.4.4 Gene expression of HUVEC individual donors

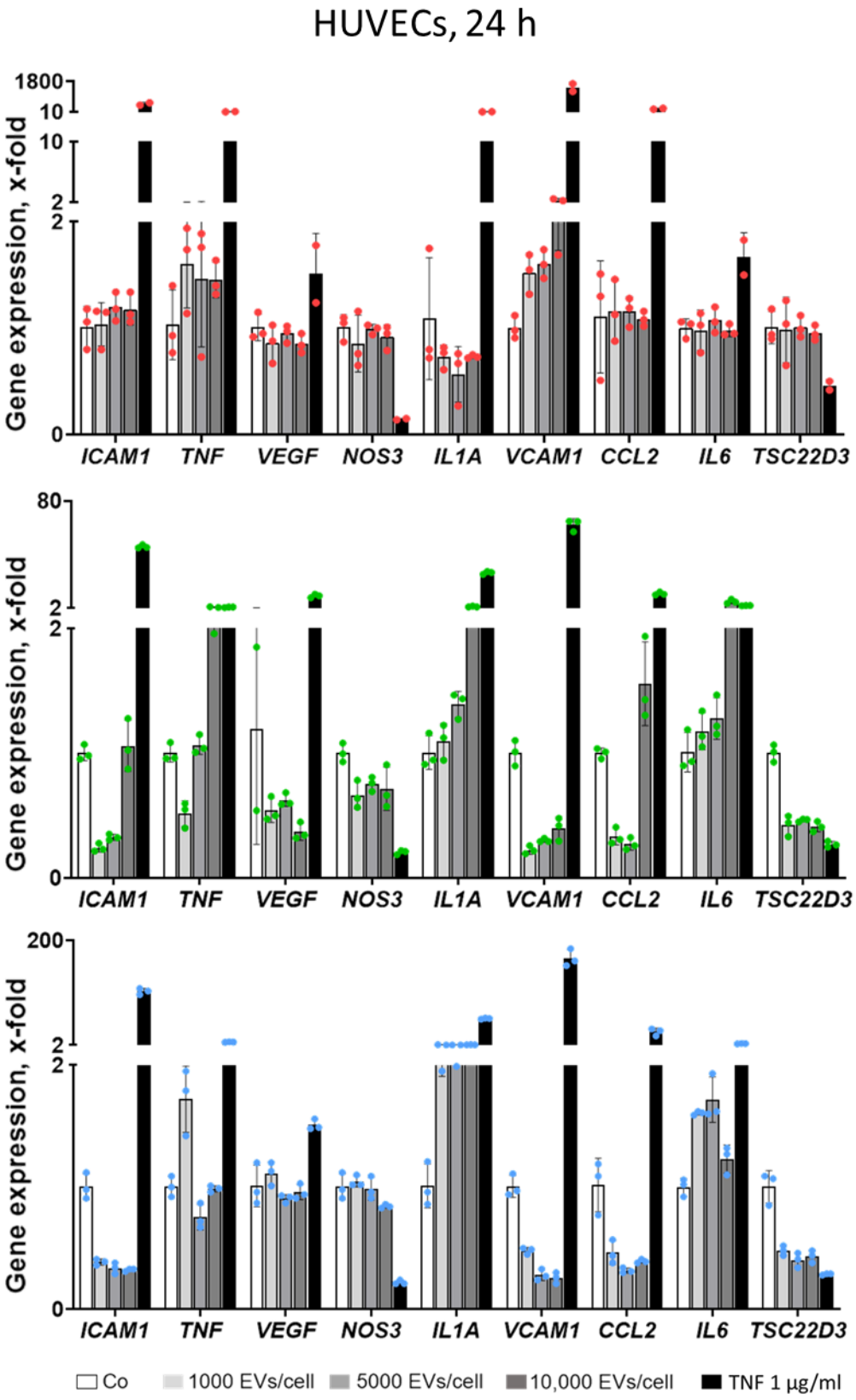

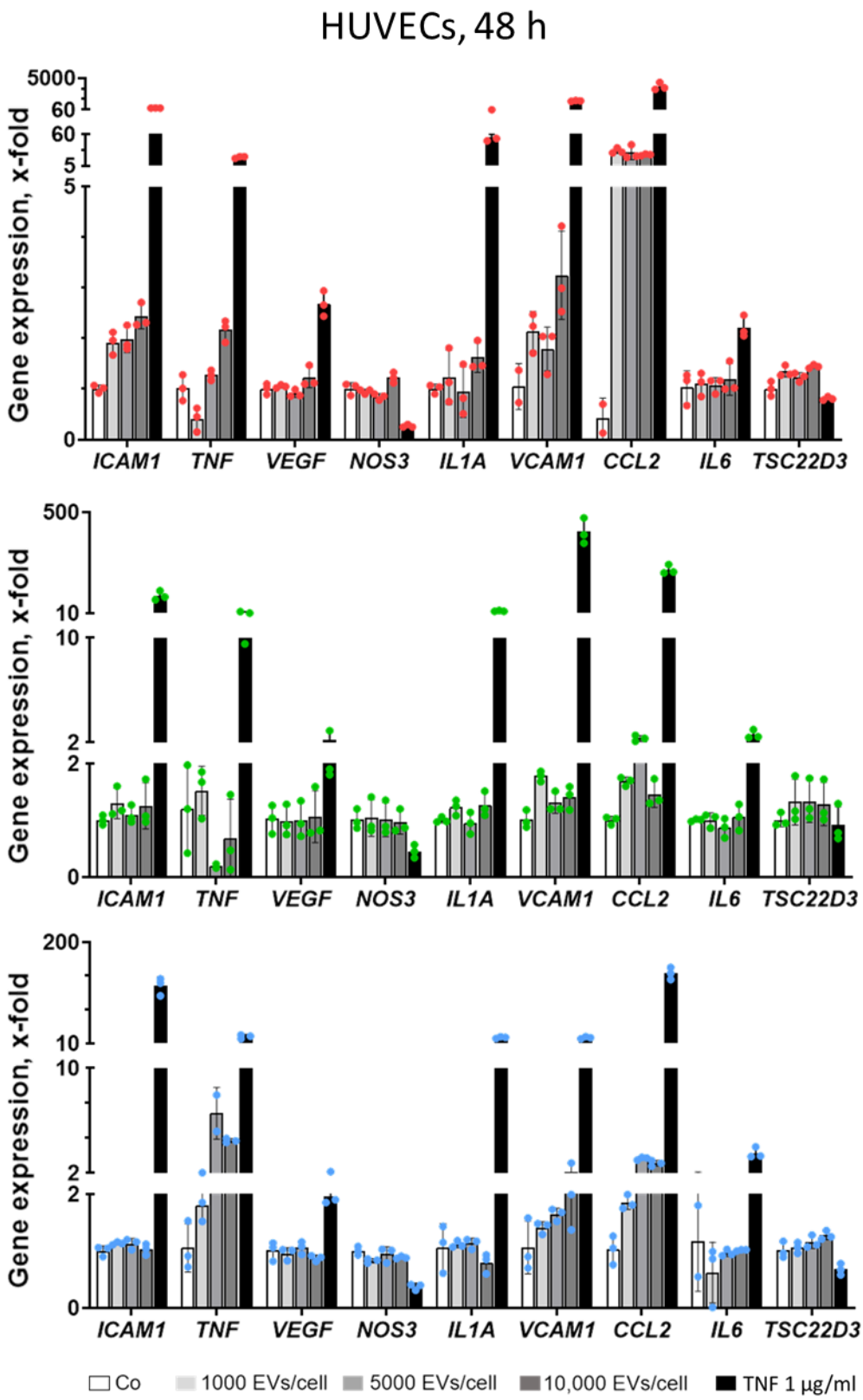
HUVECs, 48 h
Gene expression, x-fold
5000
60
60
5
5
0
ICAM1
TNF
VEGF
NOS3
IL1A
VCAM1
CCL2
IL6
TSC22D3
500
10
10
2
2
0
200
10
10
2
2
0
Co
1000 EVs/cell
5000 EVs/cell
10,000 EVs/cell
TNF 1 µg/ml

FIGURE S 4. Gene expression of HUVEC individual donors after 24 h and 48 h incubation with bacterial EVs at different EV per cell ratios (1000, 5000, and 10,000 EVs/cell).

6.4.5 Levels of TLR2 mRNA in individual HUVECs

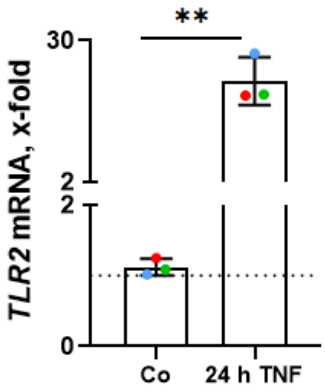

FIGURE S 5**.** Levels of *TLR2* mRNA in individual HUVECs at resting (Co) and TNF-stimulated (1 µg/ml) conditions (n=3, individual donors).

6.4.6 Flow cytometric gating strategy for EV uptake analysis in HMDMs

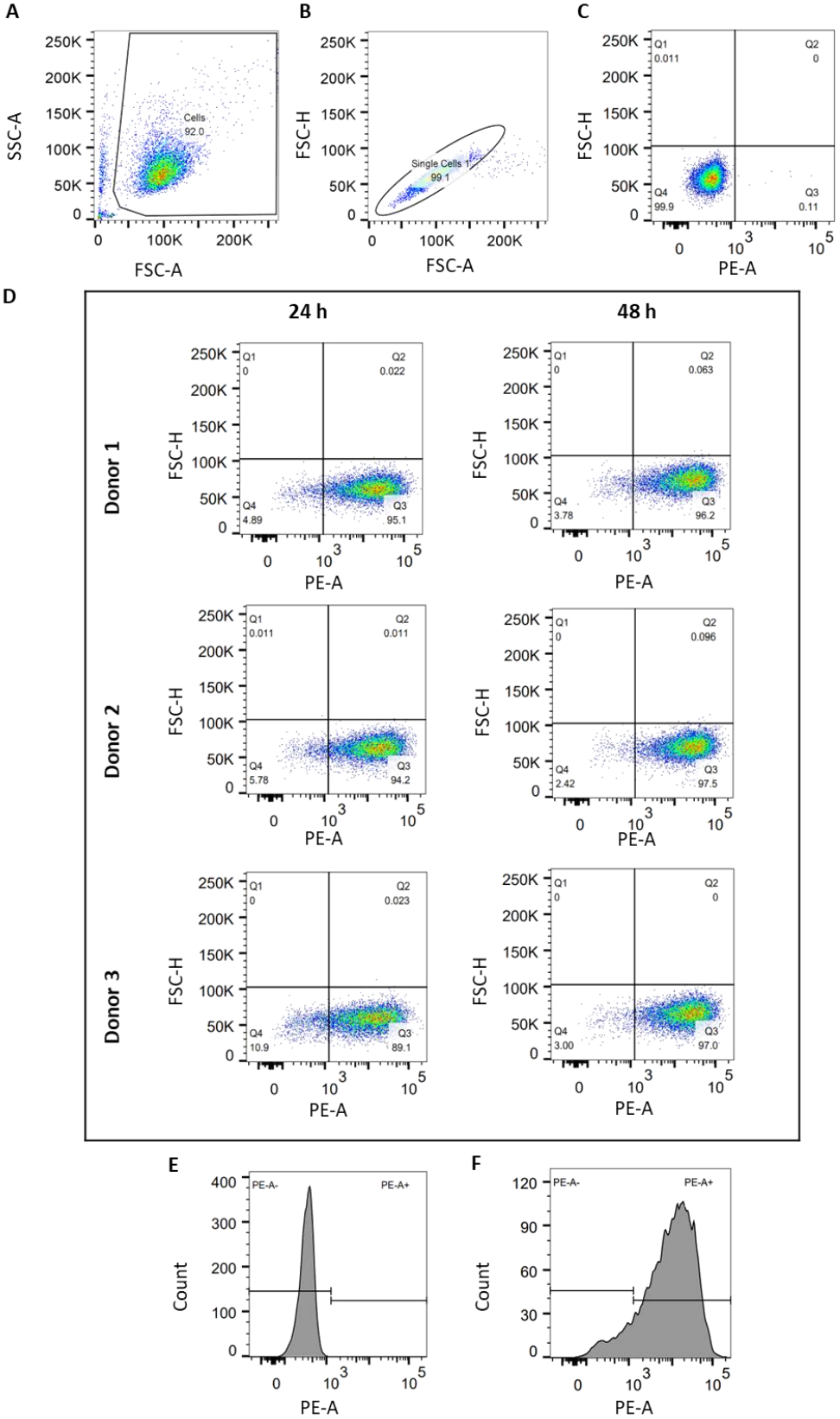

FIGURE S 6. Flow cytometric gating strategy for EV uptake analysis in HMDMs. Cells were incubated with DiI-labeled EVs (30,000 EVs/cell) for 24 and 48 h. Internalization was quantified by measuring phycoerythrin (PE-A) channel fluorescence intensity. **A)** Events in SSC-A *vs*. FSC-A. **B)** Singlets in FSC-H *vs.* FSC-A. **C)** Control cells in FSC-H *vs*. PC-A. **D)** FSC-H *vs.* PC-A of each individual donor after 24 and 48 h of incubation with EVs. Representative histogram of cells without **E)** and with EVs **F)**.

6.4.7 Flow cytometric gating strategy for EV uptake analysis in HUVECs

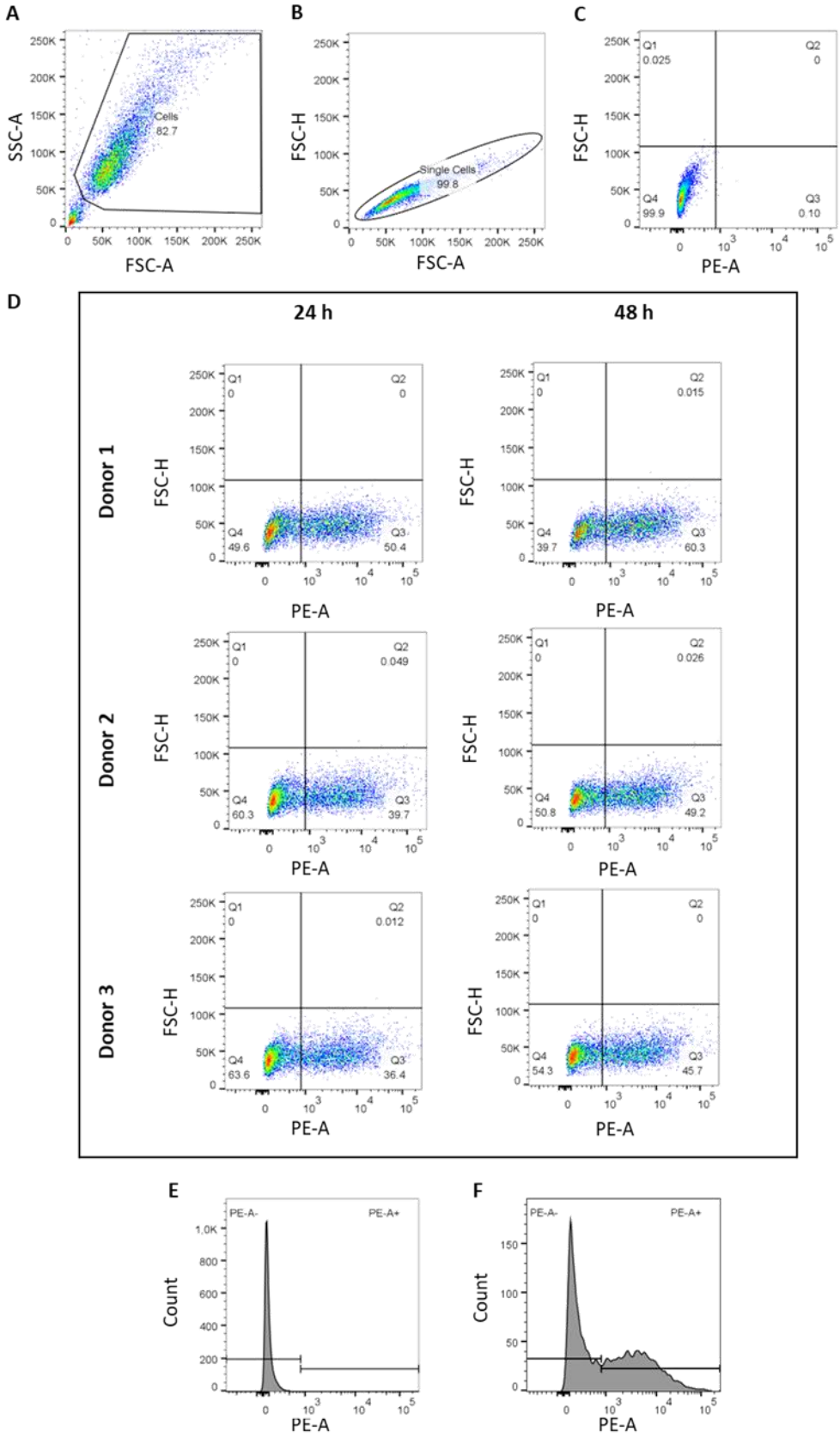

FIGURE S 7. Flow cytometric gating strategy for EV uptake analysis in HUVECs. Cells were incubated with DiI-labeled EVs (30,000 EVs/cell) for 24 and 48 h. Internalization was quantified by measuring phycoerythrin (PE-A) channel fluorescence intensity. **A)** Events in SSC-A *vs.* FSC-A. **B)** Singlets in FSC-H *vs*. FSC-A. C) Control cells in FSC-H *vs*. PC-A. **D)** FSC-H *vs.* PC-A of each individual donor after 24 and 48 h of incubation with EVs. Representative histogram of cells without **E)** and with EVs **F)**.

6.4.8 Flow cytometric gating strategy for EV uptake analysis in reporter cells

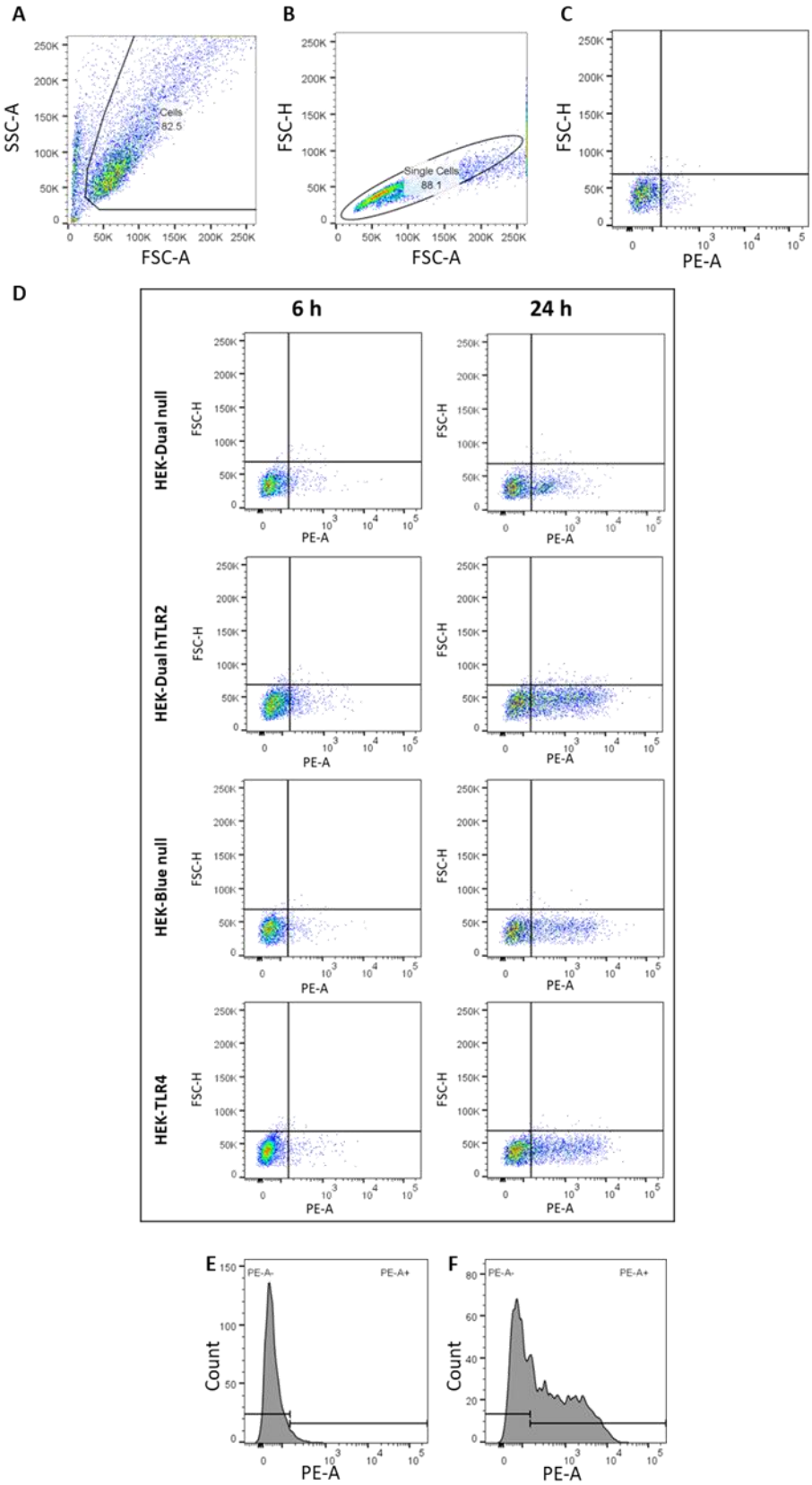

FIGURE S 8. Flow cytometric gating strategy for EV uptake analysis in reporter cells. Cells were incubated with DiI-labeled EVs (30,000 EVs/cell) for 6 h and 24 h. Internalization was quantified by measuring phycoerythrin (PE-A) channel fluorescence intensity **A)** Events in SSC-A *vs*. FSC-A. **B)** Singlets in FSC-H *vs*. FSC-A. **C)** Control cells in FSC-H *vs*. PC-A. **D)** FSC-H *vs.* PC-A of cells after 6 h and 24 h of incubation with EVs. Representative histogram of cells without (E, HEK-Dual null) and with EVs (F, HEK-Dual TLR2).

6.4.9 Flow cytometric gating strategy for surface TLR2 measurement in HUVECs

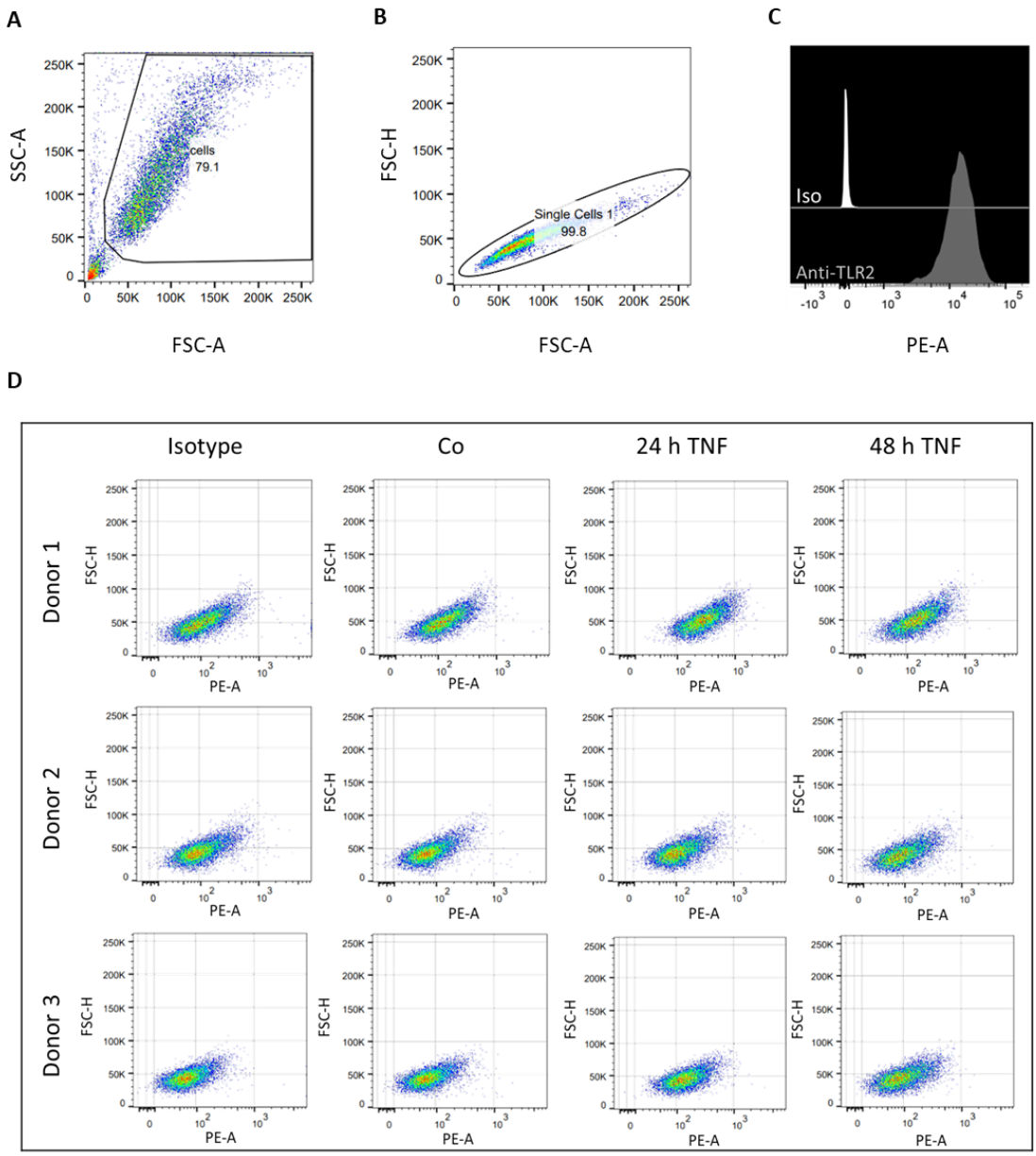

FIGURE S 9. Flow cytometric gating strategy for surface TLR2 measurement after TNF treatment (100 ng/ml) in HUVECs. HUVECs from three individual donors (n=3) were treated with TNF (100 ng/ml) for 24 and 48 h. Levels of surface TLR2 were quantified by measuring phycoerythrin (PE-A) channel fluorescence intensity. **A)** Events in SSC-A *vs*. FSC-A. **B)** Singlets in FSC-H *vs*. FSC-A. **C)** Histograms of HEK-Dual TLR2 cells incubated with anti-TLR2 antibody or the isotype control to investigate antibody specificity. **D)** FSC-H *vs*. PC-A of each individual HUVEC donor after 24 and 48 h of TNF treatment.

6.4.10 Flow cytometric gating strategy for EV uptake analysis after TNF-treatment in HUVECs

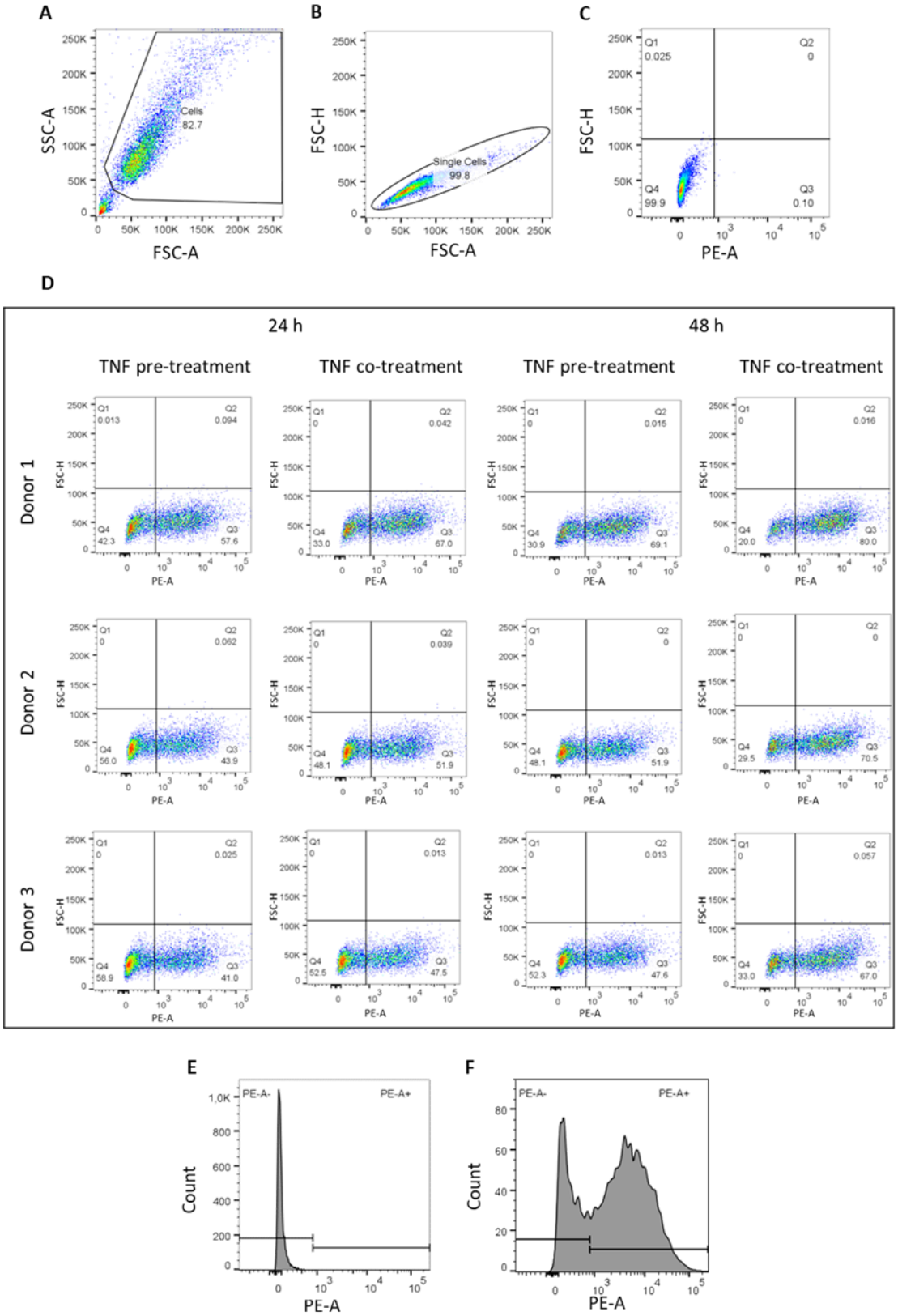

FIGURE S 10. Flow cytometric gating strategy for EV uptake analysis after TNF-treatment (100 ng/ml) in HUVECs. HUVECs from three individual donors were pre-treated with TNF (100 ng/ml) for 24 h. Cells were treated with 30,000 EVs/cell in the presence or absence of TNF for 24 and 48 h. EV uptake was quantified by measuring PE-A channel fluorescence intensity. **A)** Events in SSC-A *vs.* FSC-A. **B)** Singlets in FSC-H *vs.* FSC-A. **C)** Control cells in FSC-H *vs.* PC-A. **D)** FSC-H *vs.* PC-A of each individual donor after 24 and 48 h of pre/co-treatment and incubation with EVs. Representative histogram of cells without **E)** and with EVs **F)**.

6.4.11 C2025 hollow fiber cartridge instructions

Endothelial Cartridge Instructions

FiberCell Systems Inc.
a better way to grow cells

C2025 Specifications

Fiber number	20
Fiber I.D.	700µm
Fiber O.D.	1,300µm
Wall Thickness	300µm
Pore Size	.1µm
Lumen Surface Area	70cm^2
Outer Surface Area	85cm^2
Inoculation cell number	5-10 X 10^6
µg of Recovered RNA (est.)	50-150

FiberCell Systems Inc.
905 West 7th Street #334
Frederick, Md. 21701
Tel: (301) 471-1269
Email: info@fibercellsystems.com

Revision 6.0 1/8/14

Introduction

Thank you for your purchase of a hollow fiber bioreactor system from FiberCell Systems. A hollow fiber bioreactor cartridge will allow you to culture more cells, produce more protein and antibody at a higher concentration and in a smaller space than is possible with any other culture method. Because the cells are growing at 100X density than other techniques there will be some methods that are counter-intuitive to the ways that you may currently be growing cells.

These products are for laboratory use only. Not for diagnostic or therapeutic use in humans or animals.

Read the entire FiberCell Systems User's Manual prior to use. This provides important information on system set-up, maintenance, and daily monitoring of hollow fiber cultures. This manual is available from our web site at www.fibercellsystems.com.

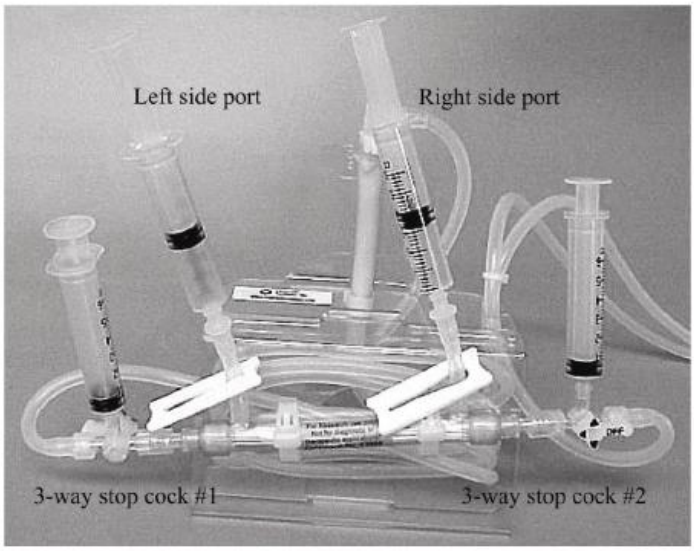

Photo: FiberCell Systems cartridge with ports identified.

Culture Guidelines

Technique:

- Correct sterile technique will ensure a long and productive life for your hollow fiber module. Shortcuts, suspect medium and poor sterile technique may result in contamination.
- Use a needle to draw liquids into syringes. Droplets of medium at the syringe/side port junction invites contamination.
- Perform all operations in the laminar flow hood. Keep the hood clean. Avoid rapid movements and working directly over the samples. If it necessary to open the hood front be sure to allow time for the air inside the hood to completely exchange.

Overview

The FiberCell Systems Polysulfone Plus cartridge (cat# C2025) contains a unique hollow fiber manufactured from a material that allows the hydrophobic binding of proteins to the fiber matrix. It is only necessary to wet out the fiber using 70% ethanol/water to activate the fiber and allow proteins to attach. This protein attachment is of the order of 10µg to 100µg per cm^2 of fiber area (70cm^2 for C2025). The fiber pore size of this material is .1µm so the protein coating will be uniformly applied to both the inner and outer surfaces of the fiber. Applications for this fiber include the study of the effects of extra-cellular matrix (ECM) composition on the growth of cells such as hepatocytes, pancreatic islets and other cell types where ECM composition may affect cell growth and differentiation. The FiberCell Systems Polysulfone Plus cartridge allows for the long term study (weeks to months) of ECM matrix on cell growth and development.

Another application for the Polysulfone Plus fiber is for the culture of endothelial cells under conditions of chronic shear stress. They are designed to be coated with appropriate matrix proteins such as fibronectin, collagen, gelatin or other proteins that facilitate the attachment of endothelial cells when inoculated onto the inside wall (lumenal wall) of the fiber. A solution of 10% FBS in standard cell culture medium can also be used. Endothelial cells attached in this manner can be subjected to various levels of reproducible shear stress for long term culture, up to 28 days or more. When grown under these conditions of chronic shear stress endothelial cells behave very differently than when grown in static culture. Endothelial cells will lay flat, form a monolayer and orient to the direction of medium flow forming tight junctions. Physiologic expression of Palade bodies can be observed and some genes can be

expressed that are not expressed in static culture. Culture of endothelial cells under chronic shear stress is considered to be a more physiologic environment and closer to the *in vivo* ideal. It is also possible to set up the FiberCell Systems Polysulfone Plus cartridge as a co-cultivation system in which endothelial cells are loaded into the lumen of the fiber and other cells types such as vascular smooth muscle or astro-glial cells are placed outside of the fiber. Examples of this can be found in the references included in the FiberCell Systems User's Manual.

Proper sterile technique is essential to maintain the long term health of this culture system. The FiberCell Systems materials used in the construction of this hollow fiber permits the easy application of various protein matrices such as collagen, fibronectin or gelatin. Also, it is possible to bind cytokines in conjunction with the proteins such as VEGF (vascular endothelial growth factor). Recovery of intact endothelial cells can be variable depending upon cell line and culture conditions. However, recovery of RNA and proteins can be achieved easily. Various microscopic techniques such as SEM, TEM, and immunohistochemical staining can be applied. Growth of endothelial cells under chronic shear stress using the FiberCell Systems' Polysulfone Plus cartridge is the most physiologic way to culture and study endothelial cell growth and function.

Set up of this system requires three steps. The first is to activate and coat the cartridge with the proteins of choice. The second is to load to endothelial cells into the cartridge. The third is to adapt the endothelial cells to the desired shear stress levels.

Activating the Endothelial Cartridge

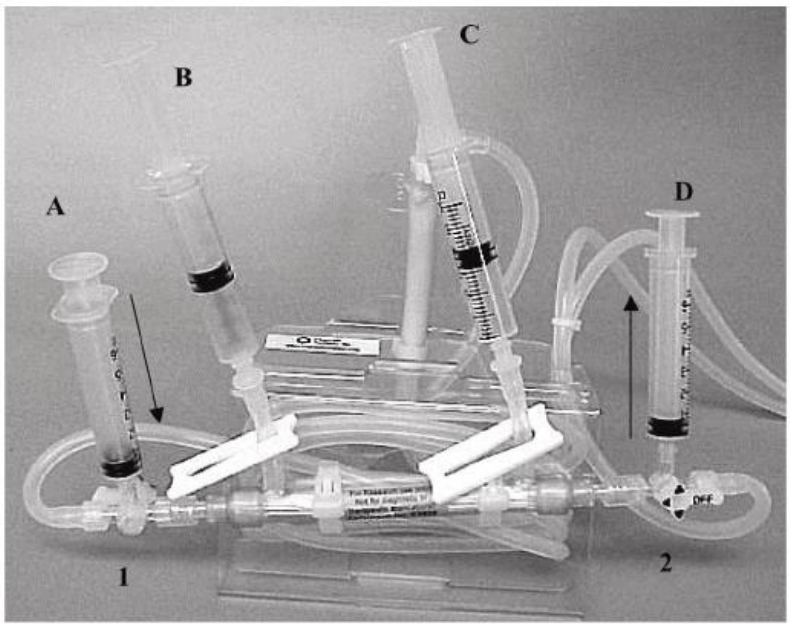

1. Prepare the following items in the laminar flow hood
   - 6 each 5 or 10ml syringes
   - 10-20 mls 70% ethanol/water sterile filtered
   - 10-20 mls sterile PBS
   - 10 mls sterile water
   - 5-10 mls of coating solution, 1mg/ml in sterile PBS. This solution can be fibronectin, collagen, gelatin, serum or other appropriate matrix proteins.
2. Fill a syringe with alcohol solution and attach it to 3-way stopcock #1. Position stopcock so that the "off" is facing away from the cartridge. Flow should go from the syringe into the cartridge.
3. Attach an empty syringe to 3-way stopcock #2. Position the "off" so that it is facing away from the cartridge. Flow should travel from the cartridge to the syringe.
4. Side port slide clamps associated with syringes B and C should be closed.

5. Flush alcohol from syringe A to syringe D. The ethanol should be in contact with the fiber for at least one minute. You will be able to see the fiber "wet out".
6. Drain any excess ethanol from the cartridge using syringe D.
7. Fill a fresh 10ml syringe with sterile distilled water. Attach to stopcock #1
8. Empty syringe D of ethanol and re-attach.
9. Rinse cartridge with sterile water. The water should be in contact with the fiber for at least 60 seconds. Flush back and forth between syringes A and D to remove alcohol. Remove excess sterile water using syringe D.
10. Fill a new syringe with protein matrix solution and attach to 3-way stopcock #1.
11. Attach a new, empty syringe to 3-way stopcock #2.
12. Attach new empty syringes to side ports B and C. Open side port slide clamp C
13. Position 3-way stopcock #2 so that the "off" is facing the cartridge.
14. Flush protein solution from syringe A to syringe C through the fiber. Flush solution back into syringe A.
15. Close side port slide clamp C. Position 3-way stopcock #2 so that the "off" is facing away from the cartridge. Flush protein solution from syringe A to syringe D.
16. Open side port slide clamp B. Position 3-way stopcock #1 so that the "off is facing away from the cartridge.
17. Flush protein solution from syringe D to syringe B and back to syringe D.
18. Ensure that the cartridge is filled with protein solution. Close both side port slide clamps and position the two 3-way stopcocks so that the "off" is facing towards the cartridge.
19. Let protein solution coat the cartridge for a minimum of one hour.
20. Position 3-way stopcocks so that the "off" is facing the syringes. Remove the syringes and replace with sterile luer caps. Initiate pre-culture for 24 hours.

Loading Endothelial Cells

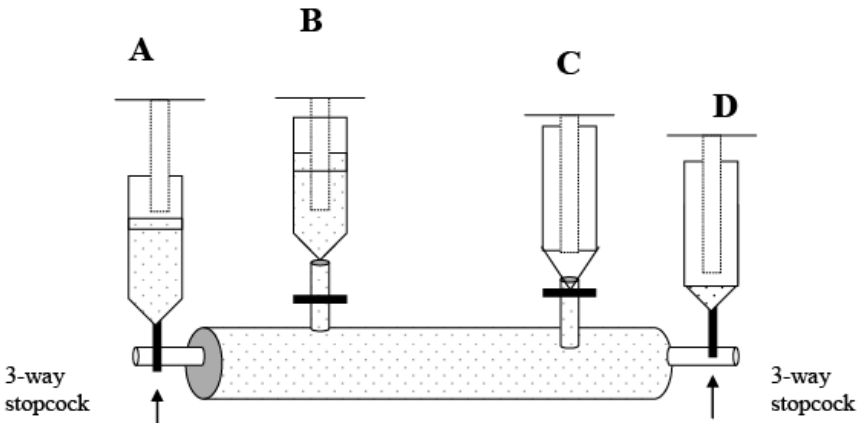

21. Prepare the following items in the laminar flow hood
    - 4 each 5 or10ml syringes
    - Freshly harvested endothelial cells from 2 T75 flasks in a volume of 10mls complete medium.
    - 18 gauge or larger needle
    - 4 sterile male luer caps
22. Attach a syringe to 3-way stopcock A and side ports B and C.
23. Using the large gauge needle draw 10 mls of the endothelial cell suspension into the 4th syringe. Remove the needle and attach the syringe to 3-way stopcock D
24. Side port slide clamps B and C should be closed. 3-way stopcocks A and D should have the "off" position facing away from the cartridge
25. Gently flush the cell suspension between syringe A and D through the inside of the cartridge 3 to 4 times. Leave half of the cell suspension in each of the syringes when finished
26. Open side port slide clamp C. Turn 3-way stopcock D so that the "off" position is turned towards the cartridge.
27. Slowly transfer medium and cells from syringe A to syringe C. Excess medium will flow through the walls of the fibers and the endothelial cells will be trapped in the lumen of the fibers.
28. Close side port slide clamp C and turn 3-way stopcock A so that the "off" position is turned towards the cartridge.
29. Open side port slide clamp B and turn 3-way stopcock D so the "off" position is turned away from the cartridge.
30. Slowly transfer medium and cells from syringe D to syringe B. Excess medium will flow through the walls of the fibers and the endothelial cells will be trapped in the lumen of the fibers.
31. Close side port slide clamp B and turn both 3-way stopcock A and D so that the "off" position is facing towards the cartridge.
32. Place the endothelial cell culture cartridge into the incubator for one hour WITHOUT flow to allow the endothelial cells to attach to the fiber. Rotate the cartridge 180 degrees after 30 minutes.
33. After the one-hour attachment period in the incubator return the cartridge to the hood. Remove the syringes and replace with sterile luer caps. Turn the 3-way stopcocks so that the "off" position is facing towards the position where the syringes were attached and will allow medium to flow through the cartridge.

Place the cartridge into the FiberCell Systems pump system and initiate flow at the lowest rate (30 pulses per minute) and shortest stroke length for approximately 12-24 hours. Check that the pump tubing is being compressed by the pump platen as the pre-culture period can occasionally distort the tubing slightly. Restore the original shape by GENTLY squeezing the tubing back into shape. This level of medium flow is sufficient to provide oxygen and nutrients to the endothelial cells without generating a level of shear that will remove the cells from the fiber. After 12 hours change the medium in the reservoir bottle. Retain the initial medium and count the cells that did not attach to the fiber. This will provide a direct indicator of the number of cells that attached to the fiber. Typically 20-40% of the cells loaded will not adhere. If desired the endothelial cell inoculation can be divided into two equal portions and the loading steps repeated.

Daily Maintenance Schedule

Day 0: Start the newly inoculated cartridge with 50mls of medium in the reservoir bottle. The will allow the accumulation of cytokines during the first few days of culture. The flow rate should be set to low, position 1 on the FiberCell Systems pump. The cartridge should remain at this flow rate for the first day of culture. Check to insure that the pump tubing has become distorted during the pre-culture period. If it is not being compressed restore the circular shape of the tubing by squeezing it gently.

Day 1-7 Adapt the cells to shear stress by increasing flow rate no more than one position increment at a time. Once the cells have been adapted to position 5, low rate it is possible to increase the rate to high and gradually select higher shear stress levels based upon the flow rate and shear stress levels in the chart below.

Check the reservoir bottle for endothelial cells that have washed from the cartridge. This will give an indication of the cells remaining in the cartridge.

Change the cell culture medium when the glucose has been 50% depleted.

Flow rate and Shear Stress

$$\tau = (4\eta Q / \pi R^3)$$

η = viscosity (dyne sec/cm^2)
Q = fluid flow rate (ml/sec) (per fiber)
R = internal radius

Viscosity of cell culture medium with 10% FBS is approximately 0.008 dyne sec/cm^2
Fluid flow rate must be converted from mls/min to mls/sec. Also, there are 20 fibers in the cartridge so this flow rate must be divided by 20

Internal radius of the fiber is 350µm (0.07 cm)

$R^3 = 0.000043$
1 ml/min flow rate per fiber = 0.0167

Shear stress at 20mls/minute = 3.95 dynes/cm^2

It is strongly recommended that you calibrate your pump system in your own laboratory for flow rate.

Flow	Shear
5 mls/min	1.2 dynes/cm2
12 mls/min	3.0 dynes/cm2
15 mls/min	3.75 dynes/cm2
24 mls/min	6.0 dynes/cm2
30mls/min	7.5 dynes/cm2
40 mlsmin	9.8 dynes/cm2
55 mls/min	14 dynes/cm2
70 mls/min	17.5 dynes/cm2
85 mls/min	21 dynes/cm2

RNA Isolation from Endothelial Cells

Overview: Endothelial cells are cultured on the inside wall of the hollow fiber module under conditions of defined shear stress and time. The cells are then lysed in situ using a guanidinium isothiocyanate solution. RNA is purified and quantitated using conventional molecular biology techniques.

Utilize all precautions to prevent contamination of the samples with RNase from the researcher and laboratory. All reagents should be RNase free. Volumes indicated are for one FiberCell Systems catalog number C2025 hollow fiber module.

Materials

Reagents

- TRIZOL Reagent, Invitrogen Inc. cat # 15596-026
  Similar RNA isolation reagents based upon the acid guanidinium thiocyanate/phenol method of Chomczynski and Sacchi are available from other vendors
- Chloroform, (molecular biology grade, without additives)
- 75% ethanol (v/v) (molecular biology grade) in DEPC-treated (RNase-free) water

- RNase-free water or 0.5% SDS solution in RNase-free water

Supplies

- sterile pipette tips
- sterile plastic pipettes, individually wrapped
- sterile 1.5 ml microfuge tubes
- 50 and 15 ml polypropylene centrifuge tubes (12,000 X g)
- disposable latex gloves (talc-free)
- sterile 10cc luer-lock syringes

Equipment

- micro-pipettes
- refrigerated centrifuge capable of 12,000 X g
- table top microfuge (refrigeration optional)
- Speed-Vac, water bath or other method of drying RNA pellets
- -20°C freezer
- UV Spectrophotometer

Cartridge Preparation

34. Remove module from the FiberCell Systems pump and place into the laminar flow hood.
35. Attach an empty 5-10 ml syringe to one of the 3-way stop cock valves. Remove the luer cap from the other 3-way stop cock. Set both 3-way stop cocks such that the "off" position is facing away from the cartridge and so that flow will proceed from the cartridge to the syringe.
36. Drain the cell culture medium from the lumen of the fibers by gently withdrawing the medium into the syringe. Discard.
37. Using the same syringe (or a fresh one) remove the luer cap from one of the side ports and attach. Remove the luer cap from the other side port and remove any cell culture medium from the ECS. Discard.
38. Close the side port slide clamps.
39. Detach the cartridge from the 3-way stop cock valves. Attach an empty 5 or 10 ml syringe to one end of the cartridge.
40. Draw 3-4 mls of cold (4°C) TRIZOL reagent into a 5 or 10 ml syringe and immediately attach it to the other end of the cartridge.
41. Flush the lysis solution both and forth between the two syringes 7-10 times and collect into one syringe. Place lysate into a 50ml conical centrifuge tube.
42. Repeat the RNA extraction 2 more times by repeating steps 7 and 8 above twice. Collect lysate into the same 50ml conical centrifuge tube.
43. Allow the pooled samples to incubate at room temperature for 5 minutes to allow for complete dissociation of the nucleoprotein complex.
44. Follow the manufacturer's recommendations for precipitation, washing and quantitation of RNA.

6.4.12 Full western blot of HUVEC EVs

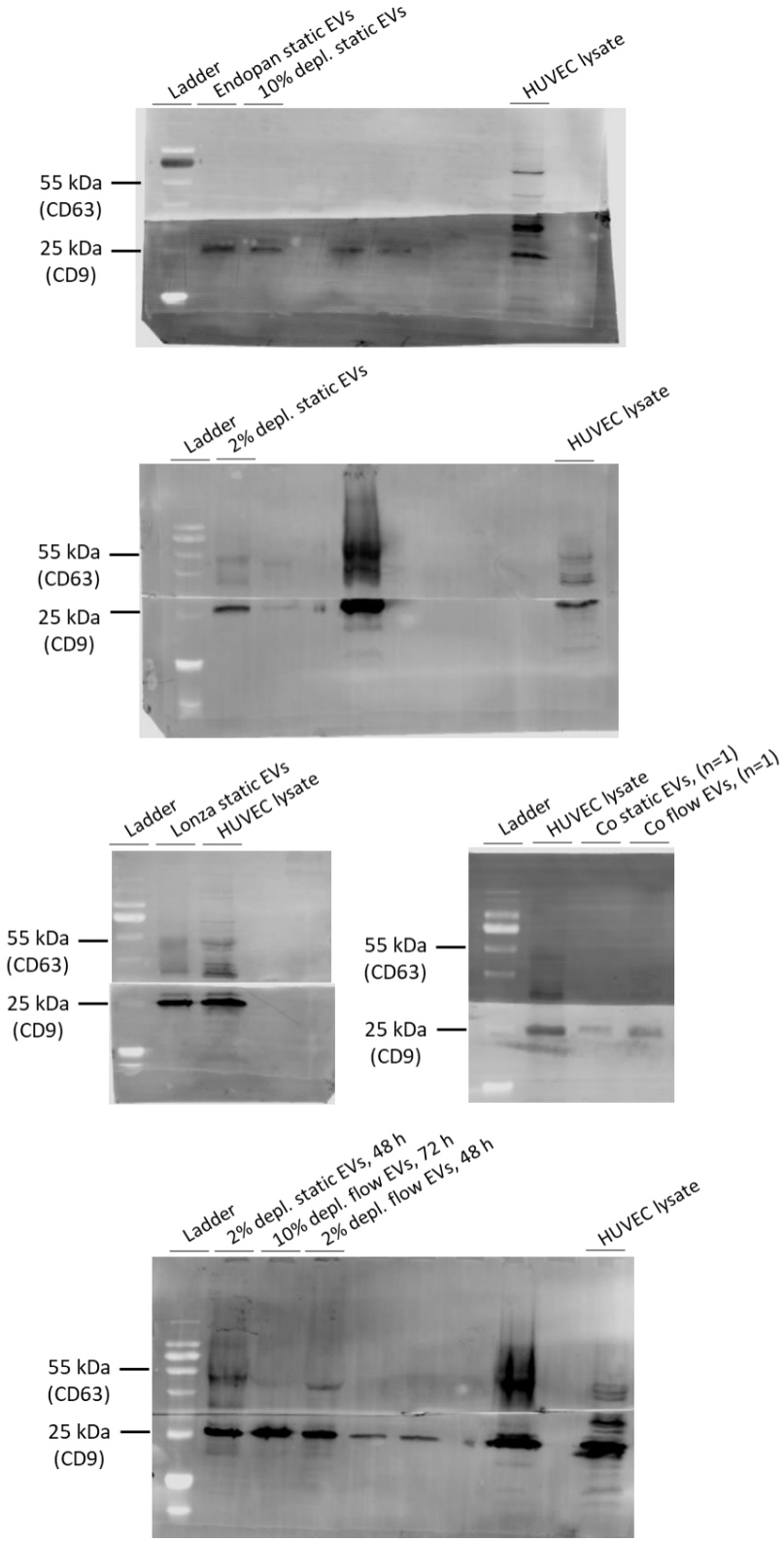

FIGURE S 11**.** Uncut western blot of HUVEC EVs from static and flow cultures (20 dynes/cm^2).

6.4.13 Cellular component terms for significantly enriched proteins in static and flow EVs

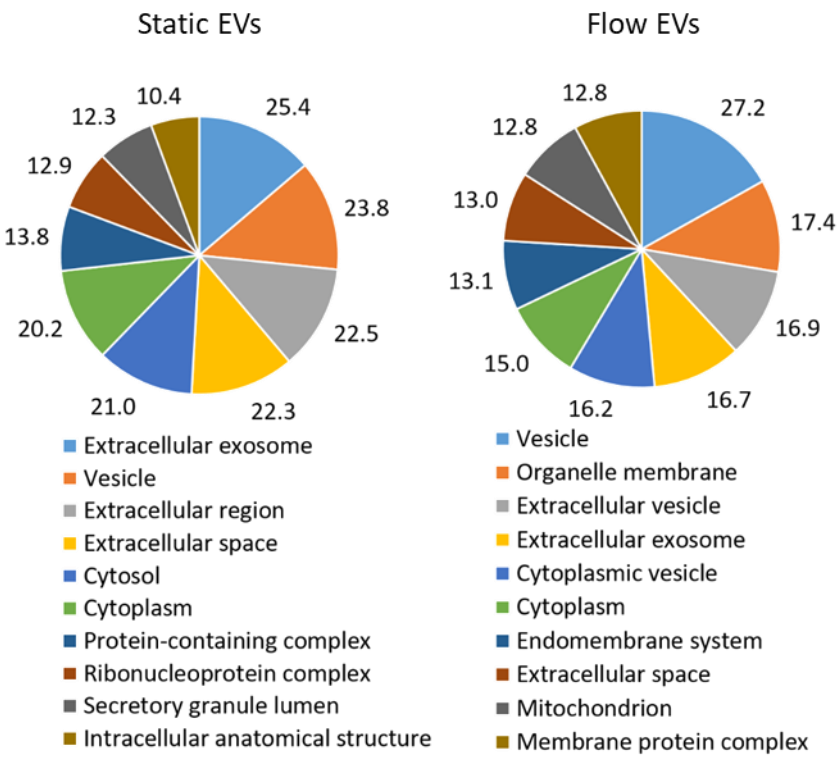

FIGURE S 12**.** Top 10 gene ontology (GO) cellular component terms for significantly enriched proteins in static and flow EVs according to the STRING database. $-\text{Log}_{10}$ (p-value) is shown for each term.

6.4.14 EV marker distribution in static and flow EVs

	F1	F2	F3	S1	S2	S3
A2M	22	26	27	28	33	28
ADAM10	6	15	9	22	14	16
AHCY	24	22	22	30	36	35
ANXA1	31	37	23	33	37	34
ANXA11	19	14	14	11	14	15
ANXA2	63	56	55	47	45	54
ANXA4	25	27	22	18	24	28
ANXA5	60	56	64	39	44	42
ANXA6	69	69	69	57	56	56
ARF6	6	8	4	7	9	7
ATP1A1	77	80	71	58	47	37
BSG	19	18	15	17	14	15
CAV1	13	8	7	11	12	9
CAV2	5	2	2	3	4	2
CD63	3	2	2	8	10	11
CD81	12	15	12	17	11	17
CD82	0	0	0	0	4	5
CD9	11	14	10	16	15	17
CHMP4B	0	0	3	5	5	3
EHD2	19	32	11	21	40	26
FLOT1	33	31	31	30	30	31
FLOT2	23	24	21	22	20	22
GAPDH	91	99	94	128	137	153
GNAI2	22	23	19	16	15	16
GNAS	8	5	4	6	5	3
GNB1	28	31	27	26	27	29
HLA-A	2	3	2	2	4	5
HSP90AA1	81	147	164	113	101	102
HSP90AB1	56	79	76	72	75	79
HSPA8	98	107	101	160	156	156
ICAM1	5	4	3	0	0	0
ICAM2	6	5	2	6	7	5
ITGB1	53	50	44	35	43	30
MFGE8	3	4	5	32	35	32
PDCD6IP	19	36	24	50	53	53
PECAM1	69	59	59	35	33	31
PKM	68	71	73	115	109	111
RAB11B	20	19	25	23	22	22
RAB14	31	36	35	40	40	46
RAB1A	24	22	21	22	20	20
RAB27A	0	2	0	0	0	0
RAB27B	7	6	8	7	4	6
RAB35	13	11	14	15	12	13
RAB5C	15	13	17	20	23	24
RAB7A	24	22	19	26	30	24
RAC1	16	14	17	15	14	14
RAP1A	4	10	3	6	5	6
RAP1B	34	27	35	39	29	37
RHOG	6	7	4	6	7	6
ROCK1	3	4	2	6	6	3
SDC4	0	0	0	0	0	2
SDCBP	28	31	25	40	48	44
SLC3A2	27	16	11	12	9	8
SNAP23	18	13	10	12	7	6
STX7	6	7	7	4	6	6
TLN1	112	144	129	147	150	136
TSG101	4	5	6	8	8	9
VAMP3	5	3	4	0	4	4
VAMP7	3	3	3	2	3	2
VPS4A	0	2	3	2	2	3

FIGURE S 13**.** EV marker distribution in static and flow EVs. Exclusive unique spectrum count raw data are shown for all three independent preparations per condition (S: static EVs, F: flow EVs). N= three biological replicates, each replicate is a mix of three HUVEC female donors.

7 Outcome

- **Optimization of EV Isolation from Human Umbilical Vein Endothelial Cells (HUVECs) Under Static and Laminar Flow Conditions**

Arefeh Kardani, Vida Mashayekhi, Marcus Koch, Gregor Fuhrmann, Alexandra K. Kiemer

Small New World 2022: Joint Meeting of ASEV & GSEV, Salzburg, Austria- Poster presentation

- **Cell-Derived Vesicles for Antibiotic Delivery—Understanding the Challenges of a Biogenic Carrier System**

Eilien Heinrich, Olga Hartwig, Christine Walt, Arefeh Kardani, Marcus Koch, Leila Pourtalebi Jahromi, Jessica Hoppstädter, Alexandra K Kiemer, Brigitta Loretz, Claus-Michael Lehr, Gregor Fuhrmann

Small 19, no. 25 (2023): 2207479, https://doi.org/10.1002/smll.202207479

- **The Internalization of *Enterococcus faecalis*-Derived Extracellular Vesicles and Their Modulatory Impact on Monocyte-Derived Macrophages and Endothelial cells**

Manuscript under preparation

- **Laminar Flow Alters EV Composition in HUVECs: A Study of Culture Medium Optimization and Molecular Profiling of Vesicle Cargo**

Arefeh Kardani, Vida Mashayekhi, Marcus Koch, Claudia Fecher-Trost, Markus R Meyer, Nicole Ludwig, Gregor Fuhrmann, Alexandra K. Kiemer

Manuscript under submission

8 Acknowledgment

I moved to Germany in 2020 to take a step forward in my life and education. Today, I am proud that I did not let even a global COVID-19 pandemic stop me from achieving my goals. I would like to express my heartfelt gratitude to everyone who supported me throughout this journey:

I sincerely appreciate Prof. Dr. Alexandra Kiemer and Prof. Dr. Gregor Fuhrmann for providing me with the opportunity to pursue my Ph.D. under their supervision and guidance. Additionally, I am grateful to all my colleagues in the Pharmaceutical Biology group and the BION team.

Special thanks to:

- Mr. Theo Ranßweiler for his technical support in providing the umbilical cords and isolating HUVECs.
- Ms. Astrid Decker for her assistance during my visa application process.
- Dr. Britta Diesel for her help in obtaining approval for BSL2 bacterial work.
- Dr. Nicole Ludwig for her assistance with RNA library preparation.
- Dr. Marcus Koch for the cryo-TEM images.
- Dr. Claudia Fecher-Trost for the proteomics analysis.
- Dr. Eilien Heinrich for introducing me to UC, NTA, and bacterial culture during my early days.
- Jan Hemmer and Annika Schomisch for their help regarding HMDMs.
- Thomas Kuhn for his guidance on the hollow fiber cartridge.
- Laura Gröger for providing the *E. faecalis* bacteria.

No words can fully express my heartfelt thanks to Dr. Vida Mashayekhi for her incredible supervision and friendship. Vida, I feel so lucky to have had you by my side. I've learned so much from you—both scientifically and personally—and I'll always cherish the moments we shared, both in the lab and outside of it. The coffee breaks, lunch chats, picnics, trips, drinks, and BBQs with you and Kamal are among my absolute favorite memories from my Ph.D. journey.

I am deeply thankful to my family, especially my mom, for all her unwavering support. Without her, I would never have come this far. I envisioned my Ph.D. graduation with her right after completing my B.Sc.. Mom, I told you I would do it—and I did! ☺